Accepted Manuscript

Aryl-1,3,5-triazine derivatives as histamine H_4 receptor ligands

Dorota Łażewska, Małgorzata Więcek, Joanna Ner, Katarzyna Kamińska, Tim Kottke, J. Stephan Schwed, Małgorzata Zygmunt, Tadeusz Karcz, Agnieszka Olejarz, Kamil Kuder, Gniewomir Latacz, Marek Grosicki, Jacek Sapa, Janina Karolak-Wojciechowska, Holger Stark, Katarzyna Kieć-Kononowicz

PII: S0223-5234(14)00551-0

DOI: 10.1016/j.ejmech.2014.06.032

Reference: EJMECH 7075

To appear in: *European Journal of Medicinal Chemistry*

Received Date: 25 January 2014

Revised Date: 17 April 2014

Accepted Date: 16 June 2014

Please cite this article as: D. Łażewska, M. Więcek, J. Ner, K. Kamińska, T. Kottke, J.S. Schwed, M. Zygmunt, T. Karcz, A. Olejarz, K. Kuder, G. Latacz, M. Grosicki, J. Sapa, J. Karolak-Wojciechowska, H. Stark, K. Kieć-Kononowicz, Aryl-1,3,5-triazine derivatives as histamine H_4 receptor ligands, *European Journal of Medicinal Chemistry* (2014), doi: 10.1016/j.ejmech.2014.06.032.

Aryl-1,3,5-triazine derivatives as histamine H_4 receptor ligands

Dorota Łażewska[1], Małgorzata Więcek[1], Joanna Ner[1], Katarzyna Kamińska[1], Tim Kottke[2], J. Stephan Schwed[2], Małgorzata Zygmunt[3], Tadeusz Karcz[1], Agnieszka Olejarz[1], Kamil Kuder[1], Gniewomir Latacz[1], Marek Grosicki[1], Jacek Sapa[3], Janina Karolak-Wojciechowska[4], Holger Stark[2,5], Katarzyna Kieć-Kononowicz[1*]

[1] *Department of Technology and Biotechnology of Drugs, Jagiellonian University Medical College, Medyczna 9 str., 30-688 Kraków, Poland;* [2]*Goethe University, Institute of Pharmaceutical Chemistry, Biozentrum, ZAFES/CMP/ICNF, Max-von-Laue-Str. 9, 60438 Frankfurt am Main, Germany;* [3]*Department of Pharmacodinamics, Jagiellonian University Medical College, Medyczna 9 str., 30-688 Kraków, Poland;* [4]*Institute of General and Ecological Chemistry, Technical University of Łódź, Żeromskiego 116 str., 90-924 Łódź, Poland;* [5]*Heinrich-Heine-University, Institute of Pharmaceutical and Medicinal Chemistry, Universitaetsstr. 1, 40225 Duesseldorf, Germany*

*****Corresponding author: tel +48 12 6205580; fax + 48 12 620 55 96
E-mail address: mfkonono@cyf-kr.edu.pl (K. Kiec-Kononowicz)

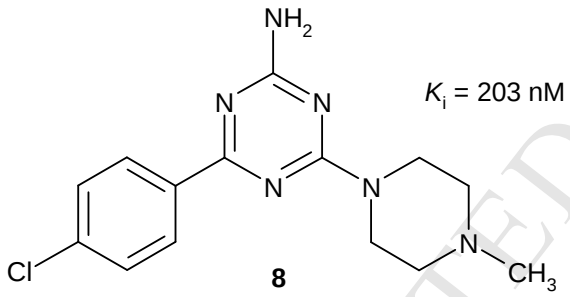

8

Highlights

- A series of 2,4,6-trisubstituted 1,3,5-triazines were obtained as potential histamine H_4R ligands
- Some compounds showed K_i values in the low submicromolar range
- Some compounds exhibited *in vivo* anti-inflammatory activity

Aryl-1,3,5-triazine derivatives as histamine H_4 receptor ligands

Dorota Łażewska[1], Małgorzata Więcek[1], Joanna Ner[1], Katarzyna Kamińska[1], Tim Kottke[2], J. Stephan Schwed[2], Małgorzata Zygmunt[3], Tadeusz Karcz[1], Agnieszka Olejarz[1], Kamil Kuder[1], Gniewomir Latacz[1], Marek Grosicki[1], Jacek Sapa[3], Janina Karolak-Wojciechowska[4], Holger Stark[2,5], Katarzyna Kieć-Kononowicz[1*]

[1] *Department of Technology and Biotechnology of Drugs, Jagiellonian University Medical College, Medyczna 9 str., 30-688 Kraków, Poland;* [2]*Goethe University, Institute of Pharmaceutical Chemistry, Biozentrum, ZAFES/CMP/ICNF, Max-von-Laue-Str. 9, 60438 Frankfurt am Main, Germany;* [3]*Department of Pharmacodinamics, Jagiellonian University Medical College, Medyczna 9 str., 30-688 Kraków, Poland;* [4]*Institute of General and Ecological Chemistry, Technical University of Łódź, Żeromskiego 116 str., 90-924 Łódź, Poland;* [5]*Heinrich-Heine-University, Institute of Pharmaceutical and Medicinal Chemistry, Universitaetsstr. 1, 40225 Duesseldorf, Germany*

*****Corresponding author: tel +48 12 6205580; fax + 48 12 620 55 96
E-mail address: mfkonono@cyf-kr.edu.pl (K. Kiec-Kononowicz)

Abstract: A series of novel 2-amino-4-(4-methylpiperazin-1-yl)-1,3,5-triazine derivatives with different aryl substituents in the 6-position was designed, synthesized and evaluated for histamine H_4 receptor (H_4R) affinity in S*f*9 cells expressing human H_4R co-expressed with G-protein subunits. Triazine derivative **8** with a 6-(*p*-chlorophenyl) substituent showed the highest affinity with hH_4R K_i value of 203 nM and was classified as an antagonist in cAMP accumulation assay. This compound, identified as a new lead structure, demonstrated also anti-inflammatory properties in preliminary studies in mice (carrageenan-induced edema test) and neither possessed significant antiproliferative activity, nor modulated CYP3A4 activity up to concentration of 25 μM. In order to discuss structure-activity relationships molecular modeling and docking studies were undertaken.

Keywords: Histamine H_4 receptor, 4-methylpiperazines, 2,4,6-trisubstituted 1,3,5-triazines, anti-inflammatory properties

1. Introduction

The human histamine H_4 receptor (hH_4R) was cloned in 2000 and has constituted an interesting target for drug development thereafter. Pharmacological studies suggest utility of H_4R antagonists/inverse agonists in the treatment of inflammatory and immunomodulatory diseases, e.g., allergic rhinitis, asthma, atopic dermatitis, colitis and pruritus.[1] Among described H_4R antagonists/inverse agonists pyrimidine-2-amine derivatives consist important lead structures with many potent compounds [for review see [2-7]]. Some of early developments

already made their way to clinical trials and promising results from the clinical studies for compounds **UR-63325** and **ZPL-38937887** were reported.[8,9]

The 1,3,5-triazine (*s*-triazine) moiety is present in many biologically active structures with the broad range of therapeutic utility. Such compounds have been proved to exhibit antimicrobial,[10,11] antimalarial activity[12] and chemotherapeutic potential.[13,14] Moreover, for some triazine dimers the ability to mimic the protein A binding to murine and human IgG antibody was described.[15] The chemistry of 1,3,5-triazine was recently reviewed by Blotny.[16] A couple of 4-(4-methylpiperazin-1-yl)-1,3,5-triazines were disclosed in the patent application from Johnson&Johnson and some of them showed high affinities (K_i < 20 nM) for hH_4R (e.g. **1**, Fig. 1).[17]

Taking together the published results on pyrimidine derivatives (e.g. **2**)[18] as well as information on triazines (e.g. **1**)[17] a search was initiated to find active compounds among 2-amino-4-(4-methylpiperazin-1-yl)-1,3,5-triazines. In this work, the synthesis, H_4R affinities, functional properties, receptor selectivity and anti-inflammatory properties of these compounds (exemplified by general structure on Fig. 2) are described. Also for selected compounds antiproliferative effect and metabolic stability was checked.

2. Results and Discussion

2.1 Chemistry

The general synthetic procedure for preparation of 2,4,6-trisubstituted 1,3,5-triazines is outlined in Scheme 1. Triazine derivatives **3**-**23** were obtained as the result of the reaction of esters **3a**-**23a** with biguanidine dihydrochloride. 4-Methylpiperazin-1-yl biguanidine dihydrochloride intermediate was obtained by the heating of cyanoguanide and 4-methylpiperazine dihydrochloride in 1-butanol.[19] All acid methyl esters were commercially available (except **7a** and **21a** which were synthesized according to the known procedure[20]). Cyclization of 4-methylpiperazin-1-yl biguanidine dihydrochloride with the appropriate carboxylic acid methyl ester in the presence of sodium methoxide have been known to yield 1,3,5-triazines.[21] The reaction was led in the boiling point and proceeded in low yields (4-35%).

2.2 Histamine H_4 receptor screening

The series of novel substituted phenyl derivatives of 1,3,5-triazine with one to three substituents at the benzene ring was screened at hH_4R in [^{3}H]histamine binding experiments (Table 1). Investigated was the SAR of the 6 substituent of the 1,3,5-triazine derivatives on the hH_4R activity. All compounds share the 4-methylpiperazinyl moiety (as basic center) and the primary aromatic amino group as additional basic center as well as hydrogen acceptor/donor functionality. These both elements are widely present in many published H_4R antagonists.[2-7] Most of the obtained compounds showed micro/submicromolar affinities.

The most potent in these group was compound **8** with chlorine substituent in the *para*-position with submicromolar affinity (K_i = 203 nM[6]). The change of chlorine position to *meta* (**5**, K_i = 408 nM) and especially to *ortho* (**4**, K_i = 1261 nM) position drastically reduced affinity. Generally, the same trend was also observed for methyl and cyano substituents (compare **6** vs **12** and **7** vs **14**). In addition, the change of chlorine in the *para*-position for

different substituents (F, Br, I, CH_3, CF_3, CN, $N(CH_3)_2$, compounds **9**-**15**), led to decrease of potency compared with that of **8**. Interestingly, compound **3**, the unsubstituted analogue, had higher affinity than the majority of the substituted derivatives.

The introduction of the second substituent (chlorine **18** or methoxy group **16**, **17**) to *meta*-position e.g. compound **5** did not improve the affinity. Two fluorine substituents in 2- and 6-position (**19**) are less beneficial than two (**20**) or three atoms (**21**) in respectively the 3,5-position and the 3,4,5-position.

Comparing the present results with the published data for pyrimidine analog of **8** (compound **2**, Fig. 1[18]) a reduction in affinity of more than one log unit was noticed. Although, it seems that the additional nitrogen in the central core (triazine ring instead of pyrimidine one) is detrimental for H_4R affinity, some compounds display submicromolar affinities. So further investigations should be done (e.g. blocking free amino group) as some related triazines with high H_4R affinities have recently been described.[17]

2.3 Functional properties at histamine H_4 receptor and selectivity over histamine H_3 receptor for selected compounds

In order to better characterize the pharmacological profile of the investigated compounds selected structures (**8** and **10**) were additionally tested for their functional properties in cAMP accumulation assay at recombinant cellular model. Their selectivity over histamine H_3 receptor (H_3R) subtype, representing the highest degree of homology with H_4R, was also evaluated.

Investigated compounds caused a blockade of the histamine-induced cAMP reduction in CHO-*h*H_4R-cAMPzen cells, co-treated with forskolin and were therefore classified as antagonists at H_4Rs. Antagonist potency (IC_{50}) was determined by performing a dose response curve in presence of H_4R agonist (histamine, 140 nM, corresponding to its EC_{80}) and forksolin (10 μM) (Fig. 3). Obtained IC_{50} values for both evaluated compounds were well in accordance with their K_i values at hH_4Rs and the order of potency also was retained in functional tests (**8**, K_i = 203 nM, IC_{50} = 512 nM; **10**, K_i = 524 nM, IC_{50} = 1630 nM).

Since H_4R shows the highest sequence homology (~60% in the transmembrane domains) to the H_3R subtype[22], considered structures were additionally tested for their interaction with H_3R. For that purpose radioligand binding assays were performed with the use of [^{3}H]N^{α}-methylhistamine and membrane preparations from HEK-293 cells stably expressing human H_3R.

Performed assays revealed that compounds **8** and **10** show low affinity for H_3R (**8**, K_i = 13.2 μM; **10**, K_i =15.0 μM) and are therefore selective towards H_4R subtype (H_3R K_i/H_4R K_i: **8**, 29-fold selectivity; **10**, 65-fold selectivity).

2.4 Anti-inflammatory activities of selected compounds

Radioligand receptor binding assay showed that some of the investigated 1,3,5-triazine derivatives have micro/submicromolar affinities for the hH_4R and act as antagonists at that receptor. These results were inspiration to study the anti-inflammatory activity of the selected 1,3,5-triazine derivatives *in vivo* in the carrageenan-induced paw edema test.[23,24] The tested

compounds (**5**, **8**, **9**, **10**, **12**, **18** and **23**) administered intraperitonally caused inhibition of carrageenan-induced edema in mice, when compared to the control (ketoprofen; Fig. 4).

Compound **10**, in all doses, throughout duration of the experiment, showed a statistically significant anti-inflammatory activity. At a dose 50 mg/kg *ip*, compound **10**, decreased carrageenan-induced edema by 90.6%, 90.0% and 91.8% in 1, 2 and 3 hours of the experiment, respectively, while at a dose 25 mg/kg, by 68.8%, 70.0% and 81.6%, respectively. Compound **10** at a dose 10 mg/kg, suppress edema paw in the range 37.5% - 63.3%. Compound **8** showed statistically significant effects in this experimental model. Given intraperitoneally at a dose 50 mg/kg, inhibited carrageenan-induced edema in 1, 2, 3 hours of the experiment by 90.6%, 92.5%, 91.8%, respectively, while at a dose 25 mg/kg, by 56.2%, 65.0% and 71.5%, respectively. The half maximal the anti-inflammatory effect was observed at the lowest dose, analogously by 46.9%, 50.0%, 59.2%. Compound **12** at a dose 50 mg/kg and 25 mg/kg, reduced carrageenan-induced edema, in the first hour of measurement by 90.6% and 50.0%, in the second hour of measurement by 75.0% and 52.5%, and in the third hour by 79.5% and 61,2%, respectively. Compound **9** given at a dose 50 mg/kg, suppress carrageenan-induced edema by 81.3%, 77.5%, 81.6% in 1, 2 and 3 hours of the experiment, respectively. The same compound, given at the lower dose 25 mg/kg, also significantly significant inhibited edema by 75%, 57.5%, 69.4%, compared to the control group. However, reduction of the dose lead to a decreased anti-inflammatory activity. Compound **5** showed statistically significant anti-inflammatory effect, given in two doses. This compound (**5**) administered at a dose 50 mg/kg and 25 mg/kg, decreased carrageenan- induced edema, throughout duration of the observation, by 81.2% - 87.7% and 46.8% - 69.3%, respectively. Compound **23** at a dose of 50 mg/kg inhibited paw edema, in the first, second and third hour, after carrageenan injection, by 65.6%, 65%, 71.4%, respectively. In lower doses (25 mg/kg or 10 mg/kg) the decrease in activity was observed. Compound **18** given in the range 50 mg/kg - 10 mg/kg, showed anti-inflammatory effect. This effect was intensified, with an increase in the duration of the experiment, reaching a maximum in the third hour, which was 51.0% (50 mg/kg), 42.8% (25 mg/kg) and 44.8% (10 mg/kg). Ketoprofen was used as the reference compound in dosages from 50 to 10 mg/kg. The largest anti-inflammatory activity was observed at the highest dose. Ketoprofen administered at a dose 50 mg/kg, reduced carrageenan-induced edema, after the first, second and third hour after injection of carrageenan, by 66.7%, 70.7%, 77.4%, respectively. Ketoprofen given intraperitoneally, at a dose of 25 mg/kg, inhibited edema, in the third hour of the experiment by 20.0%, 55.0%, 67.3%, respectively, while at a dose 10 mg/kg, suppress edema by 26.7%, 55.1% and 62.7%.

Preliminary pharmacological studies showed, that all tested compounds had anti-inflammatory effect. The strongest inhibition of paw edema was shown at a dose of 50 mg/kg in three measurement times, in the range from 42.5% to 92.5%. The compounds administered at a dose 25 mg/kg, reduced paw edema in the first, second and third hour of the experiment in the range 27.5% - 81.6%, while at a dose 10 mg/kg in the range 14.7% -63.2%. In comparison of the anti-inflammatory properties of tested compounds with the activity of the reference compound, it has been shown, that compounds **8** and **10** at all doses, throughout duration of the experiment, showed stronger anti-inflammatory activity than ketoprofen, while compounds **5** and **9** showed apparently stronger anti-inflammatory activity than ketoprofen, only in the two highest doses.

2.5 Antiproliferative assay

The most important properties in drug discovery which describe the ability of the compound to be an ideal drug candidate are absorption, distribution, metabolism, elimination and toxicity.[25] Recently, the *in vitro* studies are increasingly applied for toxicity studies during earlier stages of drug discovery. This strategy is a reliable alternative to *in vivo* methods and allows for study of greater number of compounds. Additionally, the *in vitro* tests reduce the usage of animals (3Rs approach).[26] Moreover, the toxicity tests, for example antiproliferative or cytotoxicity assays, are useful tools in conventional anticancer drug discovery and development.[27] During this study we used formazan dye based EZ4U test for the determination of antiproliferative effect of **8** and **10** on HEK-293 and IMR-32 cell lines. The incubation of HEK-293 cells in the presence of the tested compounds for 48 h showed weak antiproliferative effect. The reduction of cell viability was observed only at very high concentrations: 100 and 250 µM. However, it must to be pointed out, that in comparison to the calculated IC_{50} value of the standard drug doxorubicin (DX) against HEK-293 (455 nM) the significant antiproliferative effect **8** and **10** was observed in more than 200 fold higher concentration (Fig. 5).

Measured antiproliferative activity of the examined compounds against neuroblastoma cell line IMR-32 was similar to that observed in HEK-293 cells. Compound **8** did not show any significant effect on cells viability up to the concentration of 10 µM and **10** up to the concentration of 100 µM. However, compared to DX (calculated IC_{50}: 5.1 nM) the examined compounds did not possess the significant antiproliferative activity (Fig. 6).

2.6 Metabolic stability

The *in silico* prediction of the sites of metabolism in phase I reactions is commonly used in the preliminary stage of study on the metabolic pathway prediction. MetaSite is an example of the easy and inexpensive computational method for *in silico* prediction of metabolic transformations related to CYP450 reactions (e.g. CYP3A4). MetaSite identifies the most likely sites of metabolism in an examined compound and predicts structures of metabolites by consideration of two factors: a thermodynamic factor (enzyme-substrate recognition) and a kinetic factor describing the chemical transformations catalyzed by the enzymes.[28,29] Cytochrome P450 3A4 is known to metabolize the majority of therapeutics agents and endogenous substrates and in the recent years, many drug interactions were documented as associated with metabolic activity of this cytochrome.[30] In our study, compounds **8** and **10** were examined *in silico* in two models of metabolism: liver and CYP3A4 exclusively. For both compounds (**8** and **10**) in the used models, the highest probability of metabolism occurred at *N*-methyl group of piperazine moiety and the suggested reaction was *N*-demethylation. The locations of metabolic modifications are shown on Fig. 7. The darker color of the marked functional group indicates higher probability of its involvement in the metabolism pathway.

Moreover, we also used luminescent CYP3A4 P450-Glo™ Assay (Promega) for testing the effects of these two H_4R ligands (**8** and **10**) on CYP3A4 activities. *In vitro* studies with the recombinant human CYP3A4 isoforms are the reliable methods for evaluation of metabolic

stability and drug-drug interaction. Luminescent CYP3A4 P450-Glo™ Assay is based on the conversion of the Luciferin-PPXE, the beetle D-luciferin derivative, into D-luciferin by recombinant human CYP3A4. After addition of the firefly luciferase the measured luminescence is used to evaluate the potential inhibition/induction of CYP3A4 by tested compounds. The measured amount of light produced in that reaction is proportional to the CYP3A4 activity.[31] As is shown on Fig. 8 compounds **8** and **10** did not modulate significantly of CYP3A4 activity up to 25 μM, whereas the reference compound ketoconazole inhibited completely the CYP3A4 activity already at 10 μM.

2.7 X-ray study

From topological point of view, all studied derivatives can be expressed in terms of triazine with the fastened phenyl and piperazine rings. The mutual position of all three rings and suitable crystal architecture depends mainly on the phenyl ring substitution. At the same time, in the frame of studied group of compounds, degree of affinity to the designed receptor must be associated with rings arrangements as well as with ability to generate suitable intermolecular interactions. Thus, crystallographic studies of compounds **8** (most potent with *para*-Cl) and **17** (4-Cl-6-methoxy compound) seem to be sufficient for the description of structural phenomena for studied triazines.

In both X-ray structures for **8** and **17** (Fig. 9) benzene and piperazine rings are slightly inclined to triazine and the distances between them are almost identical (7.08 Å and 6.89 Å respectively for **8** and **17**). Hence the impact of substituents nature and position on molecule conformation seems to be insignificant.

However this impact is evident in the pattern of molecules assembling in the crystal. The main motif in both structures is based on N3-H…N strong H-bond involving free amine group (N3 nitrogen) and one of three triazine nitrogens. Thus, in **8** the N3-H…N2 attaches molecules into the dimers, while in **17** molecules are assembled in helix through N3-H…N6 hydrogen bond. The N4 triazine nitrogen does not contribute to the crystal net. In both crystals hydrogen bonds from N3 to piperazines N4' are connecting main motifs (for details see respective Fig. 10 and Fig. 11). Therefore, it is evident that benzene ring substituents nature and position are able to manipulate with the charge of N2 and N6 triazine nitrogens. In consequence ability to create complexes with designed receptor depends on the benzene substitution as was shown with the screening data.

2.8. *In silico* molecular and docking studies

In order to determine protein-ligand interactions and its possible influence on *in vitro* activity docking studies for all synthesized ligands, as well as for two reference compounds (**1**-**2**) were performed. All of the docked ligands showed moderate to good docking score values in the range of -4.185 (**13**) to -6.738 (**1**).

As it has been previously described by Jongejan[32] the H_4R has two major anchoring points: $ASP94^{3.32}$and $GLU182^{5.46}$. Two possible ligand orientations in the binding pocket of H_4R has also been found, which is in agreement with the study of Feng[33] and recent studies of Schultes[34] (Fig. 12). For all the obtained docked ligands (**3**-**23**), interactions with only $ASP94^{3.32}$ were found. However, for the most active ligands in this group (e.g. **5**, **8**-**10**, **12**) protonated methylpiperazine nitrogen is in very close proximity to $GLU182^{5.46}$ and might

form weak hydrogen bonds. For most of the compounds, hydrogen bond formation between protonated nitrogen and TYR225$^{6.51}$ was found. Stabilization of the benzene ring via π- π stacking interactions for compounds **3**, **5**, **6**, and with pyrimidine ring of compound **2** was observed.

For compounds with triazine core, benzene ring of TYR95$^{3.33}$ stabilize receptor-ligand complexes through π- π stacking interactions with triazine ring for all of tested ligands and with substituted benzene ring for compounds **1**, **3**, **6**, **17**. For compounds **1**, **3**, **5**, **6** and **17** also additional ligand stabilization through π- π stacking interactions between substituted phenyl and PHE228$^{6.54}$ was observed. For most active compounds in this series **8**-**10**, halogen atoms *para* substituted to benzene ring fits in the hydrophobic pocket formed by VAL64$^{2.53}$, ILE69$^{2.58}$ and TRP90$^{3.28}$ (Fig. 13). It can be observed that for the structural isomers of **8**, compounds **4** and **5**, what is in agreement with Surgand et.al[35] o*rtho* and *meta* substituted chlorine of **4** and **5** might not fit in the above mentioned pocket. For the most active compounds **1** and **2** protonated methylpiperazine nitrogen forms a hydrogen bond with THR178$^{5.42,}$ (Fig. 13), that seems to highly influence the stability of ligand in H_4R binding pocket, as well as ligands' *in vitro* affinity. Even though the distance between the atoms do not meet the requirements of hydrogen bond with methylated piperazine nitrogen, for most active compounds (only in binding manner A) in this series methylated piperazine nitrogen was in very close proximity to THR178$^{5.42}$ (3,2-3,6 Å). Moreover, paying attention to the activity of reference compound **2** with free amine group and its position in H_4R homology model binding pocket, it could be observed, that the amine group of compound **2** is in very close proximity to TYR225$^{6.51}$ (3,17 Å) and thus might influence higher affinity of compound **2** (*vs* e.g. **5**) to H_4R, by forming hydrogen bond of moderate strength with this moiety.

3. Conclusions

Generally, the change of the substituent in the phenyl moiety largely influenced the H_4R affinity although it seems that this part of the structure did not decide on the activity but only influenced its degree. Histamine H_4 receptor antagonist - **8**, with promising submicromolar affinity (203 nM) and good selectivity over *h*H_3R, could be a good lead structure for our further investigations. X-ray studies indicated the preferences of triazine nitrogen N2 to be the potential H-bond acceptor in complexes with designed receptor. Molecular modelling and docking studies allowed to discuss the mode of ligands interaction with elements of histamine H_4R model. Additional preliminary pharmacological studies demonstrated the *in vivo* anti-inflammatory properties of tested triazines. The selected compounds (**8** and **10**) did not show the significant antiproliferative effect and did not modulate CYP3A4 activity.

4. Experimental

4.1 Chemistry

Melting points were determined on MEL-TEMP II apparatus and are uncorrected. IR spectra were measured as KBr pellets on FT Jasco IR spectrometer. Mass spectra (LC/MS) were performed on Waters TQ Detector mass spectrometer. ^{1}H-NMR and ^{13}C NMR spectra were recorded on Varian-Mercury 300 MHz spectrometer in DMSO-d_6. Chemical shifts in

^{1}H-NMR spectra are expressed in ppm downfield from deuterated solvent signal treated as reference. Data are reported in the following order: multiplicity (br, broad; def, deformed; s, singlet; d, doublet; t, triplet; m, multiplet; Ph, phenyl; Pp, piperazine), approximate coupling constants *J* in Hertz (Hz), number of protons. LC- MS were carried out on a system consisting of a Waters Acquity UPLC, coupled to a Waters TQD mass spectrometer. Retention times (t_R) are given in minutes. The UPLC/MS purity of all final compounds was determinated (%). Elemental analyses (C, H, N) were measured on Elemental Vario-EL III instrument and are within ± 0.5% of the theoretical values. TLC was carried out using silica gel F_{254} plates (Merck). The spots were visualized with Dragendorff's reagent or by UV absorption at 254 nm.

4.1.1. General procedure for synthesis of 1,3,5-triazines (3-22)

To 10 mL of absolute methanol was added 10 mmol of sodium and then 4-methylpiperazin-1-yl biguanidine x 2HCl (5 mmol)[19] and the appropriate carboxylic acid ester (5 mmol). The reaction mixture was refluxed for 15-30 h and 10 mL of water was added and stirred in the room temperature for 0.5h. The precipitate was separated and crystallized from methanol.

4.1.2. 4-(4-methylpiperazin-1-yl)-6-phenyl-1,3,5-triazin-2-amine (3)

White solid. Mp. 171-174^{0}C. Yield:21% (280 mg). $C_{14}H_{18}N_6$ (MW 270.33). ^{1}H-NMR [DMSO-d_6]: δ=8.28 (m, 2H, Ph 2,6-*H*), 7.41-7.53 (m, 3H, Ph 3,4,5-*H*), 6.89 (br s, 2H, -N*H*$_2$), 3.78 (br s, 4H, Pp-2,6-*H*), 2.33 (t, 4H, *J*=4.87 Hz, Pp-3,5-*H*), 2.19 (s, 3H, C*H*$_3$). ^{13}C NMR [DMSO-d_6]: δ (ppm) 170.1, 167.7, 165.2, 137.4, 131.7, 128.6, 128.2, 54.9, 46.3, 43.0. IR (KBr) [cm^{-1}] ν= 3348 (br NH_2). LC/MS$^{+/-}$: purity: 100%, t_R=2.40,(ESI) *m/z* $[M+H]^+$ 271.19.

4.1.3. 4-(4-methylpiperazin-1-yl)-6-(2-chloro-phenyl)-1,3,5-triazin-2-amine (4)

White solid. Mp. 214-216^{0}C. Yield:5% (80 mg). $C_{14}H_{17}N_6Cl$ (MW 304.79). ^{1}H-NMR [DMSO-d_6]: δ=7.62-7.57 (m, 1H, Ph-3-*H*), 7.50-7.34 (m, 3H, Ph-4,5,6-*H*), 6.97 (br s, 2H, N*H*$_2$), 3.73-3.65 (m, 4H, Pp-2,6-*H*), 2.30-2.20 (br s, 4H, Pp-3,5-*H*), 2.17 (s, 3H, C*H*$_3$). ^{13}C NMR [DMSO-d_6]: δ (ppm) 172.0, 167.3, 164.7, 138.0, 131.2, 130.4, 127.3, 54.8, 46.2. IR (KBr) [cm^{-1}] ν= 3298, 3121 (br NH_2). LC/MS$^{+/-}$: purity: 100%, t_R=2.54, (ESI) *m/z* $[M+H]^+$ 305.16.

4.1.4. 4-(4-methylpiperazin-1-yl)-6-(3-chloro-phenyl)-1,3,5-triazin-2-amine (5)

White solid. Mp 196-198^{0}C. Yield:11% (160 mg). $C_{14}H_{17}N_6Cl$ (MW 304.79). ^{1}H-NMR [DMSO-d_6]: δ=8.25-8.21 (m, 1H-Ph-2-*H*), 8.21-8.19 (m, 1H, Ph-6-*H*), 7.60-7.55 (m, 1H, Ph-4-*H*), 7.49 (t, 1H, *J* = 7.7 Hz, Ph-5-*H*), 6.98 (br s, 2H, N*H*$_2$), 3.90-3.65 (br s, 4H, Pp-2,6-*H*), 2.40-2.30 (m, 4H, Pp-3,5-*H*), 2.19 (s, 3H, C*H*$_3$). IR (KBr) [cm^{-1}] ν= 3384 (br NH_2). ^{13}C NMR [DMSO-d_6]: δ (ppm) 168.8, 167.6, 165.2, 139.6, 133.6, 131.4, 130.7, 127.8, 126.8, 54.8, 46.2. LC/MS$^{+/-}$: purity: 99.7%, t_R=2.54, (ESI) *m/z* $[M+H]^+$ 305.25. Anal. Calcd for $C_{14}H_{17}N_6Cl$: C55.16, H5.62, N27.58; Found: C55.30, H5.69, N27.65.

4.1.5. 4-(4-methylpiperazin-1-yl)-6-(3-methyl-phenyl)-1,3,5-triazin-2-amine (6)

White solid. Mp 187-190^{0}C. Yield:11% (160 mg). $C_{15}H_{20}N_6$ (MW 284.36). ^{1}H-NMR [DMSO-d_6]: δ=8,05-8,08 (m, 2H, Ph 4,5-*H*), 7,31-7,34 (m, 2H, Ph-2,6-*H*), 6,86 (br s, 2H, -N*H*$_2$), 3,78 (br.s, 4H, Pp 3,5-*H*), 2,33 (t.def, 7H, Pp-3,5-*H* + PhC*H*$_3$), 2,19 (s, 3H, C*H*$_3$). ^{13}C

NMR [DMSO-d_6]: δ (ppm) 170.2, 167.6, 165.3, 137.7, 137.4, 132.3, 128.7, 128.5, 125.5, 54.9, 46.3, 43.0, 21.5. IR (KBr) [cm^{-1}] ν= 3323, 3140 (br NH_2). LC/$MS^{+/-}$: purity: 98.8%, t_R=2.93, (ESI) *m/z* $[M+H]^+$ 285.29. Anal. Calcd for $C_{15}H_{20}N_6$: C63.36; H7.09; N29.55; Found: C63.25; H7.20; N29.34.

4.1.6. 4-(4-methylpiperazin-1-yl)-6-(3-cyano-phenyl)-1,3,5-triazin-2-amine (7)

White solid. Mp 242-243^{0}C. Yield:13% (190 mg). $C_{15}H_{17}N_7$ (MW 295.34). ^{1}H-NMR [DMSO-d_6]: δ=8.61-8.53 (m, 2H, Ph-2,6-*H*), 7.99 (dt, J_1= 7.7 Hz, J_2 = 1.5 Hz, 2H, Ph-4-*H*), 7.69 (t, J_2=7.7 Hz, 1H, Ph-5-H), 7.04 (br s, 2H, NH_2), 3.80 (br s, 4H, Pp-2,6-*H*), 2.34 (def t, 4H, Pp-3,5-*H*), 2.20 (s, 3H, CH_3). ^{13}C NMR [DMSO-d_6]: δ (ppm) 168.3, 167.5, 165.08, 138.6, 135.0, 132.7, 131.6, 130.2, 119.1, 111.9, 54.8, 39.90, 46.2, 43.0. IR (KBr) [cm^{-1}] ν= 3431, 3294 (br NH_2). LC/$MS^{+/-}$: purity: 99.4%, t_R=2.82, (ESI) *m/z* $[M+H]^+$ 296.26. Anal. Calcd for $C_{15}H_{17}N_7$: C61.00, H5.80, N33.20; Found: C60.59, H5.84, N32.70.

4.1.7. 4-(4-methylpiperazin-1-yl)-6-(4-chloro-phenyl)-1,3,5-triazin-2-amine (8)

White solid. Mp 229-231^{0}C. Yield: 20% (300 mg). $C_{14}H_{17}N_6Cl$ (MW 304.79). ^{1}H-NMR [DMSO-d_6]: δ=8.30-8.20 (m, 2H, Ph-2,6-*H*), 7.60-7.45 (m, 2H, Ph-3,5-*H*), 6.94 (br s, 2H, NH_2), 3.90-3.65 (br s, 4H, Pp-2,6-*H*), 2.40-2.30 (m, 4H, Pp-3,5-*H*), 2.19 (s, 3H, CH_3). ^{13}C NMR [DMSO-d_6]: δ (ppm) 169.2, 167.6, 165.2, 136.4, 136.3, 130.0, 128.8, 54.8, 46.2. IR (KBr) [cm^{-1}] ν= 3322, 3138 (br NH_2). LC/$MS^{+/-}$: purity: 100%, t_R=3.60, (ESI) *m/z* $[M+H]^+$ 305.23. Anal. Calcd for $C_{14}H_{17}N_6Cl$: C55.16, H5.62, N27.58; Found: C54.79, H5.75, N27.59.

4.1.8. 4-(4-methylpiperazin-1-yl)-6-(4-fluoro-phenyl)-1,3,5-triazin-2-amine (9)

White solid. Mp 198-200^{0}C. Yield:15% (210 mg). $C_{14}H_{17}N_6F$ (MW 288.33). ^{1}H-NMR [DMSO- d_6]: δ= 8.36-8.29 (m, 2H, Ph-2,6-*H*), 7.29-7.24 (m, 2H, Ph-3,5-*H*), 6.91 (br s, 2H, NH_2), 3.90-3.65 (br s, 4H, Pp-2,6-*H*), 2.34-2.31 (m, 4H, Pp-3,5-*H*), 2.19 (s, 3H, CH_3). ^{13}C NMR [DMSO-d_6]: δ (ppm) 169.2, 167.6, 165.2, 133.9, 130.7, 130.6, 115.7, 115.4, 54.8, 46.2, 43.0. IR (KBr) [cm^{-1}] ν= 3318, 3138 (br NH_2). LC/$MS^{+/-}$: purity: 96.3%, t_R=2.83, (ESI) *m/z* $[M+H]^+$ 289.21.

4.1.9. 4-(4-methylpiperazin-1-yl)-6-(4-bromo-phenyl)-1,3,5-triazin-2-amine (10)

White solid. Mp 243-245^{0}C. Yield:17% (350 mg). $C_{14}H_{17}N_6Br$ (MW 349.23). ^{1}H-NMR [DMSO-d_6]: 8.20 (d, *J*= 8.7 Hz, 2H, Ph-2,6-*H*), 7.66 (d, *J*= 8.7 Hz, 2H, Ph-3,5-*H*), 6.95 (br s, 2H, NH_2), 3.78 (br s, 4H, Pp-2,6-*H*), 2.33 (t, *J*=4.9 Hz, 4H, Pp-3,5-*H*), 2.19 (s, 3H, CH_3). ^{13}C NMR [DMSO-d_6]: δ (ppm) 169.3, 167.6, 165.2, 136.7, 131.742.99, 46.22, 54.81, 125.44, 130.23, , IR (KBr) [cm^{-1}] ν= 3325, 3141 (br NH_2). LC/$MS^{+/-}$: purity: 100%, t_R=3.77, (ESI) *m/z* [M+] 349.24. Anal. Calcd for $C_{14}H_{17}N_6Br$: C48.15, H4.91, N24.06; Found: C48.15, H5.06, N24.09.

4.1.10. 4-(4-methylpiperazin-1-yl)-6-(4-iodo-phenyl)-1,3,5-triazin-2-amine (11)

Light yellow solid. Mp 242-245^{0}C. Yield:18% (360 mg). $C_{14}H_{17}N_6I$ (MW 396.23). ^{1}H-NMR [DMSO-d_6]: δ= 8.04 (d, *J*=8.7 Hz, 2H, Ph-2,6-*H*), 7.84 (d, *J*=8.5 Hz, 2H, Ph-3,5-*H*), 6.91 (br s, 2H, NH_2), 3.78 (br s, 4H, Pp-2,6-*H*), 2.33 (t, *J*=5.1Hz, 4H, Pp-3,5-*H*), 2.20 (s, 3H, CH_3). ^{13}C NMR [DMSO-d_6]: δ (ppm) 169.5, 167.6, 165.1, 137.6, 137.0, 130.2, 99.3, 54.8, 46.2. IR

(KBr) [cm^{-1}] ν= 3324, 3142 (br NH_2). LC/$MS^{+/-}$: purity: 98.6%, t_R=3.95, (ESI) *m/z* $[M+H]^+$ 397.23. Anal. Calcd for $C_{14}H_{17}N_6I$: C42.44, H4.32, N21.21; Found: C42.33, H4.37, N20.81.

4.1.11. 4-(4-methylpiperazin-1-yl)-6-(4-methylphenyl)-1,3,5-triazin-2-amine (12)

White solid. Mp. 216-219^{0}C. Yield:16% (223 mg). $C_{15}H_{20}N_6$ (MW 284.36). ^{1}H-NMR [DMSO-d_6]: δ=8.19 (d, *J*=8,1 Hz, 2H, Ph 2,6-*H*), 7.27 (d, *J*=8.0 Hz, 2H, Ph 3,5-*H*), 6.84 (br s, 2H, -N*H*$_2$), 3.79 (br s, 4H, Pp 2,6-*H*), 2.35 (m, 7H, Pp-3,5-*H* +Ph-C*H*$_3$), 2.21 (s, 3H, C*H*$_3$). ^{13}C NMR [DMSO-d_6]: δ (ppm) 170.1, 167.6, 165.2, 141.5, 134.7, 129.2, 128.2, 54.9, 46.3, 42.9, 21.5. IR (KBr) [cm^{-1}] ν= 3319 (br NH_2). LC/$MS^{+/-}$: purity: 100%, t_R=2.92, (ESI) *m/z* $[M+H]^+$ 285.29. Anal. Calcd for $C_{15}H_{20}N_6$: C63.36, H7.09, N29.55; Found: C63.92, H7.16, N29.43.

4.1.12. 4-(4-methylpiperazin-1-yl)-6-(4-trifluoromethylphenyl)-1,3,5-triazin-2-amine (13)

White solid. Mp 204-205^{0}C. Yield:6% (100 mg). $C_{15}H_{17}N_6F_3$ (MW 338.34). ^{1}H-NMR [DMSO-d_6]: δ=8.47 (d, 2H, *J*= 8.79 Hz, Ph-2,6-*H*), 7.85 (d, 2H, *J*= 8.75 Hz, 7.03 (br s, 2H, N*H*$_2$), 3.81 (br s, 2H, Pp-2,6-*H*), 2.36 (t, 4H, *J*=4.9 Hz, 4H, Pp-3,5-*H*), 2.21 (s, 3H, C*H*$_3$). ^{13}C NMR [DMSO-d_6]: δ (ppm) 168.9, 167.6, 165.1, 141.4, 141.3, 131.7, 131.3, 128.9, 126.4, 125.7, 125.6, 122.8, 54.8, 46.2, 43.0, 43.0. IR (KBr) [cm^{-1}] ν= 3336, 3145 (br NH_2). LC/$MS^{+/-}$: purity: 99.5%, t_R=4.10, (ESI) *m/z* $[M+H]^+$ 339.26. Anal. Calcd for $C_{15}H_{17}N_6F_3$: C53.25, H5.06, N24.84; Found: C53.03, H4.98, N25.11.

4.1.13. 4-(4-methylpiperazin-1-yl)-6-(4-cyanophenyl)-1,3,5-triazin-2-amine (14)

White solid. Mp. 208-211^{0}C. Yield 12% (170 mg). $C_{15}H_{17}N_7$ (MW 295.35). ^{1}H-NMR [DMSO-d_6]: δ=8.40 (dd, J_1= 8.5 Hz; J_2= 4.9 Hz, 2H, Ph-2,6-*H*), 7.93 (dd, J_1= 8.2 Hz, J_2 = 5.1 Hz, 2H, Ph-3,5-*H*), 7.05 (br s, 2H, N*H*$_2$), 3.80 (br s, 4H, Pp-2,6-*H*), 2,33 (def t, 4H, Pp-3,5-*H*), 2.19 (s, 3H, C*H*$_3$). LC/$MS^{+/-}$: (ESI) $[M+H]^+$ 296. Anal. Calcd for $C_{15}H_{17}N_7$: C61.00, H5.80, N33.20; Found: C60.62, H5.96, N32.96.

4.1.14. 4-(4-methylpiperazin-1-yl)-6-(4-(dimethylamino)phenyl)-1,3,5-triazin-2-amine (15)

White solid. Mp. 253-256 ^{0}C. Yield 4% (60 mg). $C_{16}H_{23}N_7$ (MW 313.40). ^{1}H-NMR [DMSO-d_6]: 8.11 (d, *J*= 8.98 Hz, 2H, Ph-2,6-*H*), 6.70 (d, *J*= 9.0 Hz, 2H, Ph-3,5-*H*), 6.66 (br s, 2H, N*H*$_2$), 3.76 (br s, 4H, Pp-2,6-*H*), 2.96 (s, 6H, N-(C*H*$_3$)$_2$), 2.31 (t, *J*=4.9 Hz, 4H, Pp-3,5-*H*), 2.19 (s, 3H, C*H*$_3$). ^{13}C NMR [DMSO-d_6]: δ (ppm) 170.2, 167.5, 165.2, 152.8, 129.7, 124.3, 111.3, 54.9, 46.2, 42.8, 39.9. IR (KBr) [cm^{-1}] ν= 3277, 3079 (br NH_2). LC/$MS^{+/-}$: purity: 99.6%, t_R=2.26, (ESI) *m/z* $[M+H]^+$ 314.40. Anal. Calcd for $C_{16}H_{23}N_7$: C61.32, H7.40, N31.28; Found: C61.47, H7.45, N31.19.

4.1.15. 4-(4-methylpiperazin-1-yl)-6-(3-chloro-4-methoxyphenyl)-1,3,5-triazin-2-amine (16)

White solid. Mp 233-235^{0}C. Yield:8% (130 mg). $C_{15}H_{19}N_6OCl$ (MW 334.81). ^{1}H-NMR [DMSO- d_6]: δ=8.25 (s, 1H, Ph-2-*H*), 8.21 (d, 2H, *J*= 8.5 Hz, Ph-6-*H*), 7.21 (d, 1H, *J* = 8.7 Hz, Ph-5-*H*), 6.98 (br s, 2H, N*H*$_2$), 3.91 (s, 3H, OC*H*$_3$), 3.90-3.65 (br s, 4H, Pp-2,6-*H*), 2.40-2.30 (m, 4H, Pp-3,5-*H*), 2.19 (s, 3H, C*H*$_3$). ^{13}C NMR [DMSO-d_6]: δ (ppm) 168.7, 167.5, 165.1, 157.3, 130.7, 129.5, 128.6, 121.3, 112.7, 56.8, 54.9, 46.3. IR (KBr) [cm^{-1}] ν= 3434 (br

NH_2). LC/$MS^{+/-}$: purity: 97.4%, t_R=3.37, (ESI) *m/z* $[M+H]^+$ 335.28. Anal. Calcd for $C_{15}H_{19}N_6OCl$: C53.81, H5.72, N25.10; Found: C53.73, H5.84, N25.19.

4.1.16. 4-(4-methylpiperazin-1-yl)-6-(3-chloro-6-methoxyphenyl)-1,3,5-triazin-2-amine (17)

White solid. Mp 198-200^{0}C. Yield:31% (520 mg). $C_{15}H_{19}N_6OCl$ (MW 334.81). ^{1}H-NMR [DMSO- d_6]: δ=7.45-7.39 (m, 2H, Ph-4,6-*H*), 7.08 (d, 1H, *J* = 9.5 Hz, Ph-3-*H*), 6.88 (br s, 2H, NH_2), 3.80-3.60 (m, 7H, Pp-2,6-*H* + OCH_3), 2.35-2.20 (m, 4H, Pp-3,5-*H*), 2,17 (s, 3H, CH_3). ^{13}C NMR [DMSO-d_6]: δ (ppm) 171.3, 167.1, 164.85, 156.4, 130.5, 130.3, 129.8, 124.2, 114.6, 56.6, 54.7, 46.2, 42.9. IR (KBr) [cm^{-1}] ν= 3358 (br NH_2). LC/$MS^{+/-}$: purity: 100%, t_R=2.35, (ESI) *m/z* $[M+H]^+$ 335.28. Anal. Calcd for $C_{15}H_{19}N_6OCl$: C53.81, H5.72, N25.10; Found: C53.46, H5.80, N24.85.

4.1.17. 4-(4-methylpiperazin-1-yl)-6-(3,4-dichlorophenyl)-1,3,5-triazin-2-amine (18)

White solid. Mp. 214-216^{0}C. Yield:3% (40 mg). $C_{14}H_{16}N_6Cl_2$ (MW 339.22). ^{1}H-NMR [DMSO-d_6]: δ=8.39 (d, *J*=2.1 Hz, 1H, Ph-2-*H*), 8.21 (dd, *J*=10.1 Hz, *J*=2.1 Hz, 1H, Ph-6-*H*), 7.73 (d, *J*=8.5 Hz, 1H, Ph-5-*H*), 7.01 (br s, 2H, -NH_2), 3.78 (br s, 4H, Pp-3,5-*H*), 2.33 (t, *J*=4.2 Hz, 4H, Pp-3,5-*H*), 2.19 (s, 3H, CH_3). ^{13}C NMR [DMSO-d_6]: δ (ppm) 168.1. 167.5, 165.1, 138.1, 134.3, 131.6, 131.1, 129.7, 128.2, 54.8, 46.2, 43.0. IR (KBr) [cm^{-1}] ν= 3371 (br NH_2). LC/$MS^{+/-}$: purity: 100%, t_R=4.37, (ESI) *m/z* $[M+H]^+$ 339.20.

4.1.18. 4-(4-methylpiperazin-1-yl)-6-(2,6-difluorophenyl)-1,3,5-triazin-2-amine (19)

White solid. Mp. 218-219^{0}C. Yield 3% (40 mg). $C_{14}H_{16}N_6F_2$ (MW 306.32). ^{1}H-NMR [DMSO-d_6]: δ=7.50 (m, 1H, Ph-4-*H*), 7.03 (m, 4H, Ph-3,5-*H* + NH_2), 3.68 (br s, 4H, Pp-2,6-*H*), 2.29 (br s, 4H, Pp-3,5-*H*), 2.18 (s, 3H, CH_3).). ^{13}C NMR [DMSO-d_6]: δ (ppm) 167.0, 166.4, 164.6, 161.6, 161.5, 158.2, 131.5, 112.5, 112.1, 54.7, 46.2, 42.9. IR (KBr) [cm^{-1}] ν= 3328, 3157 (br NH_2). LC/$MS^{+/-}$: purity: 98.9%, t_R=2.28, (ESI) *m/z* $[M+H]^+$ 307.29.

4.1.19. 4-(4-methylpiperazin-1-yl)-6-(3,5-difluorophenyl)-1,3,5-triazin-2-amine (20)

White solid. Mp. 225-227^{0}C. Yield:5% (72 mg). $C_{14}H_{16}N_6F_2$ (MW 306.32). ^{1}H-NMR [DMSO-d_6]: δ=7.89-7.82 (m, 2H, Ph-2,6-*H*), 7-46-7.37 (m, 1H, Ph-4-*H*), 7.03 (br s, 2H, NH_2), 3.80 (br s, 4H, Pp-2,6-*H*), 2.33 (t, *J* = 4.87 Hz, 4H, Pp-3,5-*H*), 2.19 (s, 3H, CH_3). ^{13}C NMR [DMSO-d_6]: δ (ppm) 167.9, 165.1, 164.4, 161.2, 141.6, 111.1, 110. 8, 107.0, 54.8, 46.2, 43.1. IR (KBr) [cm^{-1}] ν= 3386 (br NH_2). LC/$MS^{+/-}$: purity: 100%, t_R=3.51, (ESI) *m/z* $[M+H]^+$ 307.29. Anal. Calcd for $C_{14}H_{16}N_6F_2$: C54.89; H5.27; N27.42; Found: C54.62; H5.02; N27.72.

4.1.20. 4-(4-methylpiperazin-1-yl)-6-(3,4,5-trifluorophenyl)-1,3,5-triazin-2-amine (21)

White solid. Mp. 186-188^{0}C. Yield 3% (25 mg). $C_{14}H_{15}N_7F_3$ (MW 324.29). ^{1}H-NMR [DMSO-d_6]: δ=8.04 (m, 2H, Ph-2,6-***H***), 7.05 (br s, 2H, NH_2), 3.78 (br s, 4H, Pp-2,6-***H***), 2.32 (t, *J*=4.9 Hz, 4H, Pp-3,5-***H***), 2.19 (s, 3H, C$\boldsymbol{H_3}$). ^{13}C NMR [DMSO-d_6]: δ (ppm) 167.4, 165.0, 152.4, 149.1, 134.4, 112.6, 112.3, 112.3, 54.8, 46.1, 43.0. LC/$MS^{+/-}$: purity: 96.2%, t_R=3.94, (ESI) *m/z* $[M+H]^+$ 325.24.

4.1.21. 4-(4-methylpiperazin-1-yl)-6-(3,5-dimethylphenyl)-1,3,5-triazin-2-amine (22)

White solid. Mp.156-160^{0}C. Yield 8% (129 mg). $C_{16}H_{22}N_6$ (MW 299.39). ^{1}H-NMR [DMSO-d_6]: δ=7.88 (s, 2H, Ph-2,6-*H*), 7.12 (s, 2H, Ph-4-*H*), 6.86 (br s, 2H, -N*H*$_2$), 3.77 (br s, 4H, Pp 2,6-H), 2.30 (m, 10H, Pp-3,5-*H* + Ph-3,5-C*H*$_3$), 2.19 (s, 3H, C*H*$_3$). ^{13}C NMR [DMSO-d_6]: δ (ppm) 175.1, 172.3, 167.0, 142.3, 142.1, 137.8, 130.8, 59.6, 51.0, 47.7, 44.7, 26.2. IR (KBr) [cm^{-1}] ν= 3378 (br NH$_2$). LC/MS$^{+/-}$: purity: 100%, t_R=3.47, (ESI) *m/z* $[M+H]^+$ 299.31. Anal. Calcd for $C_{16}H_{22}N_6$: C64.40, H7.43, N28.16; Found: C64.37, H7.76, N27.70.

4.1.22. 4-(4-methylpiperazin-1-yl)-6-(3,4-dimethylphenyl)-1,3,5-triazin-2-amine (23)

White solid. Mp. 223-226^{0}C. Yield 18% (259 mg). $C_{16}H_{22}N_6$ (MW 299.39). ^{1}H-NMR [DMSO-d_6]: δ=7.88 (s, 2H, Ph-2,6-*H*), 7.12 (s, 2H, Ph-4-*H*), 6.86 (br s, 2H, -N*H*$_2$), 3.77 (br s, 4H, Pp 2,6-*H*), 2.30 (m, 10H, Pp-3,5-*H* + Ph-3,4-C*H*$_3$), 2.19 (s, 3H, C*H*$_3$). ^{13}C NMR [DMSO-d_6]: δ (ppm) 170.2, 167.6, 165.3, 140.2, 136.3, 135.0, 129,8, 129.2, 125.9, 54.9, 46.3, 20.0. IR (KBr) [cm^{-1}] ν= 3289 (br NH$_2$). LC/MS$^{+/-}$: purity: 100%, t_R=3.27, (ESI) *m/z* $[M]^+$ 299.31. Anal. Calcd for $C_{16}H_{22}N_6$: C64.40, H7.43, N28.16; Found: C64.28, H7.46, N27.98.

4.2 Pharmacology

4.2.1. *In vitro* [^{3}H]histamine binding assay on *h*H$_4$R

Before the experiments, cell membranes were sedimented by a 10-min centrifugation at +4°C and 16,000 × *g* and resuspended in binding buffer (12.5 mM $MgCl_2$, 1 mM EDTA and 75 mM Tris/HCl, pH 7.4). Competition binding experiments were carried out by incubating membranes, 35-40 μg/well (prepared from Sf9 cells transiently expressing hH$_4$R, co-expressed with G- protein $G\alpha_{i2}$ and $G\beta_1\gamma_2$ subunits) in a final volume of 200 μL containing binding buffer and [^{3}H]histamine (10 nM). Assays were run in triplicates with four to seven appropriate concentrations between 0.1 nM and 100 μM of the test compound. Incubations were performed for 60 min at room temperature and shaking at 250 rpm. Non-specific binding was determined in the presence of 10 μM unlabeled JNJ7777120. Bound radioligand was separated from free radioligand by rapid filtration through GF/B filters pretreated with 0.3% (mass/vol) polyethylenimine (PEI) solution and washed three times with 0.3 mL of ice-cold binding buffer (+4°C). The amount of radioactivity collected on the filter was determined by liquid scintillation counting. Competition binding data were analyzed by the software GraphPad Prism™ (version 3.02, San Diego, CA, USA) using non-linear least squares fit. Affinity values (K_i) were expressed as mean ± standard deviation (SD) and mean absolute deviation (MD). K_i values were calculated from the IC_{50} values according to Cheng–Prusoff equation[36].

4.2.2. cAMP accumulation assay in cells expressing *h*H$_4$R

Intracellular cAMP accumulation was measured with homogenous TR-FRET immunoassay, using LANCE *Ultra* cAMP kit (PerkinElmer). Frozen *γ*-irradiated recombinant CHO cells, expressing the human histamine H_4 receptor were thawed completely in a 37°C water bath and resuspended in stimulation buffer (HBSS, 100μM RO-201724, 5mM HEPES, 0.1% BSA, pH 7.4). An antagonist dose-response experiments were performed in a total assay volume of 20 μl in white 384-well plates, using 600 cells/well. Cell stimulation was performed for 30 min at room temperature, and histamine (140 nM), forskolin (10 μM) and

antagonists in appropriate concentrations (in range 3-100 μM) were added simultaneously to cell suspension. After incubation, five microliters of europium (Eu) chelate-labeled cAMP tracer and 5μl of U*Light*-labeled anti-cAMP mAb working solutions were added, mixed and incubated for 1 h. TR-FRET signal was read on an EnSpire microplate reader (PerkinElmer). Measured TR-FRET signal was translated into actual quantities of produced cAMP on the basis of cAMP standard curve and obtained results were presented as % of maximal response. Sigmoidal dose-response curve fitting was performed with use of GraphPad Prism™ software (version 5.01, San Diego, CA, USA). Showed results represent the mean of three separate experiments, each performed in triplicates.

4.2.3. *In vitro* [^{3}H]N^{α}-methylhistamine binding assay on *h*H_3R

Prior to the binding experiments, thawed cell membranes were homogenized by sonication in ice-cold binding buffer (12.5 mM $MgCl_2$, 100 mM NaCl and 75 mM Tris/HCl, pH 7.4). Competition binding experiments were carried out in total volume of 200μl per sample. [^{3}H]N^{α}-methylhistamine (2 nM) was incubated with HEK293-*h*H_3R cells membranes (20–25 μg/well) and different concentrations of the tested compound. Assays were run at least in duplicates with seven appropriate concentrations of investigated ligand, spanning from 0.01 nM to 100 μM. Samples were incubated for 90 min at 25 °C with shaking (250 rpm). Non-specific binding was determined in the presence of selective histamine H_3 receptor inverse agonist/antagonist - pitolisant (10 μM). The bound radioligand was separated from free radioligand by filtration through GF/B filters, pre-treated with 0.3% (m/v) PEI, followed by three washing steps with 0.3 ml/well of ice-cold washing buffer (50 mM Tris/HCl, 120 mM NaCl, pH 7.4). Competition binding data were analyzed similarly as for H_4R affinity studies, utilizing GraphPad Prism™ software non-linear least squares fit (version 3.02, San Diego, CA, USA) and Cheng–Prusoff equation[36].

4.2.4. *In vivo* Anti-inflammatory activity

The activity of compounds was determined *in vivo* using the Carrageenan-Induced Edema Model in mice. Male albino Swiss mice (18-25 g) were used for these studies. The animals were housed and fed in a laboratory kept at constant temperature of 22°C under the standard conditions (12:12 h L:D cycle, standard pellet diet, tap water). Each experimental group consisted of 8 animals/dose and all the animals were used only once. Treatment of the used laboratory animals in the present study was in full accordance with the respective Polish and European regulations and was approved by the Local Ethics Committee at the Jagiellonian University, Cracow, Poland.

4.2.4.1. Determination of anti-inflammatory activities of investigated compounds

Male Swiss albino mice (18–25 g) were used in hind paw edema test. Mice were divided into four groups, one of them being the control. In order to produce inflammation, 0.1 ml of 1% carrageenan solution in water was injected into hind paws subplantar tissue of mice, according to the modified method of Winter[23] and Lence[24]. The development of paw edema was measured with a plethysmometr (Plethysmometr 7140, Ugo Basile). Prior to this administration, paw diameters were measured by dividers and recorded. The investigated

compounds were administered at doses of 10, 25, 50 mg/kg, intraperitonally (as a suspension in methylcellulose), prior to carrageenan injection. Methylcellulose was administered by the same route, to the control group (methylcellulose had no effect on edema, data not shown). After these administrations, paw diameters were measured at 1, 2, and 3 hours, % of edema and edema inhibition was calculated according to the formulas given below.

Edema % = (N'×100)/N.

Edema inhibition % = (N–N'×100)/N.

N: paw diameters measured 1, 2 and 3 hours after injection of carrageenan to the control group – paw diameters at the beginning.

N': paw diameters measured 1, 2, and 3 hours after injection of carrageenan to the test groups – paw diameters at the beginning.

Data are expressed as mean ± SEM (Table 2; supplemental material)**.** A value of $P < 0.05$ was considered statistically significant. The obtained data were evaluated by the Student's t-test for grouped data. The software package GraphPad Prism™ (version 6.0, San Diego, CA, USA) was used to process data.

4.2.5. Antiproliferative assay

4.2.5.1 Cell lines

HEK-293 and IMR-32 cell lines were cultured in Dulbecco's Modified Eagle's Medium - DMEM (Gibco). Complete growth media contained 10 % fetal bovine serum (FBS), 100 $mg \cdot mL^{-1}$ streptomycin and 100 $U \cdot mL^{-1}$ penicillin. Cells were cultured at 37°C in an atmosphere containing 5% CO_2. Neuroblastoma IMR-32 cell line was provided by Department of Oncogenomics, Academisch Medisch Centrum, Amsterdam, Holland. Human embryonic kidney HEK-293 cell line (ATCC CRL-1573) was kindly donated by Prof. Dr. Christa Müller (Pharmaceutical Institute, Pharmaceutical Chemistry I, University of Bonn).

4.2.5.2 *In vitro* antiproliferative assay

The cells were seeded in 96-well plates at a concentration of 2×10^4 cells/well (IMR-32) or 1.5×10^4 cells/well (HEK-293) in 200 µl culture medium and routinely cultured for 24 h to reach 60 % confluence. Next, the stock solutions of examined compounds in DMSO were diluted into fresh growth medium and added into the microplates at the final concentrations 0.01 µM – 250 µM. The maximal DMSO concentration did not exceed 1%. After 48 h of incubation 20 µl of EZ4U labeling mixture (EZ4U Non-radioactive cell proliferation and cytotoxicity assay**,** Biomedica) was added to the each well and the cells were incubated under the same conditions for 5 h. The absorbance of the samples was measured using a microplate reader (PerkinElmer) at 492 nm. The activity of the standard drug doxorubicin (DX) was estimated in the same way at the concentrations: 0.001-50 µM for IMR-32 cells and at 0.005-100 µM for HEK-293 cells. GraphPad Prism™ software (version 5.01, San Diego, CA, USA) was used to calculate the IC_{50} values.

4.3. Physicochemical studies

4.3.1. Metabolic stability

4.3.1.1. *In silico* study

The metabolic biotransformation of H_4R ligands **8** and **10** was studied *in silico* by using computational procedure MetaSite 4.1.1 provided by Molecular Discovery Ltd. The potential sites of metabolism were analyzed using either liver or cytochrome CYP3A4 computational model exclusively.

4.3.1.2. *In vitro* CYP3A4 P450-Glo™ Assay

The luminescent CYP3A4 P450-Glo™ Assay was purchased from Promega. The CYP3A4 inhibitor ketoconazole was purchased from Sigma-Aldrich. The enzymatic reactions were performed in white polystyrene, nontreated, flat-bottom multiwall ½ AreaPlate™ - 96 (PerkinElmer). The luminescence signal was measured with a microplate reader in luminescence mode (PerkinElmer). The CYP3A4 P450-Glo™ assays were performed according to the manufacturer's procedure. The mixture consisting 0.5 pmol of CYP3A4 membranes and 4X Luciferin-PPXE in 100mM Tris-HCl was titrated in 96-well plate. Next, an equal volume of the test compound or Luciferin-Free Water or ketoconazole (inhibition control) was added to give one-half of the final reaction volume. After the 10-minute pre-incubation one-half of the final volume of 2X NADPH regeneration system was added to initiate CYP3A4 reaction. The final concentrations of TR7 and TR18 were 0.025 μM – 25 μM, the CYP3A4 inhibitor ketoconazole 0.025 μM - 10 μM and Luciferin-PPXE 25 mM. The total volume of DMSO did not exceed of recommended by manufacturer 0.2 %. The reaction mixture with inactive control membranes (control) was prepared simultaneously as was described above. The reaction mixture was incubated at 37 °C for 30 minutes. Afterwards, to initiate the luminescence the reconstituted Luciferin Detection Reagent containing firefly luciferase was added. The luminescence was measured after 20 minutes incubation of the reaction mixture at room temperature. For calculation the total luminescence the average luminescence of the control reaction containing inactive membranes was subtracted from the luminescence of CYP3A4 containing reactions. The luminescence of the reactions containing Luciferin-Free Water instead of the tested compound indicated the total (100%) CYP3A4 activity.

4.3.2. X-ray crystal structures determination

The relevant crystals were obtained from methanol solutions. Pertinent crystallographic parameters are summarized in Table 3 and selected metric parameters are presented in Table 4 (supplemental material). The structures were solved by direct methods and refined with SHELXTL[37]. E-map provided positions for all non-H-atoms. The full-matrix least-squares refinement was carried out on F^2's using anisotropic displacement factors for all non-H-atoms. All C-bound H atoms were placed in idealized locations and were refined using a riding model, with C–H = 0.93 Å and $U_{iso}(H) = 1.2U_{eq}(C)$. The H-atoms attached to nitrogens were located in difference Fourier map and refined with the restraints N-H = 0.86 Å and $U_{iso} = 1.2U_{eq}(N)$.

Further details on the CIF files are available from the Cambridge Crystallographic Data Center, 12 Union Road, Cambridge CB2 1EZ quoting the deposition numbers CCDC 913574 & 913575 (Fax: Int code + (1223)336-033; E-mail: deposit@ccdc.cam.ac.uk).

Crystal data for **8**: C_{14} H_{17} N_6 Cl_5, M = 304.79, monoclinic, space group $P2_1/c$, a = 6.4519(4) Å, b = 16.5378(14) Å, c = 13.9923(10) Å, β= 91.056(7)°, V = 1492.73(19) $Å^3$, Z = 4, D_x = 1.356 g cm^{-3}, T = 293 K, μ = 0.259 mm^{-1}, λ = 0.71073 Å, data/parameters = 2649/ 191; final R_1 = 0.0678.

Crystal data for **17**: C_{15} H_{19} N_6 O Cl S, M = 334.81, monoclinic, space group Cc, a = 12.9909(5) Å, b = 18.2448(7) Å, c = 7.3449(4) Å, β = 113.968(5)°, V = 1590.75(14)$Å^3$, Z = 4, D_x = 1.398 g cm^{-3}, T = 293 K, μ = 0.255 mm^{-1}, λ = 0.71073 Å, data/parameters = 2607/ 211; final R_1 = 0.0258.

4.3.3. *In silico* molecular and docking studies

4.3.3.1. Homology model

Histamine H_4 receptor homology model used in this studies was built on the basis of previously described and published crystal structure of histamine H_1 receptor (PDB entry: 3RZE), paying attention to mutagenesis data described by Jongejan et al.[32].

After the alignment of sequences, a total of 100 models was obtained using Modeller[38]. Models were then fitted to H_1R crystal structure using Schrödinger software[39]. Missing side chains were added using Prime module, H-bonds optimization and energy minimization (using OPLS2005 forcefield) was then performed using Protein Prepararion Wizard implemented in Schrödinger suite. Structures evaluation and stereochemical analyses were performed using PROCHECK[40], and Ramachandran plots. Further docking studies allowed to choose one model used for docking studies. Obtained model lacks the large intracellular loop, due to its length difference in desired (H_4R) and template (H_1R) model.

4.3.3.2. Ligands

For this study two crystal structures of ligands, **5** and **18** were used. For the tested set of compounds energetically optimal conformers were found using ConfGen and prepared using LigPrep module. For all of the structures 5 energetically best conformations were used for docking. All of the tested compounds were used in their *N*-protonated form.

Receptor grid was generated by GlideGrid module and validated with known histamine H_4 receptor ligands 4-methylhistamine and JNJ 7777120, according to the procedure described by Feng[33]. Docking studies were performed *via* GlideDock module. Results were interpreted by the means of Docking Score functions. Receptor-ligand interactions were visualized using PyMOL[41].

Acknowledgments

We grateful thank Prof. R. Seifert (Hannover, Germany) for providing S*f*9 cells and baculovirus stock solutions encoding for the human histamine H_4 receptor and G-protein $G_{\alpha i2}$ and $G_{\beta 1\gamma 2}$ subunits.

The authors acknowledge the partial support of ESF COST Action BM0806 'Recent advances in histamine receptor H_4R research', financed by EU-FP7, of Grant No. 594/N-COST/2009/0, National Science Center, granted on the basis of decision No DEC-2011/02/A/NZ4/00031, of the European COST Actions BM1007, CM1103, CM1207, of Else Kröner-Fresenius Foundation (EKFS), Research Training Group Translational Research Innovation – Pharma (TRIP), of Fraunhofer-Institut für Molekularbiologie und Angewandte Ökologie IME, Projektgruppe Translationale Medizin und Pharmakologie TMP (Fh-TMP), and that of LOEWE OSF.

References

1. E. Zampeli, E. Tiligada, The role of histamine H_4 receptor in immune and inflammatory disorders. Br. J. Pharmacol. 157 (2009) 24-33.
2. E. Tiligada, E. Zampeli, K. Sander, H. Stark, Histamine H_3 and H_4 receptors as novel drug targets. Expert Opin. Investig. Drugs 18 (2009) 1519-31.
3. H. Engelhardt, R.A. Smits, R. Leurs, E. Haaksma, I.J.P. de Esch, A new generation of anti-histamines: histamine H_4 receptor antagonists on their way to the clinic. Curr. Opin. Drug Discov. Devel. 12 (2009) 628-43.
4. C.M. Marson, Targeting the histamine H_4 receptor. Chem. Rev. 111 (2011) 7121-56.
5. C. Saravanan, S.K. Bharti, S. Jaggi, S.K. Singh, Histamine H_4 receptor: a novel target for inflammation therapy. Mini Rev. Med. Chem. 11 (201) 143-58.
6. D. Łażewska, K. Kieć-Kononowicz, Azines as histamine H_4 receptor antagonists. Front. Biosci. (Schol. Ed) 4 (2012) 967-87.
7. R. Kiss, G.M. Keserű, Histamine H_4 receptor ligands and their potential therapeutic applications: an update. Expert Opin. Ther. Pat. 22 (2012) 205-21.
8. www.palaupharma.com
9. www.ziarcopharma.com
10. M. Saleh, S. Abbott, V. Perron, C. Lauzon, C. Penney, B. Zacharie, Synthesis and antimicrobial activity of 2-fluorophenyl-4,6-disubstituted [1,3,5]triazines. Bioorg. Med. Chem. Lett. 20 (2010) 945-9.
11. R.V. Patel, P. Kumari, K.H. Chikhalia, Microwave assisted synthesis and determination of in-vitro antimicrobial efficacy of well characterized s-triazinyl piperazines and piperidines. Acta Pol. Pharm. 69 (2012) 423-32.
12. H. Ojha, P. Gahlot, A.K. Tiwari, M. Pathak, R. Kakkar, Quantitative structure activity relationship study of 2,4,6-trisubstituted-s-triazine derivatives as antimalarial inhibitors of Plasmodium falciparum dihydrofolate reductase. Chem. Biol. Drug Des. 77 (2011) 57-62.
13. F. Sączewski, A. Bułakowska, P. Bednarski , R. Grunert, Synthesis and anticancer activity of novel 2,4-diamino-1,3,5-triazne derivatives. Eur. J. Med. Chem. 41 (2006) 219-25.
14. Z. Hu, T. Ma, Z. Chen, Z. Ye, G. Zhang, Y. Lou, Y. Yu, Solid-phase synthesis and antitumor evaluation of 2,4-diamino-6-aryl-1,3,5-triazines. J. Comb. Chem. 11 (2009) 267-73.
15. B. Zacharie, S.D. Abbott, J.-F. Bienvenu, A.D. Cameron, J. Cloutier, J-S. Duceppe, A. Ezzitouni, D. Fortin, K. Houde, C. Lauzon, N. Moreau, V. Perron, N. Wilb, M. Asselin, A. Doucet, M-E. Fafardf, D. Gaudreau, B. Grouix, F. Sarra-Bournet, N. St-Amant, L. Gagnon, C.L. Penney, 2,4,6-trisubstituted triazines as protein a mimetics for the treatment of autoimmune diseases. J. Med. Chem. 53 (2010) 1138-54.
16. G. Blotny, Recent applications of 2,4,6-trichloro-1,3,5-triazine and ist derivatives in organic synthesis. Tetrahedron 62 (2006) 9507-9522.
17. M. Gaul, B. Zhao, X. Zhu, Substituted nitrogen-containing heteroaryl derivatives useful as modulators of the histamine H_4 receptor. (Janssen Pharmaceutica). WO2009035671 (2009).
18. R.J. Altenbach, R.M. Adair, B.M. Bettencourt, L.A. Black, S.R. Fix-Stezel, S.M. Gopalakrishnan, G.C. Hsieh, H. Liu, K.C. Marsh, M.J. McPherson, I. Milicic, T.R. Miller, T.A. Vortherms, U. Warrior, J.M. Wetter, N. Wishart, D.G. Witte, P. Honore, T.A. Esbenshade, A.A. Hancock, J.D. Brioni, M.D. Cowart, Structure-activity studies on a series of a 2-aminopyrimidine-containing histamine H_4 receptor ligands. J. Med. Chem. 51 (2008) 6571-6580.

19. Z. Brzozowski, Z. Kamiński, I. Kozakiewicz, S. Angielski, J. Rogulski, Synthesis and hypoglycemic activity of various N-(2-pyrazoline-1-carbaimidoyl)-guanidine derivatives. Acta Pol. Pharm. 36 (1979) 401-410.
20. K. Kulig, M. Ignasik, B. Malawska, Synthesis of 3,3- and 4,4-alkyl-phenyl-substituted pyrrolidin-2-one derivatives. Pol. J. Chem. 83 (2009) 1629-36.
21. Z. Brzozowski, F. Sączewski, M. Gdaniec, Synthesis, structural characterization and antitumor activity of novel 2,4-diamino-1,3,5-triazine derivatives. Eur. J. Med. Chem. 35 (2000) 1053-64.
22. L.B. Hough, Genomics meets histamine receptors: new subtypes, new receptors. Mol. Pharmacol. 59 (2001) 415-419.
23. C.A. Winter, E.A. Risley, G.W. Nuss, Carrageenin-induced edema in hind paw of the rat as an assay for anti-inflammatory drugs. Proc. Soc. Exp. Boil. Med. 111 (1962) 544-547.
24. P. Lence, A new device for plethysmoscopic measuring of small objects. Arch. Int. Pharmacodyn. 136 (1962) 237-240.
25. E.H. Kerns, L. Di, Drug-like properties: Concepts, structure design and methods. M.A. Burlington, Academic Press.
26. R. Smith, Animal research: the need for a middle ground: Let's promote the three Rs of animal research: replacement, reduction, and refinement. BMJ.322 (2001) 248-249.
27. A.S. Narang, D.S. Desai (2009). Anticancer drug development. Pharmaceutical Perspectives of Cancer Therapeutics (pp. 49-92). Springer US.
28. G. Cruciani, E. Carosati, B. De Boeck, K. Ethirajulu, C. Mackie, T. Howe, R. Vianello, MetaSite: understanding metabolism in human cytochromes from the perspective of the chemist. J Med Chem.48 (2005) 6970-6979.
29. D. Boyer, J.N. Bauman, D.P. Walker, B. Kapinos, K. Karki, A.S. Kalgutkar, Utility of MetaSite in improving metabolic stability of the neutral indomethacin amide derivative and selective cyclooxygenase-2 inhibitor 2-(1-(4-chlorobenzoyl)-5-methoxy-2-methyl-1H-indol-3-yl)-N-phenethyl-acetamide. Drug Met Disp. 37 (2009) 999-1008.
30. P. Anzenbacher, E. Anzenbacherova, Cytochromes P450 and metabolism of xenobiotics. Cell Mol Life Sci. 58 (2001) 737-747.
31. J.J. Cali, D. Ma, M. Sobol, D.J. Simpson, S. Fracjman, T.D. Good, W.J. Daily, D. Liu, Luminogenic cytochrome P450 assays. Expert Opin Drug Metab Toxicol. 2 (2006) 629-645.
32. A. Jongejan, H.D. Lim, R.A. Smits, I.J.P. de Esch, E. Haaksama, R. Leurs, Delineation of agonist binding to the human histamine H_4 receptor using mutational analysis, homology modeling, and *ab initio* calculations. J. Chem. Inf. Model. 48 (2008) 1455-1463.
33. Z. Feng, T. Hou, Y. Li, Docking and MD study of histamine H_4R based on the crystal structure of H_1R. J. Mol. Graph. Model. 39 (2013) 1-12.
34. S. Schultes, S. Nijmeijer, H. Engelhardt, A.J. Kooistra, H.F. Vischer, I.J.P. de Esch, E.E.J. Haaksma, R. Leurs, C. de Graaf. Mapping histamine H_4 receptor-ligand binding modes. Med. Chem. Commun. 4 (2013) 193-204.
35. J.S. Surgand, J. Rodrigo, E. Kellenberger, D. Rognan, A chemogenomic analysis of the transmembrane binding cavity of human G-Protein-Coupled Receptors. Proteins 62 (2006) 509-538.
36. Y.C. Cheng, W.H. Prusoff, Relationship between the inhibition constant (K1) and the concentration of inhibitor which causes 50 per cent inhibition (I50) of an enzymatic reaction. Biochem. Pharmacol. 22 (1973) 3099-3108.
37. G.M. Sheldrick, A short history of SHELX. Acta Crystallogr. Sect A 64 (2008) 112-122.
38. Modeller 9.11; http://salilab.org/modeller/; (Accessed November 5th 2013)
39. Schrödinger Maestro Version 9.3.5, Schrödinger, LLC
40. R.A. Laskowski, J.A.C. Rullmann, M.W. MacArthur, R. Kaptein, J.M. Thornton. AQUA and PROCHECK-NMR: Programs for checking the quality of protein structures solved by NMR. J. Mol. NMR 8 (1996) 477-486.
41. PyMOL(TM), Version 1.4.1. Schrödinger, LLC

Table 1. Histamine H_4R affinities of synthesized compounds **3-23**.

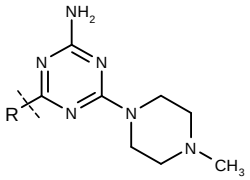

No	R	Histamine H_4R affinity[a] K_i [nM] ± SD (MD)	n[(m)]
3		1099 ± 485 (345)	**3**[(3)]
4		1261 ±332 (235)	**2**[(2)]
5	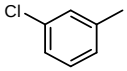	408 ± 134 (99)	**3**[(3)]
6	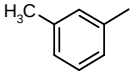	1747 ± 1500 (1061)	**2**[(2)]
7	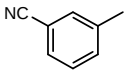	5161 ± 2440 (1726)	**1**[(2)]
8[b]	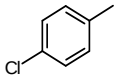	203 ± 65 (47)	**3**[(3)]
9	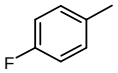	378 ± 96 (73)	**3**[(3)]
10[c]	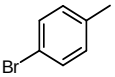	524 ± 225 (159)	**2**[(2)]
11	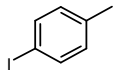	2391 ± 1477 (1044)	**1**[(2)]
12	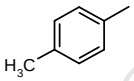	431 ± 99 (72)	**2**[(4)]
13	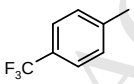	4239 ± 673 (477)	**1**[(2)]
14	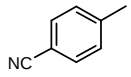	2358 ± 1277 (903)	**1**[(2)]
15	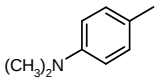	64490 ± 31396 (22200)	**2**[(2)]
16	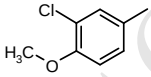	1472 ± 57 (41)	**2**[(2)]
17	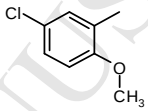	6007 ± 1538 (1088)	**2**[(3)]
18	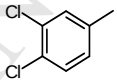	790 ± 320 (226)	**3**[(3)]
19	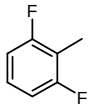	5077 ± 445 (315)	**1**[(2)]
20	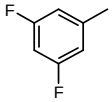	1191 ± 71 (50)	**1**[(2)]
21	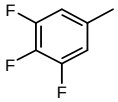	1787 ± 71 (50)	**1**[(2)]
22	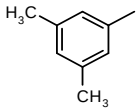	10567 ± 5110 (3614)	**1**[(2)]
23	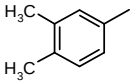	834 ± 494 (379)	**2**[(3)]

[a] [^{3}H]Histamine displacement with membrane preparation of Sf9 cells expressing human histamine H_4 receptor, co-expressed with G protein $G\alpha_{i2}$ and $G\beta_1\gamma_2$ subunits. Each determination was performed with four or seven different concentration points (initial screening with four concentration points with at least two independent measurements, for compounds with good affinity values, i.e. K_i < 1000 nM, seven concentration points in at least three independent experiments were performed) ranging from 0.01 nM to 100 μM test compound concentration in triplicates.

SD: standard deviation; MD: mean absolute deviation; n: number of experiments in triplicates, m: number of measurements

[b] K_i value of **8** at human histamine H_3 receptor: 13.2 ± 0.8 μM

[c] K_i value of **10** at human histamine H_3 receptor: 15.0 ± 2.2 μM

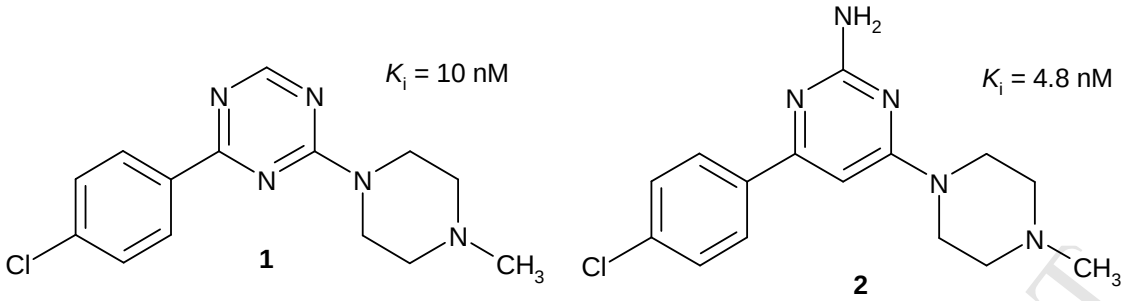

Figure 1. Structures and H_4R affinities of (4-methylpiperazin-1-yl)-1,3,5-triazine (**1**[17]) and -pyrimidine-2-amine derivatives (**2**[18]).

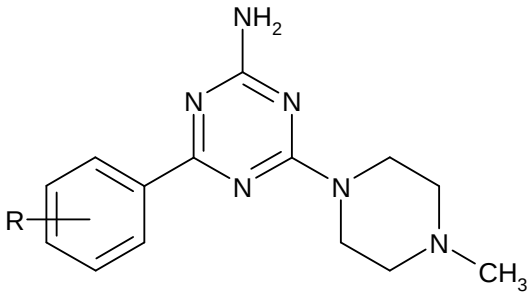

R= mono/di/trisubstituted with F, Cl, Br, I, CH_3, CF_3, CN, OCH_3, $N(CH_3)_2$

Figure 2. General structure of synthesized compounds.

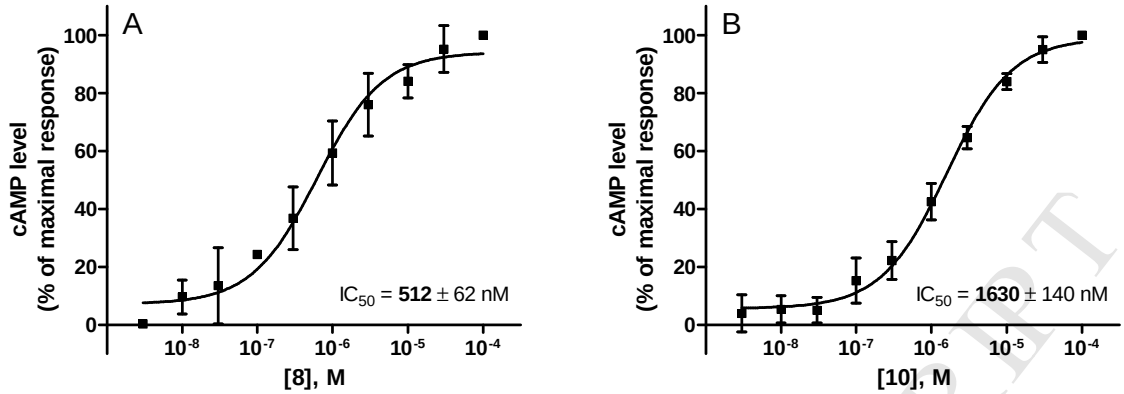

Figure 3. cAMP accumulation studies in CHO cells expressing the human histamine H_4 receptor, co-treated with forskolin, histamine and tested compounds: **8** (A) and **10** (B).

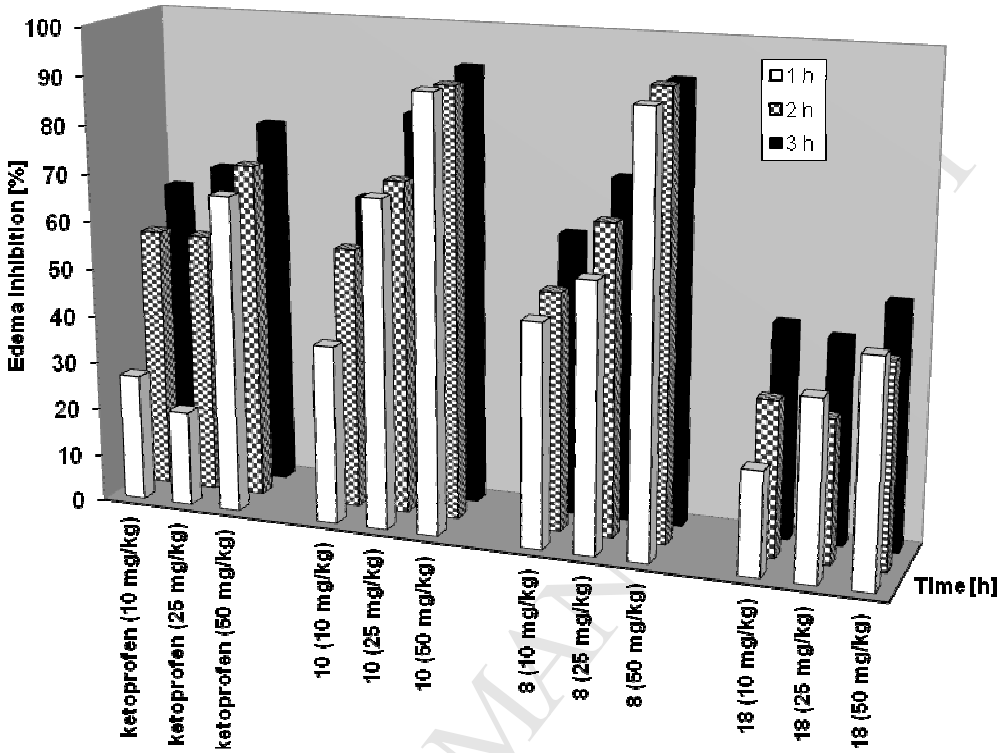

Figure 4. Anti-inflammatory effect of compounds **8**, **10** and **18** (doses: 10 mg/kg, 25 mg/kg and 50 mg/kg) on paw edema induced by subplantar injection of carrageenan.

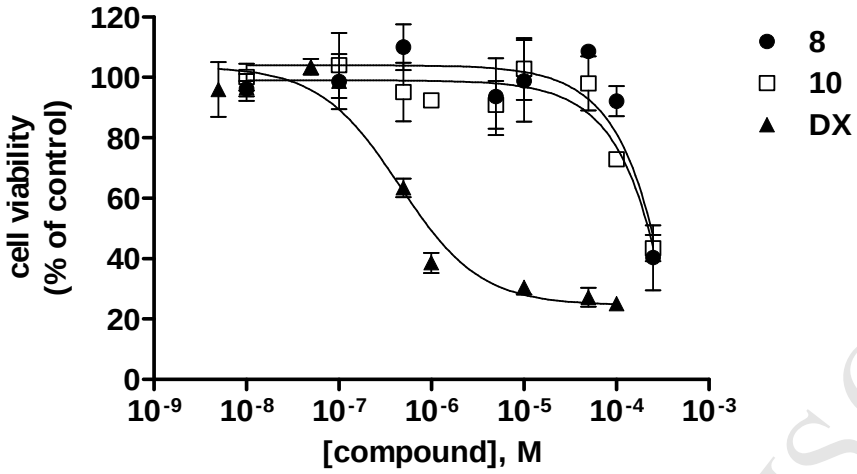

Figure 5. The antiproliferative effect of **8**, **10** and **DX** (reference) against HEK-293 cell line.

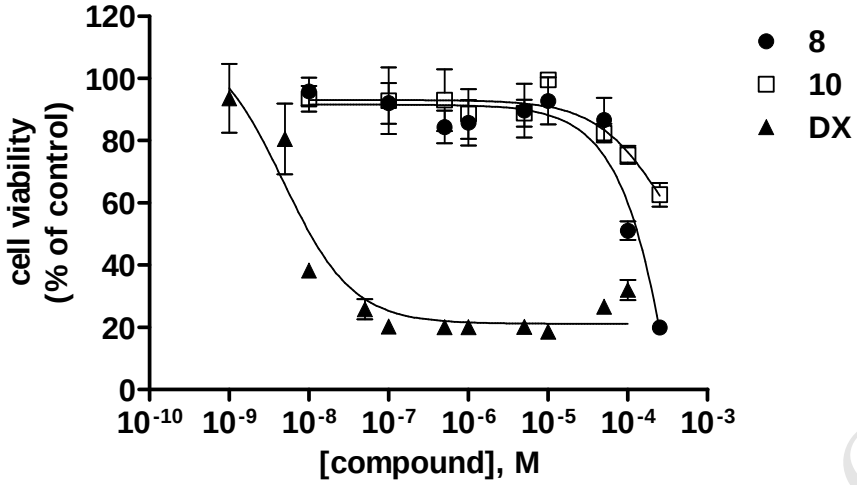

Figure 6. The antiproliferative effect of **8**, **10** and **DX** (reference) against IMR-32 cell line.

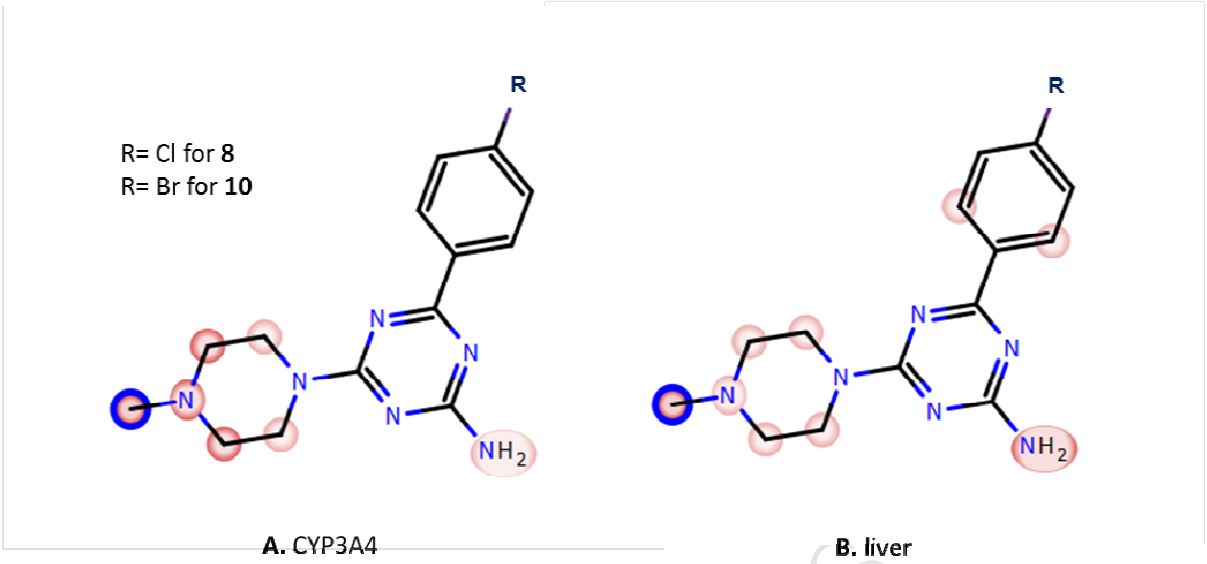

Figure 7. Plots of MetSite predictions for sites of metabolism for **8** and **10** by liver and CYP3A4.

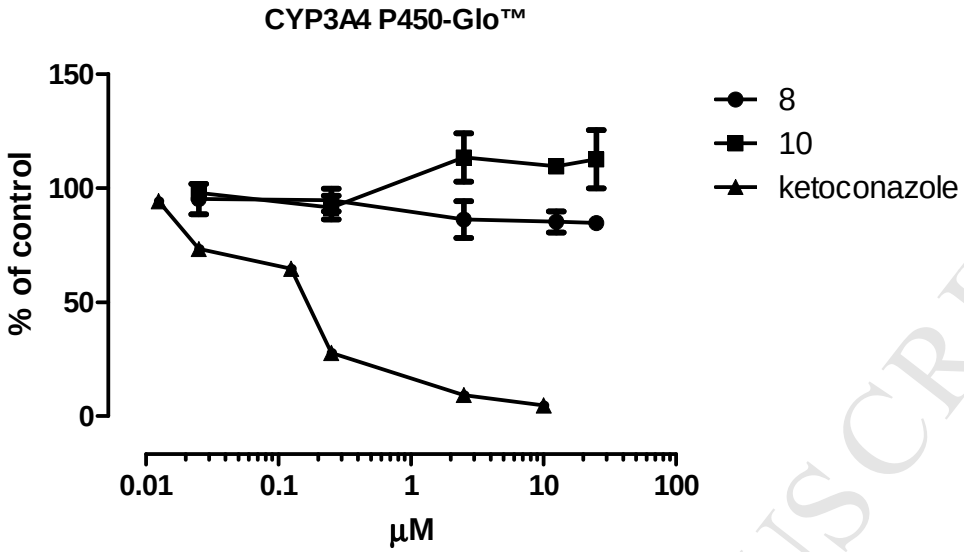

Figure 8. The effect of **8**, **10** and ketoconazole on CYP3A4 activity.

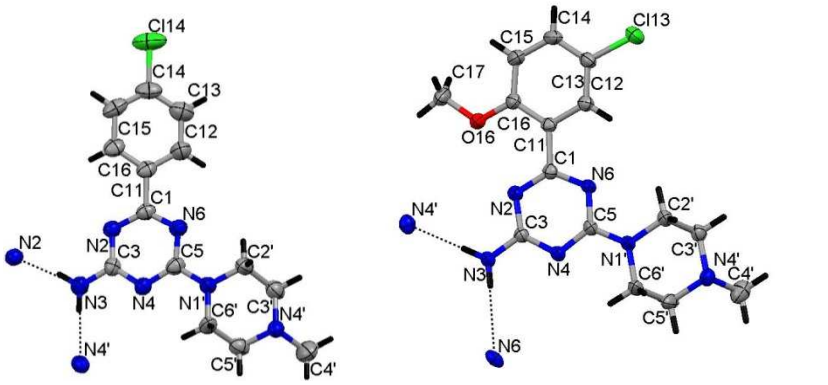

N3-H…N2 = 3.097 Å

N3-H…N4' = 3.069 Å

N3-H…N6 = 3.223 Å

N3-H…N4' = 2.946 Å

Figure 9. ORTHEP drawing of the **8** and **17** molecules with hydrogen bonds marked as dotted line.

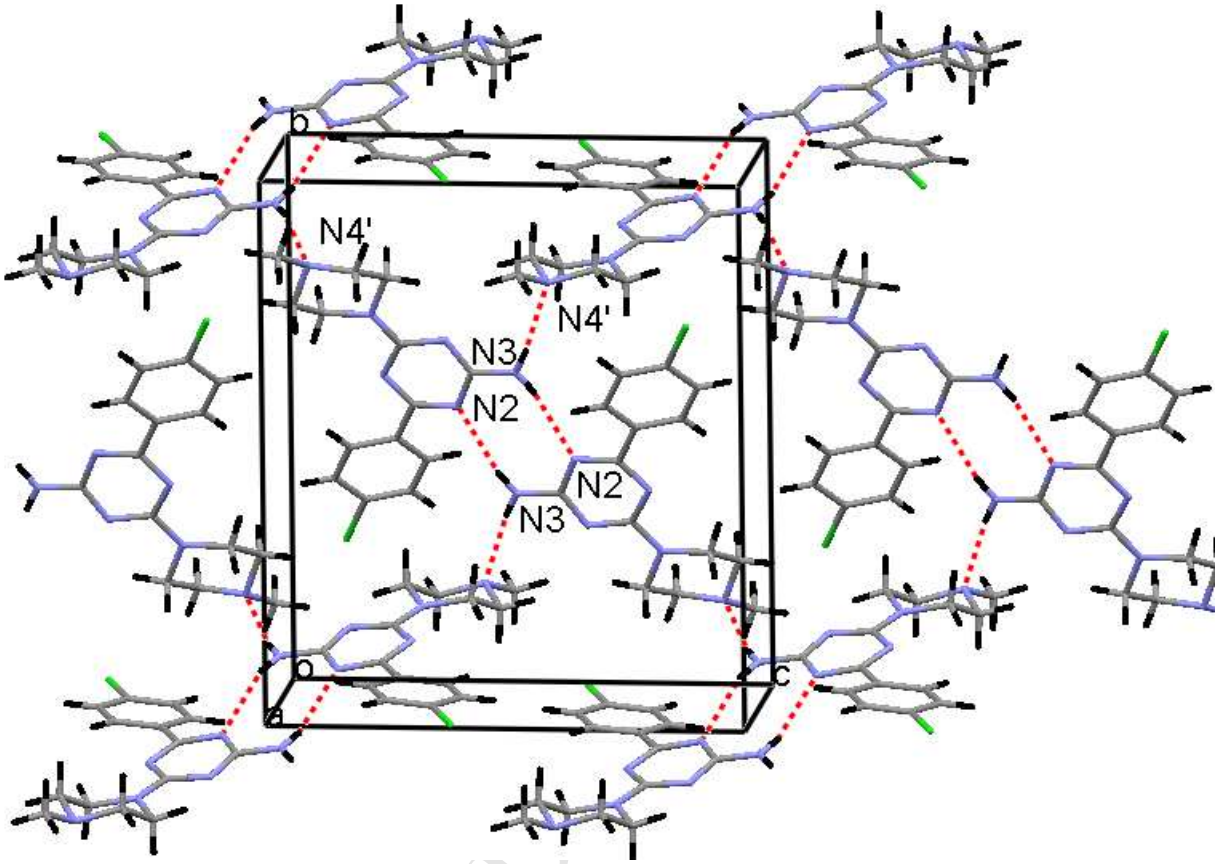

Figure 10. Unit cell packing for **8**.

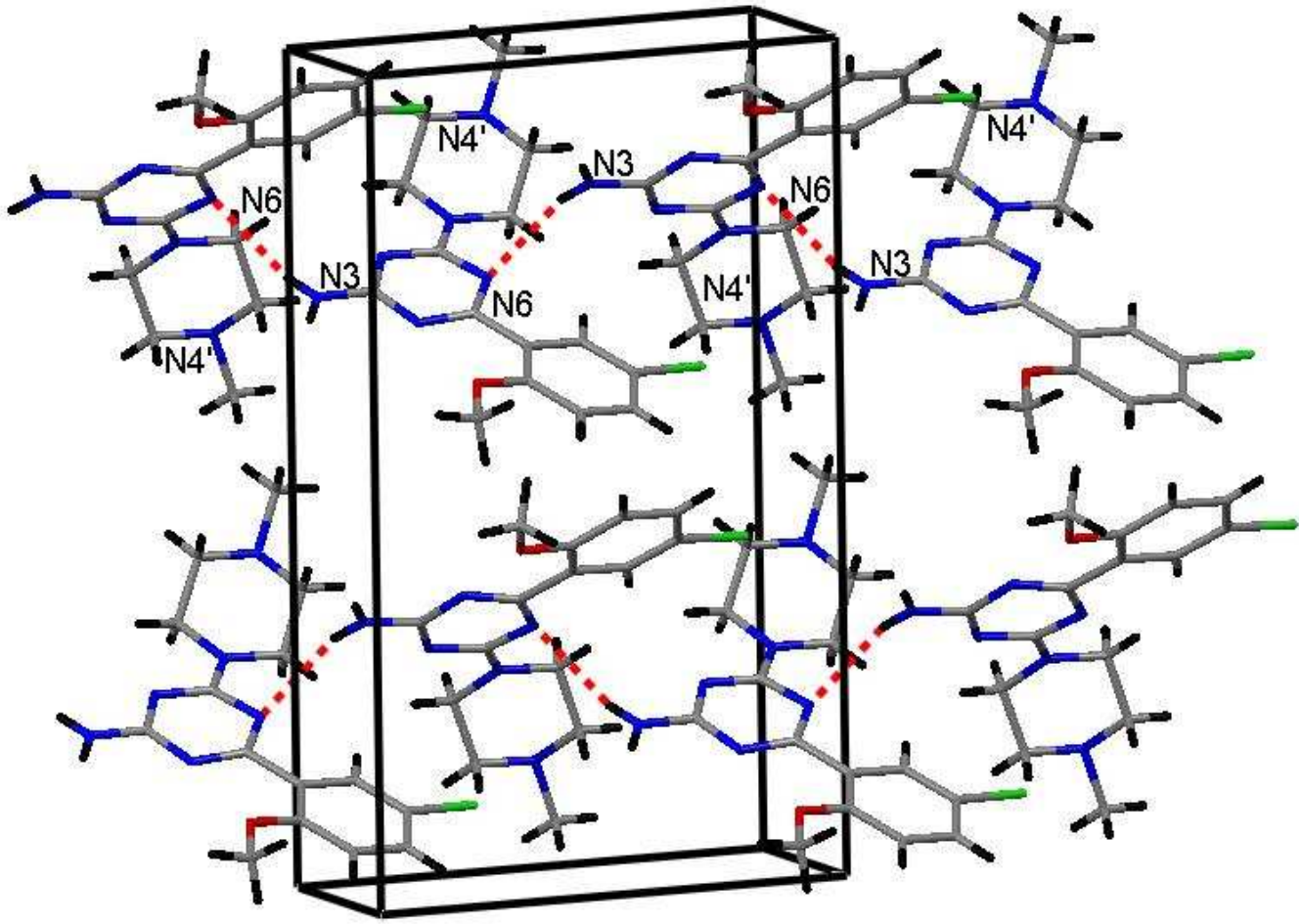

Figure 11. Unit cell packing for **17**.

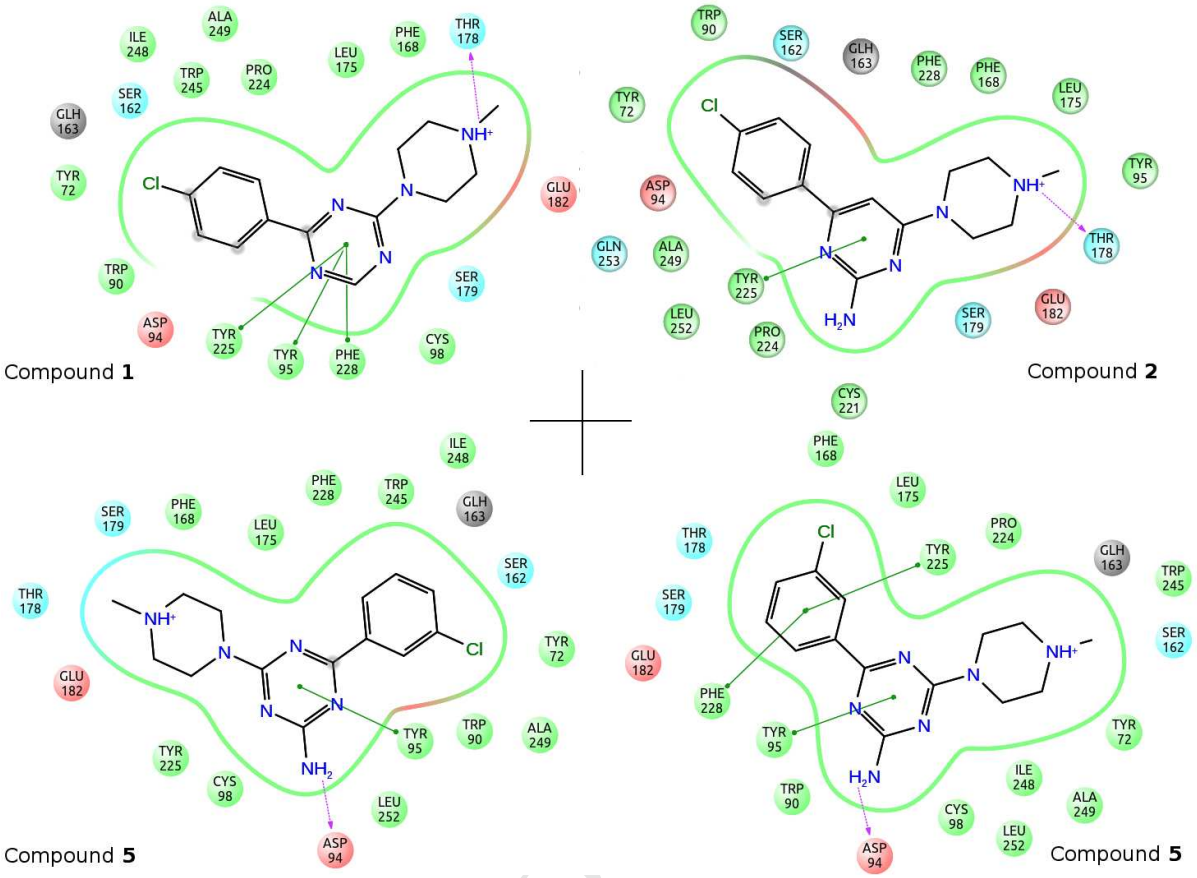

Figure 12: Ligand interaction diagrams for chosen positions of the best docking score values for compounds **1**, **2** and for compound **5** in two binding manners (A – left, B-right). Hydrogen bonds are shown as magenta spotted lines. Green spotted lines represent π-π stacking.

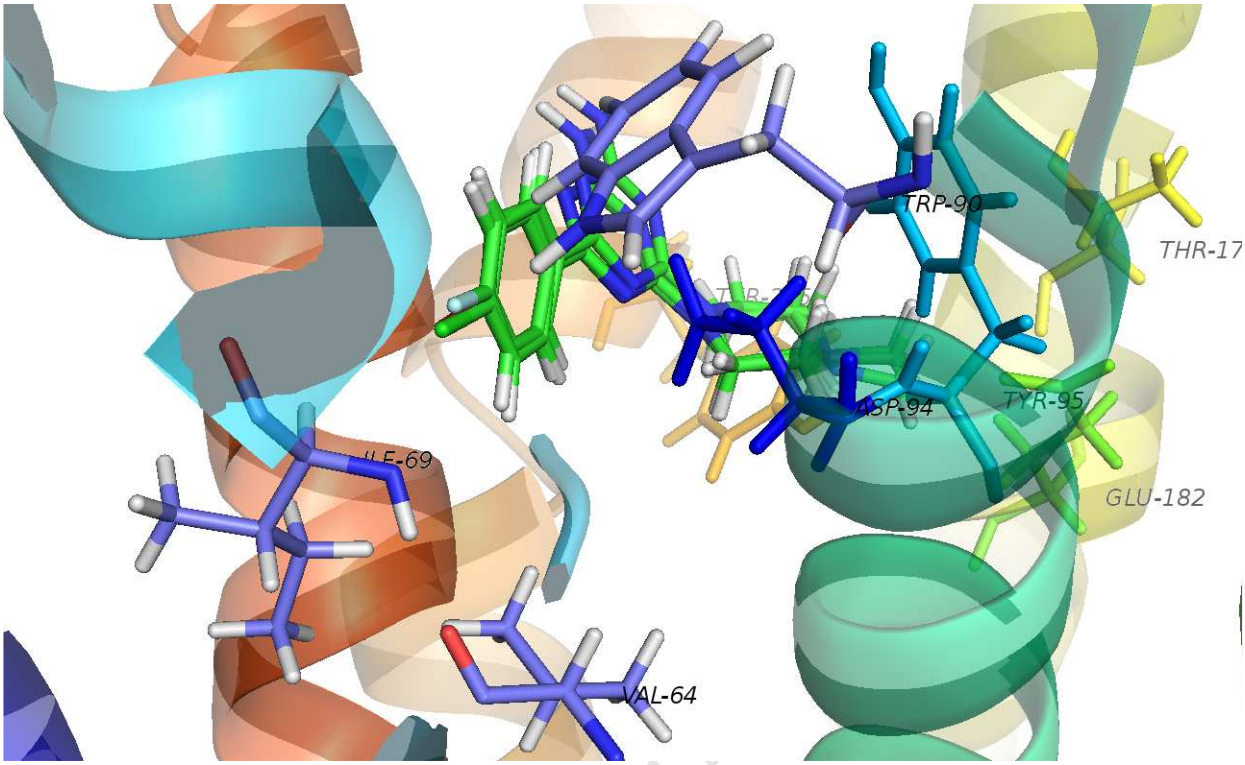

Figure 13: Compounds **8** and **10** (green color for carbons, white for hydrogens),in the binding pocket of histamine H_4 receptor homology model hydrophobic „pocket" formed by VAL64$^{2.53}$, ILE69$^{2.58}$ and TRP90$^{3.28}$ (light blue color for carbons, white for hydrogens, dark blue for oxygen, red for amine group).

Scheme 1. Synthetic route leading to 2,4,6-trisubstituted 1,3,5-triazines. Reagents and conditions: (A) BuOH, temperature gradually increased from 50 to 90^0C during 1h, 5h reflux; (B) MeONa, reflux from 15-30h.

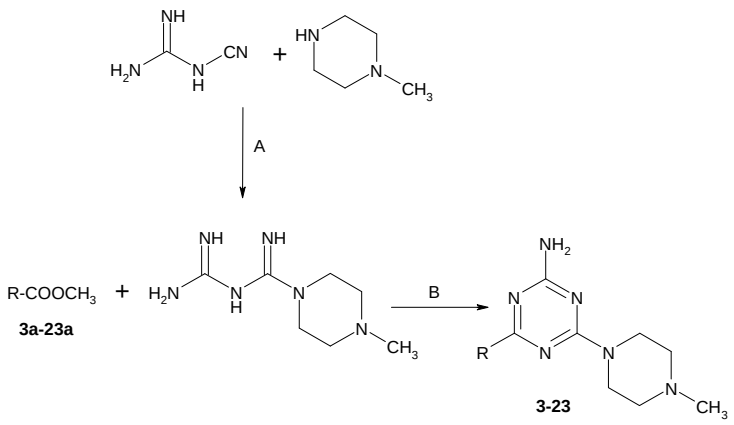

Figures and Scheme captions

Figure 1 Structures and H_4R affinities of (4-methylpiperazin-1-yl)-1,3,5-triazine (**1**[17]) and -pyrimidine-2-amine derivatives (**2**[18]).

Figure 2. General structure of synthesized compounds.

Figure 3. cAMP accumulation studies in CHO cells expressing the human histamine H_4 receptor, co-treated with forskolin, histamine and tested compounds: **8** (A) and **10** (B).

Figure 4. Anti-inflammatory effect of compounds **8**, **10** and **18** (doses: 10 mg/kg, 25 mg/kg and 50 mg/kg) on paw edema induced by subplantar injection of carrageenan.

Figure 5. The antiproliferative effect of **8**, **10** and **DX** (reference) against HEK-293 cell line.

Figure 6. The antiproliferative effect of **8**, **10** and **DX** (reference) against IMR-32 cell line.

Figure 7. Plots of MetSite predictions for sites of metabolism for **8** and **10** by liver and CYP3A4.

Figure 8. The effect of **8**, **10** and ketoconazole on CYP3A4 activity.

Figure 9. ORTHEP drawing of the **8** and **17** molecules with hydrogen bonds marked as dotted line.

Figure 10. Unit cell packing for **8**.

Figure 11. Unit cell packing for **17**.

Figure 12. Ligand interaction diagrams for chosen positions of the best doscing score values for compounds **1**, **2** and for compound **5** in two binding manners (A – left, B-right). Hydrogen bonds are shown as magenta spotted lines. Green spotted lines represent π-π stacking.

Figure 13. Compounds **8**-**10** in the binding pocket of histamine H_4 receptor homology model.

Scheme 1. Synthetic route leading to 2,4,6-trisubstituted 1,3,5-triazines. Reagents and conditions: (A) BuOH, temperature gradually increased from 50 to 90^0C during 1h, 5h reflux; (B) MeONa, reflux from 15-30h.

SUPPLEMANTAL MATERIALS

Table 2. Anti-inflammatory effect of tested compounds on carrageenan-induced paw edema in mice.

Compound	Dose [mg/kg]	Change in the volume of edema [μL]		
		1h	2h	3h
Control	-	64±5	80±8	98±8
5	50	12±4***	12±5***	12±2***
	25	34±5**	30±3,2***	30±3***
	10	50±18	64±8	113±13
7	50	12±7***	18±5***	18±4***
	25	16±6***	34±8**	30±6***
	10	36±5**	60±7	60±9*
8	50	6±2***	6±4***	8±4***
	25	28±11*	28±11**	28±11***
	10	34±5**	40±9**	40±9**
10	50	6±4***	8±2***	8±4***
	25	20±13*	24±17*	18±13***
	10	40±14	36±16*	36±16**
12	50	6±3***	20±5***	20±5***
	25	32±6**	38±1*	38±12**
	10	30±9*	48±7*	48±7**
18	50	34±8*	46±8*	48±9**
	25	40±6	56±3	56±3**
	10	50±8	54±7	54±8*
23	50	22±9**	28±10**	28±10***
	25	40±8	58±15	58±15*
	10	44±10	54±17	60±17
Ketoprofen	50	21±7***	23±5***	22±9***
	25	51±9	36±8**	32±10**
	10	47±2	36±10**	37±8**

differences significant *vs.* control group, *p<0.05; **p<0.01; ***p<0.001

Table 3. Crystal data and structure refinement details for **8** and **17**.

	8	**17**
Empirical formula	$C_{14}H_{17}N_6Cl_5$	$C_{15}H_{19}N_6OCl$
Formula weight	304.79	334.81
Temperature	293 K	293 K
Radiation	Mo(Kα)=0.71073 Å	Mo(Kα)=0.71073 Å
Crystal system	monoclinic	monoclinic
Space group	$P2_1/c$	Cc
Unit cell dimensions	a = 6.4519(4) Å b = 16.5378(14) Å c = 13.9923(10) Å β = 91.056(7) °	a = 12.9909(5) Å b = 18.2448(7) Å c = 7.3449(4) Å β = 113.968(5) °
Volume $(Å)^3$	1492.73(19)	1590.75(14)
Z, density (g/m^3)	4, 1.356	4, 1.398
μ (mm^{-1})	0.259	0.255
Crystal size (mm)	0.2 x 0.15 x 0.3	0.15 x 0.15 x 0.3
Diffractometer	KM-4 -CCD	

Table 4. Selected metric parameters of compound **8** and **17**.

a. H- bonds geometry					
	D-H⊙⊙⊙A	Symm. code	H⊙⊙⊙A [Å]	D⊙⊙⊙A [Å]	D-H⊙⊙⊙A [˚]
8	N3-H3B⊙⊙⊙N2	1-x,1-y,1-z	2.30	3.097(4)	154
	N3-H3A⊙⊙⊙N4'	x,1/2-y,-1/2+z	2.24	3.069(4)	161
17	N3-H3A⊙⊙⊙N6	-1/2+x,-1/2-y,-1/2+z	2.42	3.223(3)	156
	N3-H3B⊙⊙⊙N4'	-1/2+x,-1/2-y,1/2+z	2.09	2.946(3)	171

b. Bond lengths in triazine ring [Å]						
	N2-C1	C3-N2	N4-C3	C5-N4	N6-C5	C1-N6
8	1.333(5)	1.346(5)	1.326(5)	1.335(5)	1.350(5)	1.311(5)
17	1.320(3)	1.358(3)	1.338(3)	1.333(3)	1.351(3)	1.333(3)

Uniwersytet Jagiellonski
Collegium Medicum
Pracownia Spektroskopii NMR
Aug 30 2013
Probka: TR-18
Rozpuszczalnik: dmso

Pulse Sequence: s2pul

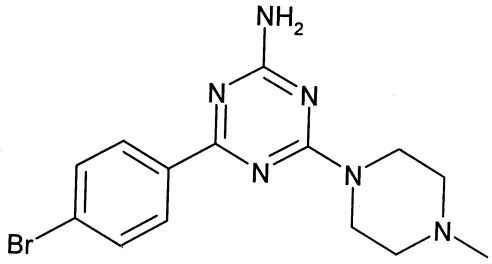

10

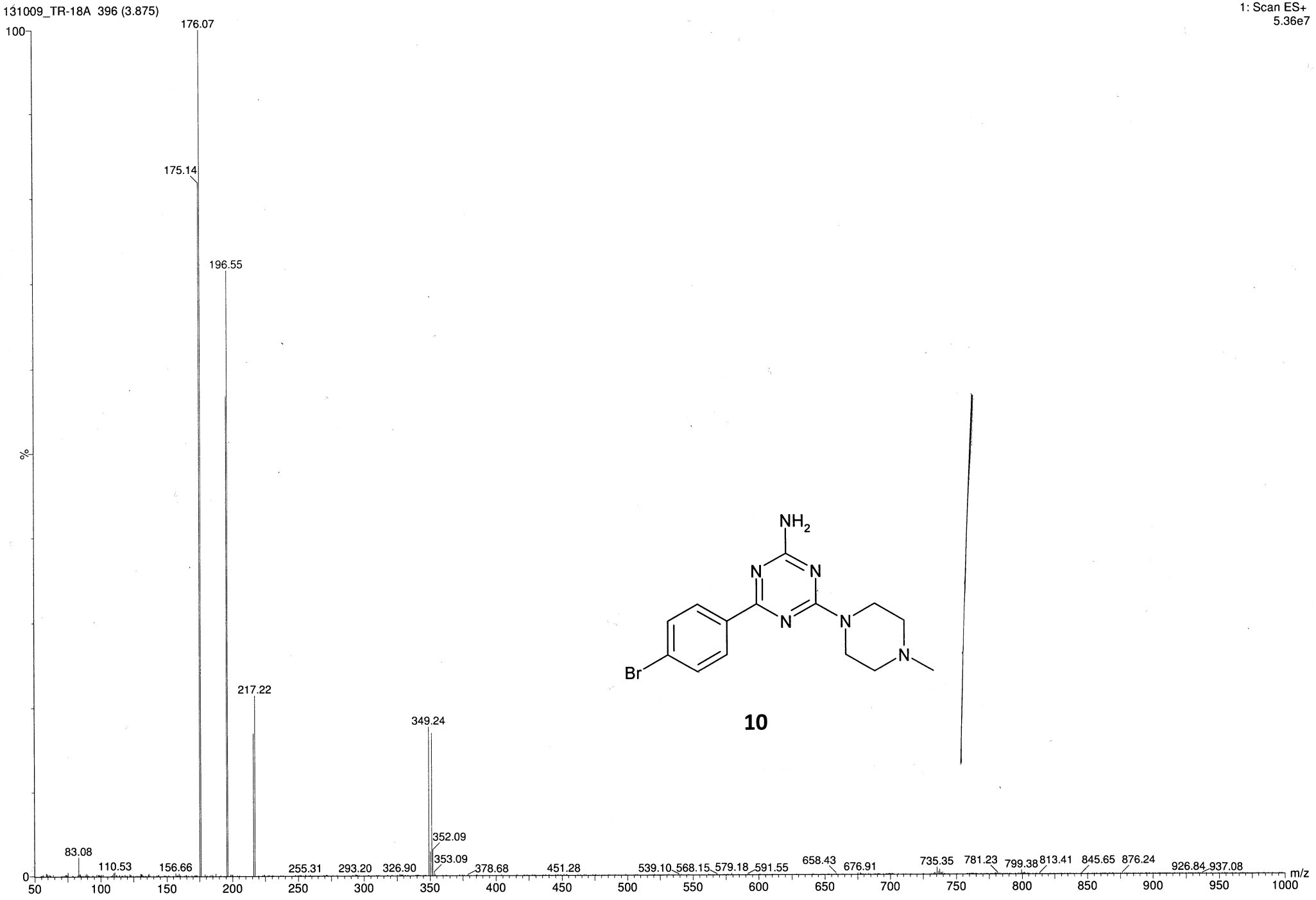
131009_TR-18A 396 (3.875)
1: Scan ES+
5.36e7
100
%
0
176.07
175.14
196.55
217.22
349.24
352.09
353.09
83.08
110.53
156.66
255.31
293.20
326.90
378.68
451.28
539.10
568.15
579.18
591.55
658.43
676.91
735.35
781.23
799.38
813.41
845.65
876.24
926.84
937.08
50
100
150
200
250
300
350
400
450
500
550
600
650
700
750
800
850
900
950
1000
m/z
NH2
N
N
N
N
N
Br

10

Uniwersytet Jagiellonski
Collegium Medicum
Pracownia Spektroskopii NMR
Jun 28 2013
Probka: TR-16
Rozpuszczalnik: dmso

Pulse Sequence: s2pul

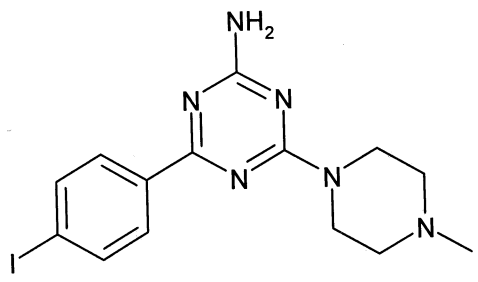

11

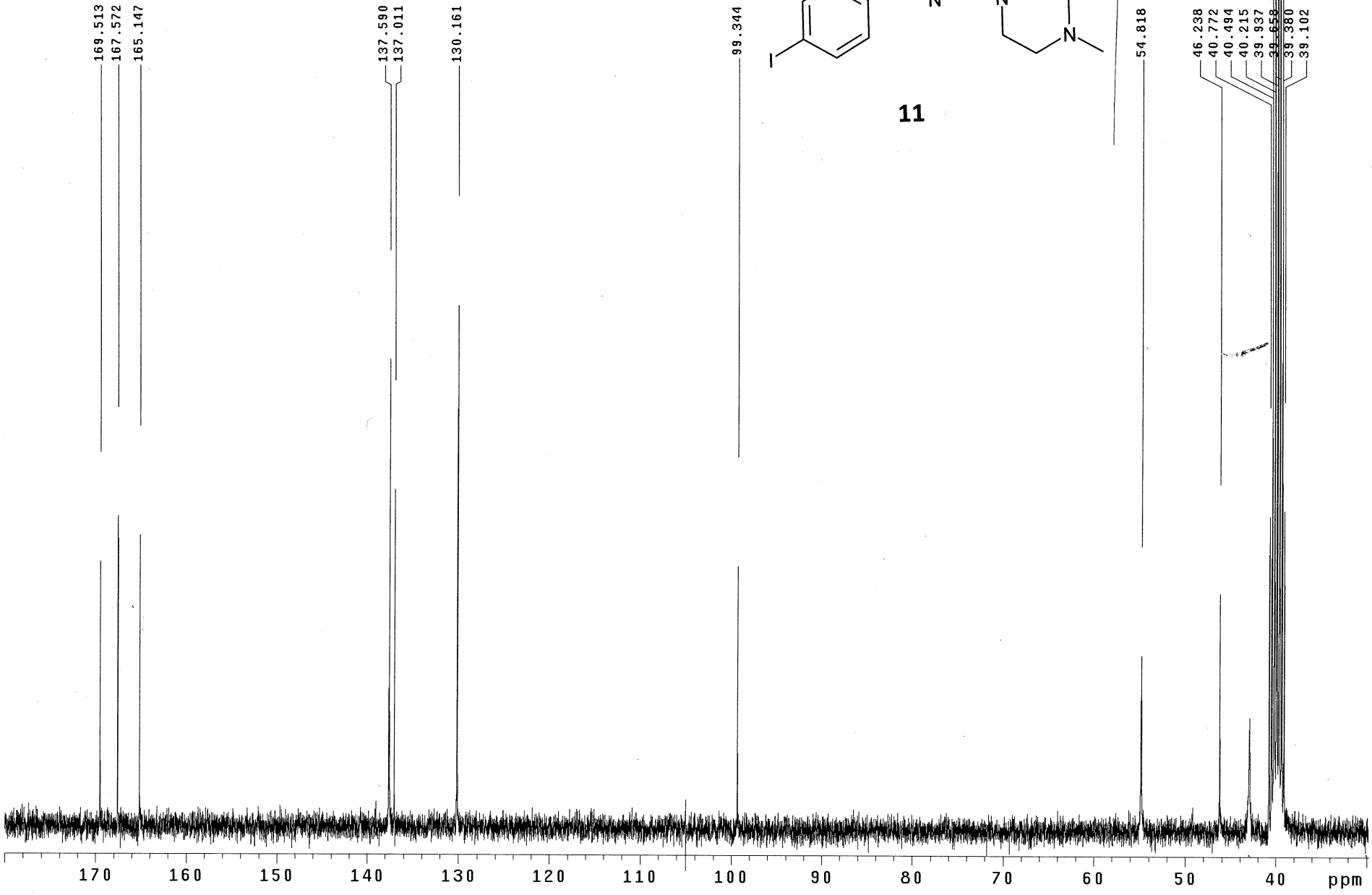

131009_TR-16A 375 (3.694)

1: Scan ES+
2.18e6

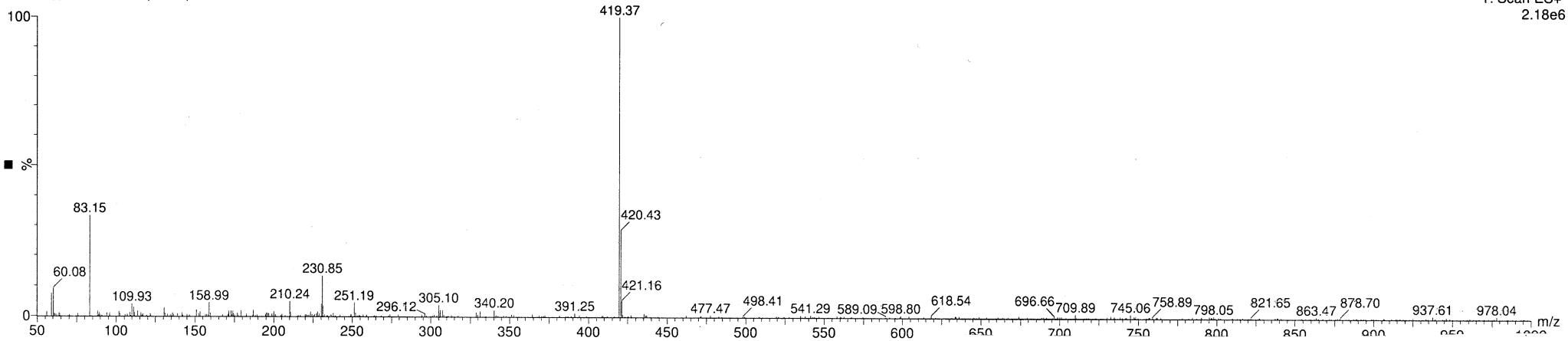

131009_TR-16A 424 (4.112)

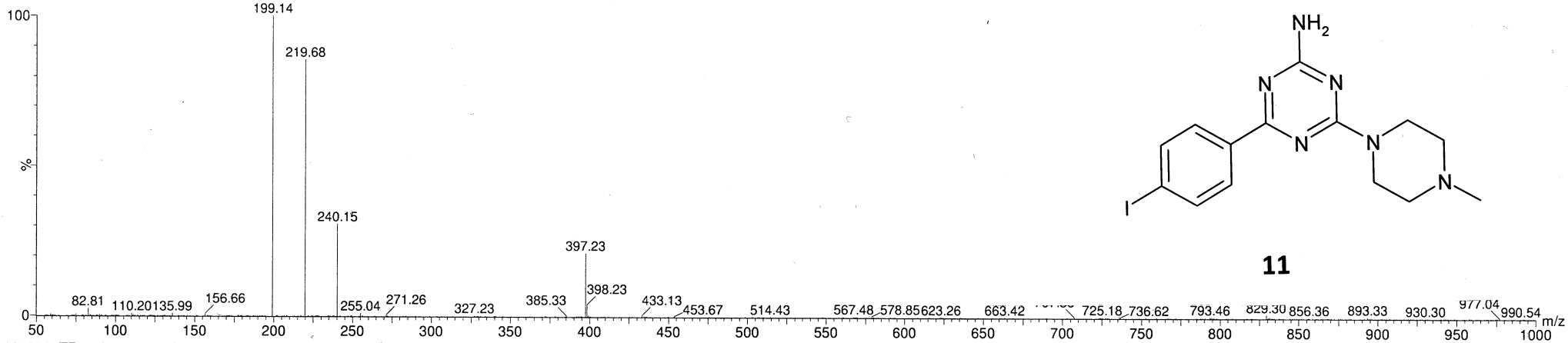

11

131009_TR-16A 584 (5.475)

1: Scan ES+
2.89e5

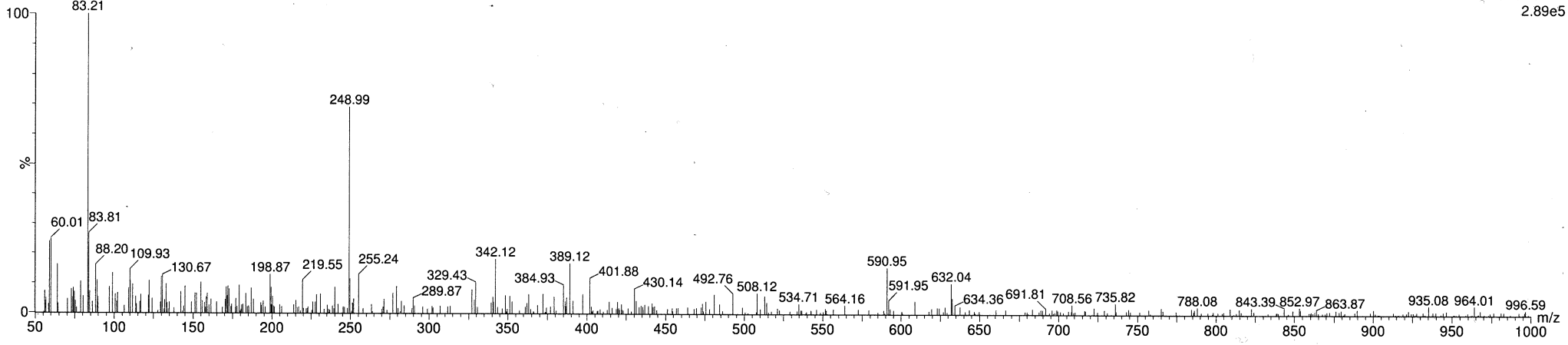

DN-8A

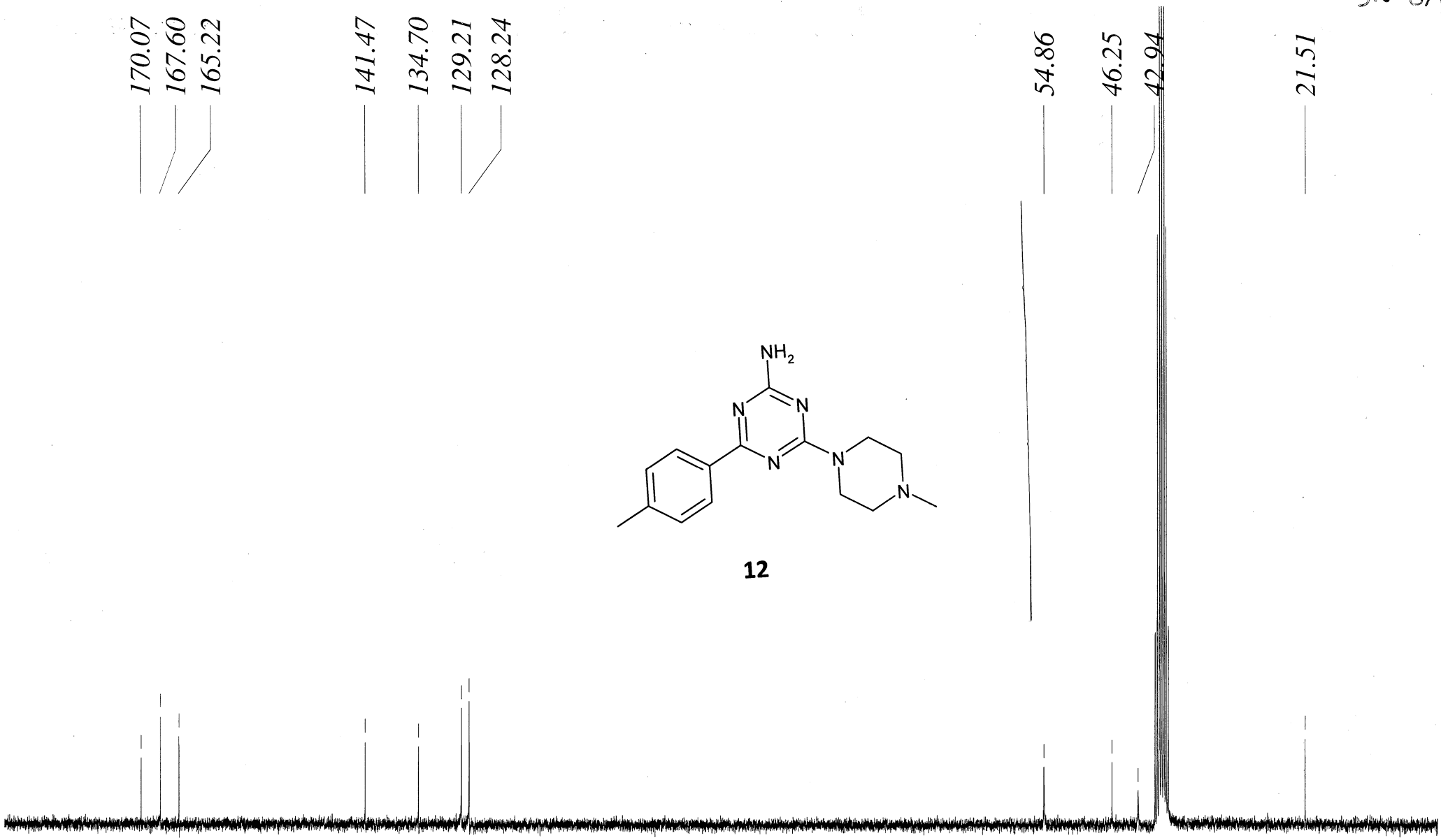
170.07
167.60
165.22
141.47
134.70
129.21
128.24
54.86
46.25
42.94
21.51
NH2
N
N
N
N
N

12

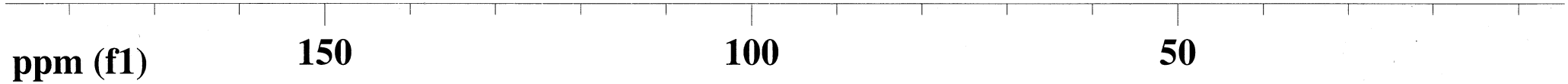
ppm (f1)
150
100
50

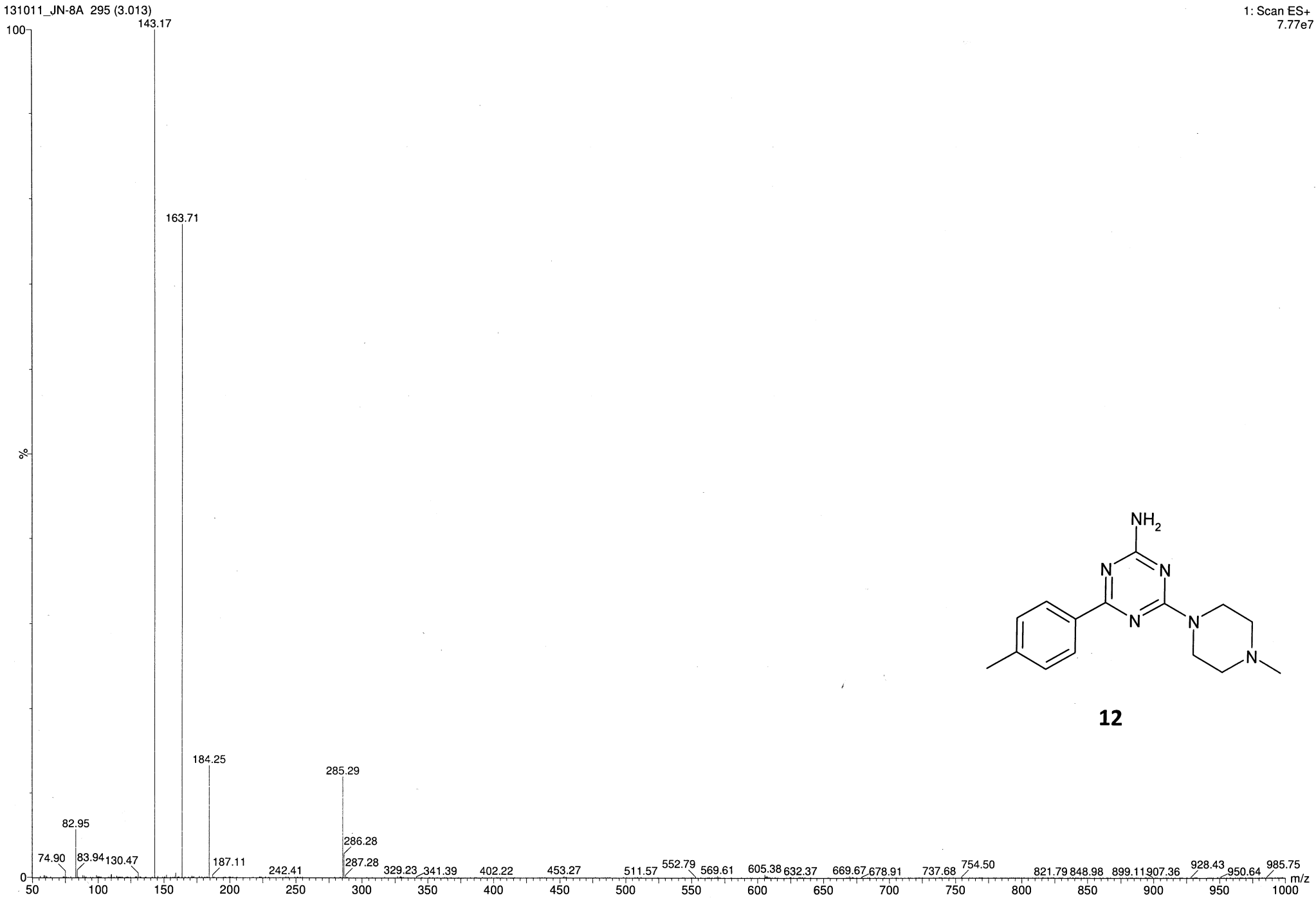
131011_JN-8A 295 (3.013)
1: Scan ES+
7.77e7
100
%
0
143.17
163.71
184.25
285.29
82.95
286.28
74.90
83.94
130.47
187.11
242.41
287.28
329.23
341.39
402.22
453.27
511.57
552.79
569.61
605.38
632.37
669.67
678.91
737.68
754.50
821.79
848.98
899.11
907.36
928.43
950.64
985.75
m/z
50
100
150
200
250
300
350
400
450
500
550
600
650
700
750
800
850
900
950
1000
NH2
N
N
N
N
N

12

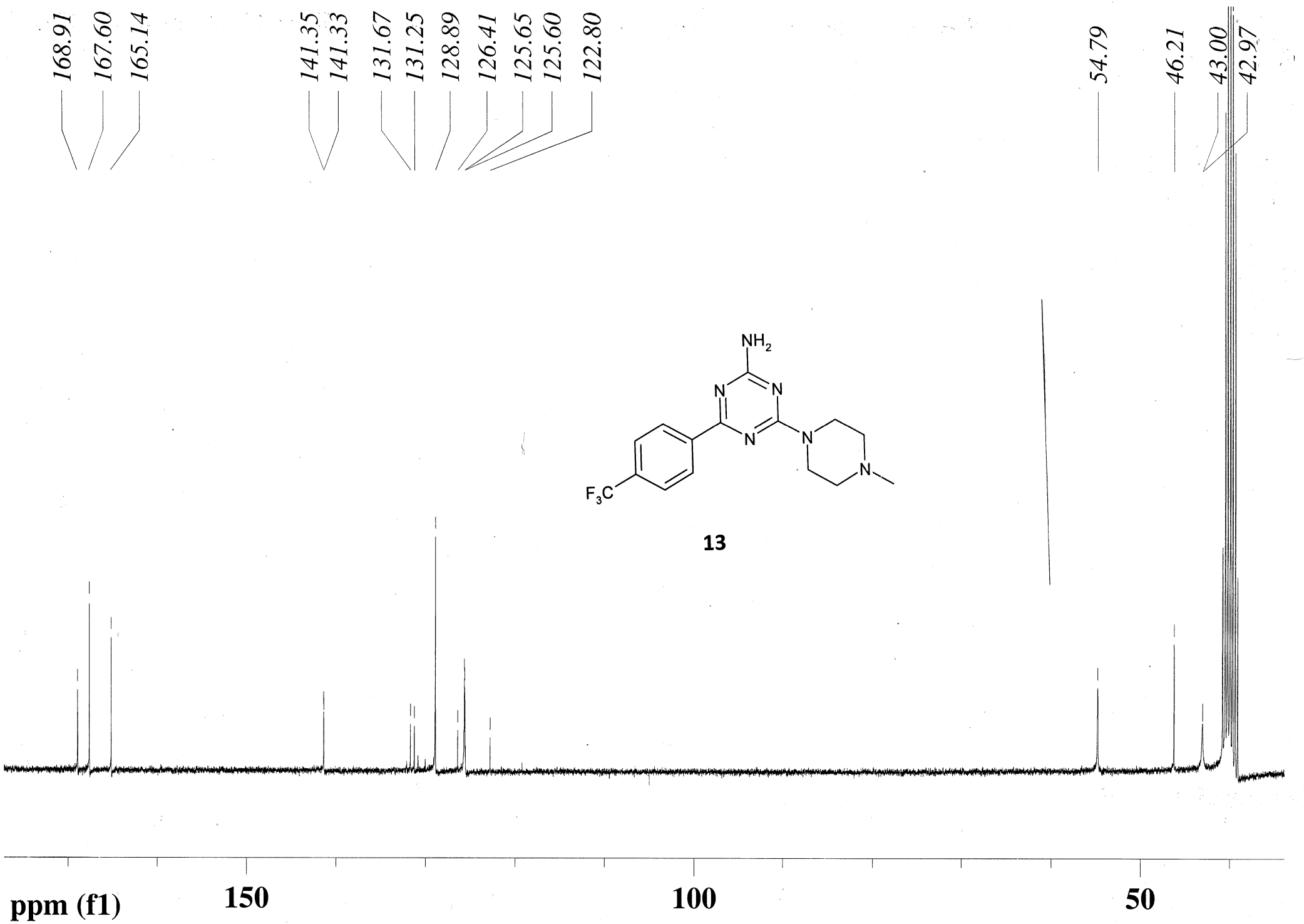
168.91
167.60
165.14
141.35
141.33
131.67
131.25
128.89
126.41
125.65
125.60
122.80
54.79
46.21
43.00
42.97
NH2
N
N
N
N
N
F3C
13
ppm (f1)
150
100
50

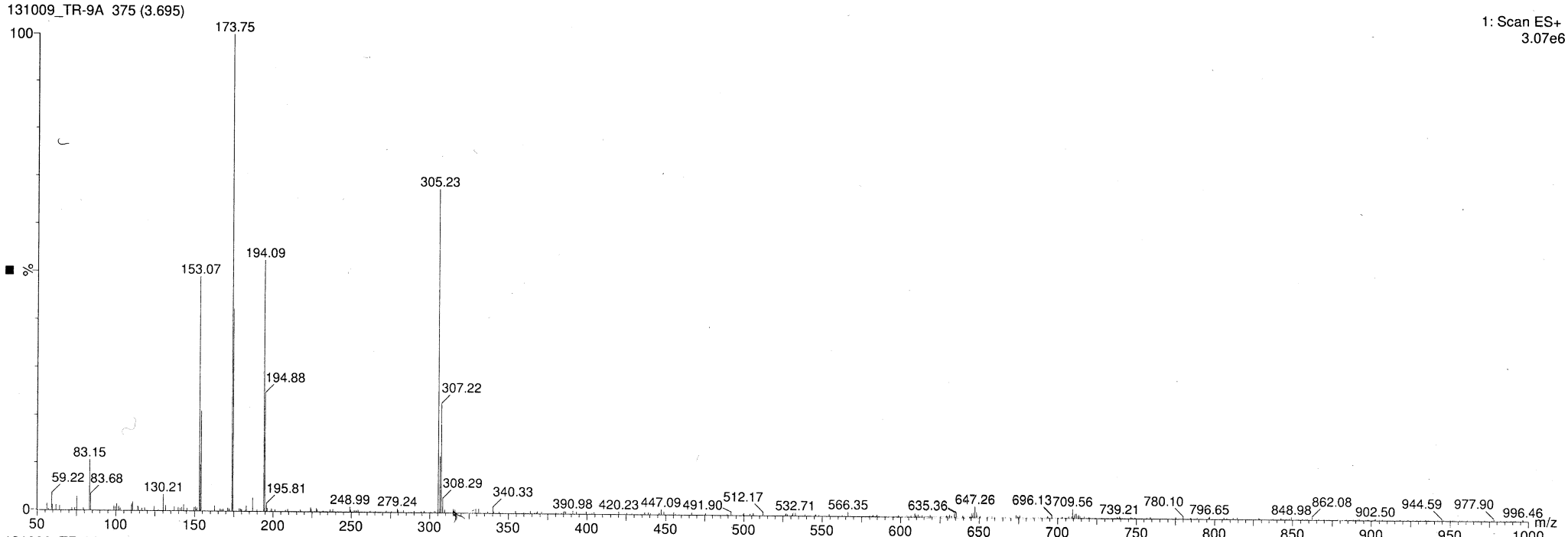
131009_TR-9A 375 (3.695)
1: Scan ES+
3.07e6
100
%
0
173.75
305.23
194.09
153.07
194.88
307.22
83.15
59.22
83.68
130.21
195.81
248.99
279.24
308.29
340.33
390.98
420.23
447.09
491.90
512.17
532.71
566.35
635.36
647.26
696.13
709.56
739.21
780.10
796.65
848.98
862.08
902.50
944.59
977.90
996.46
50
100
150
200
250
300
350
400
450
500
550
600
650
700
750
800
850
900
950
1000
m/z

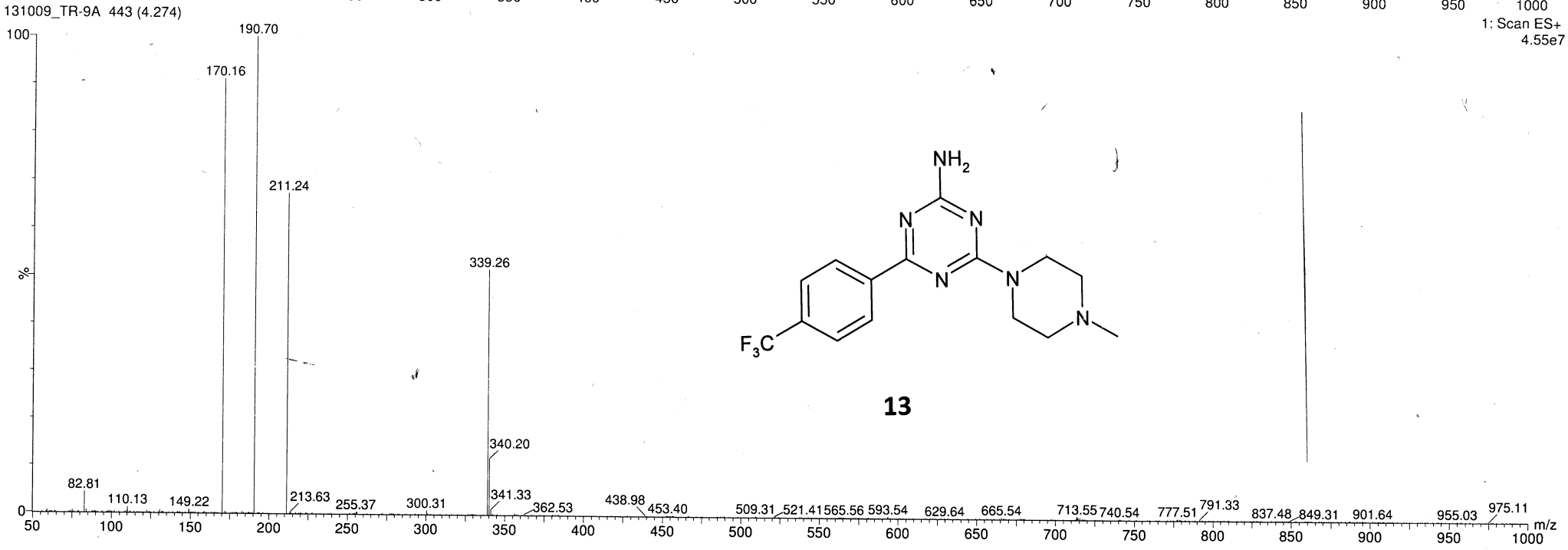
131009_TR-9A 443 (4.274)
1: Scan ES+
4.55e7
100
%
0
190.70
170.16
211.24
339.26
340.20
82.81
110.13
149.22
213.63
255.37
300.31
341.33
362.53
438.98
453.40
509.31
521.41
565.56
593.54
629.64
665.54
713.55
740.54
777.51
791.33
837.48
849.31
901.64
955.03
975.11
50
100
150
200
250
300
350
400
450
500
550
600
650
700
750
800
850
900
950
1000
m/z

NH2
N
N
N
N
N
F3C

13

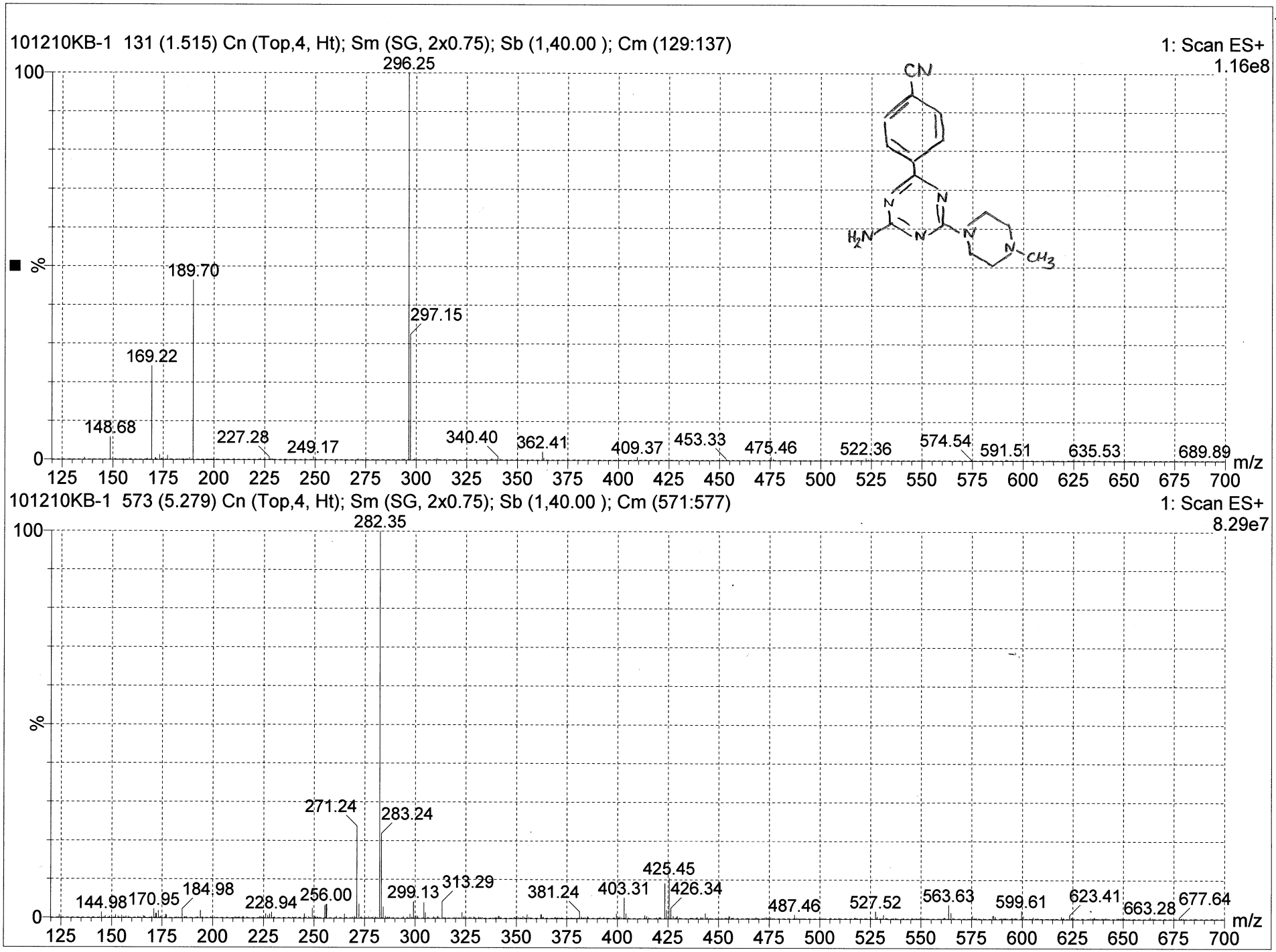
101210KB-1 131 (1.515) Cn (Top,4, Ht); Sm (SG, 2x0.75); Sb (1,40.00); Cm (129:137)
1: Scan ES+
1.16e8
100
%
0
296.25
189.70
297.15
169.22
148.68
227.28
249.17
340.40
362.41
409.37
453.33
475.46
522.36
574.54
591.51
635.53
689.89
m/z
125 150 175 200 225 250 275 300 325 350 375 400 425 450 475 500 525 550 575 600 625 650 675 700
CN
N
N
N
N
N
H_2N
CH_3
101210KB-1 573 (5.279) Cn (Top,4, Ht); Sm (SG, 2x0.75); Sb (1,40.00); Cm (571:577)
1: Scan ES+
8.29e7
100
%
0
282.35
271.24
283.24
425.45
313.29
144.98
170.95
184.98
228.94
256.00
299.13
381.24
403.31
426.34
487.46
527.52
563.63
599.61
623.41
663.28
677.64
m/z
125 150 175 200 225 250 275 300 325 350 375 400 425 450 475 500 525 550 575 600 625 650 675 700

TR-30

39.92
42.83
46.22
54.86
111.33
124.27
129.67
152.81
165.17
167.47
170.16

15

ppm (f1)
150
100
50

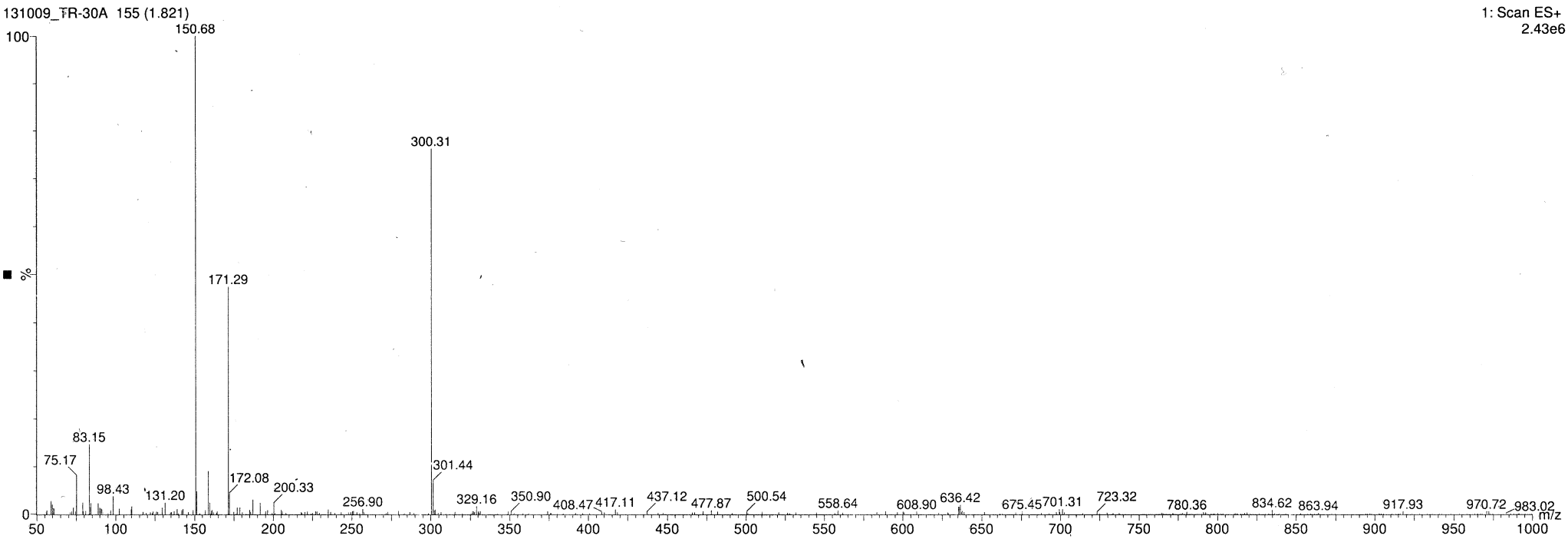
131009_TR-30A 155 (1.821)
1: Scan ES+
2.43e6
100
%
0
150.68
300.31
171.29
83.15
75.17
98.43
131.20
172.08
200.33
256.90
301.44
329.16
350.90
408.47
417.11
437.12
477.87
500.54
558.64
608.90
636.42
675.45
701.31
723.32
780.36
834.62
863.94
917.93
970.72
983.02
m/z
50 100 150 200 250 300 350 400 450 500 550 600 650 700 750 800 850 900 950 1000

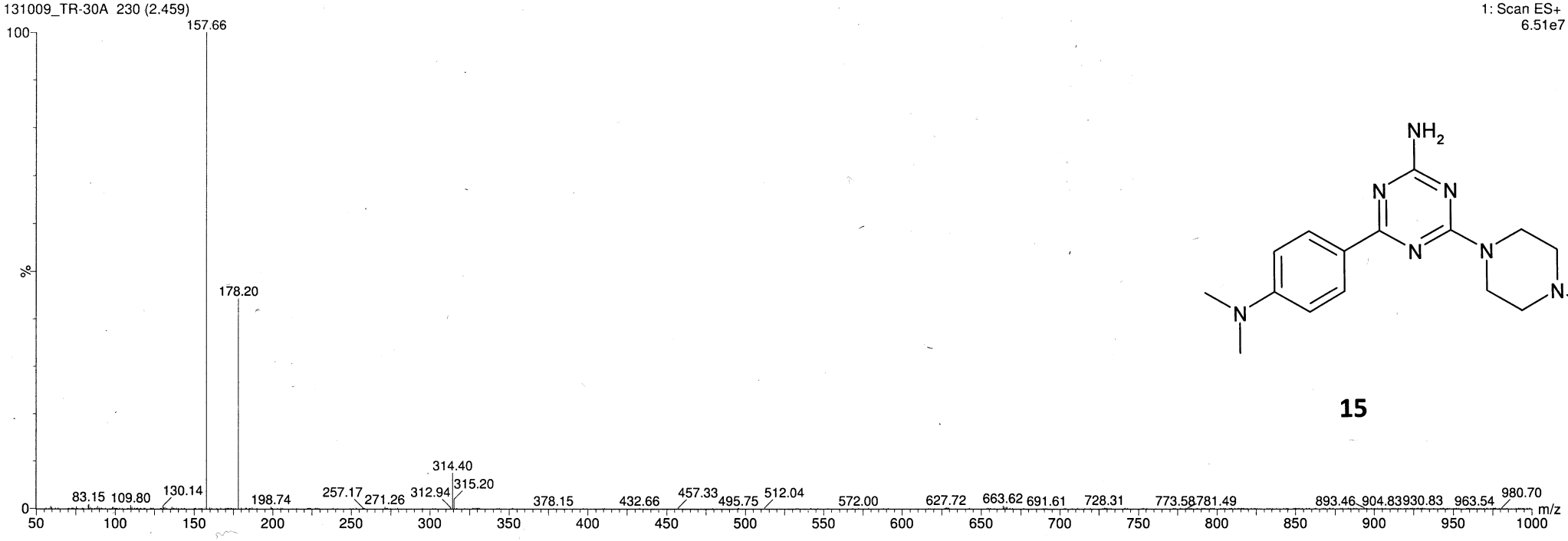
131009_TR-30A 230 (2.459)
1: Scan ES+
6.51e7
100
%
0
157.66
178.20
83.15
109.80
130.14
198.74
257.17
271.26
312.94
314.40
315.20
378.15
432.66
457.33
495.75
512.04
572.00
627.72
663.62
691.61
728.31
773.58
781.49
893.46
904.83
930.83
963.54
980.70
m/z
50 100 150 200 250 300 350 400 450 500 550 600 650 700 750 800 850 900 950 1000

NH2
N
N
N
N
N
N

15

Uniwersytet Jagiellonski
Collegium Medicum
Pracownia Spektroskopii NMR
Jul 11 2013
Probka: TR-4
Rozpuszczalnik: dmso

Pulse Sequence: s2pul

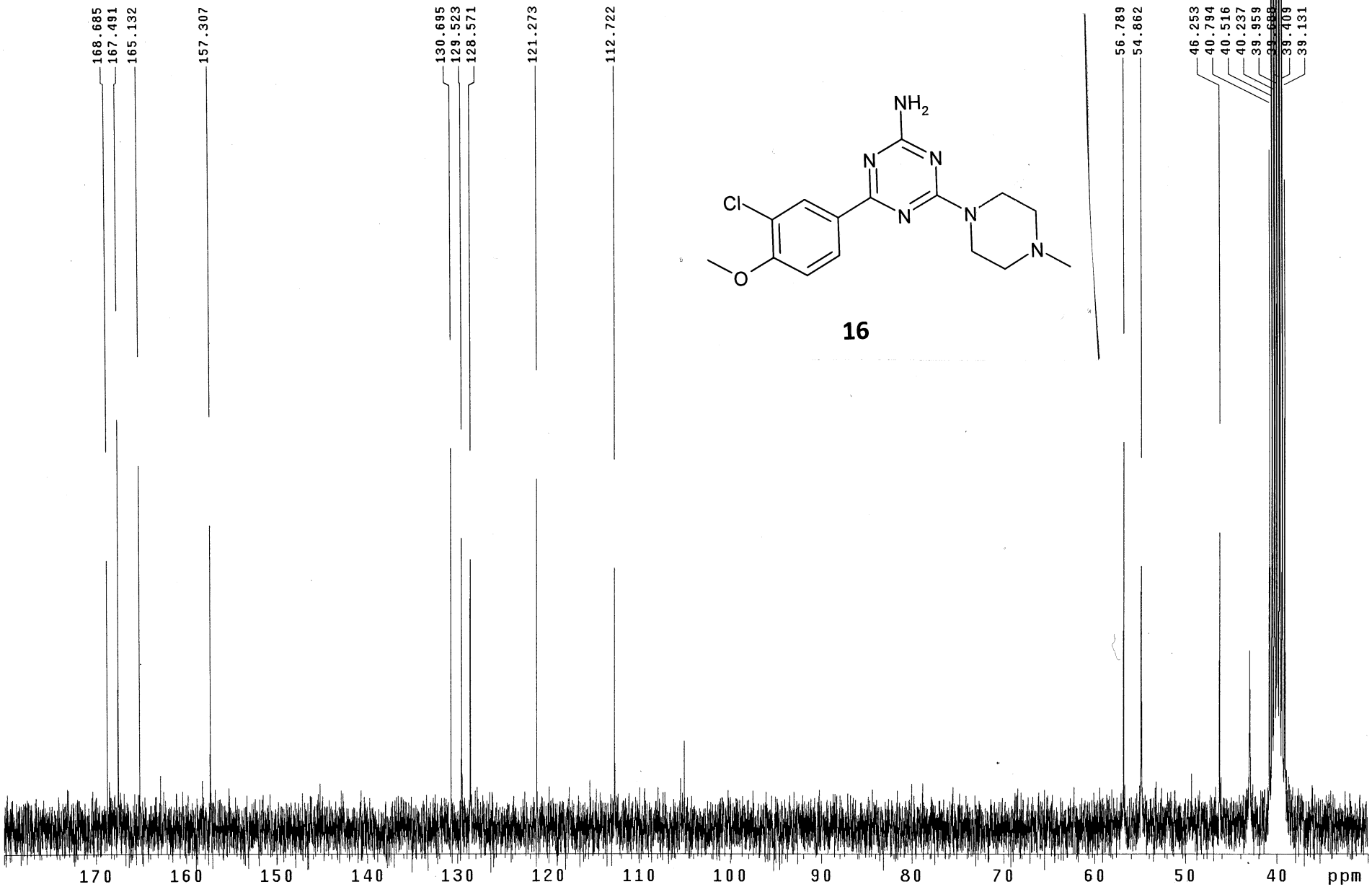

16

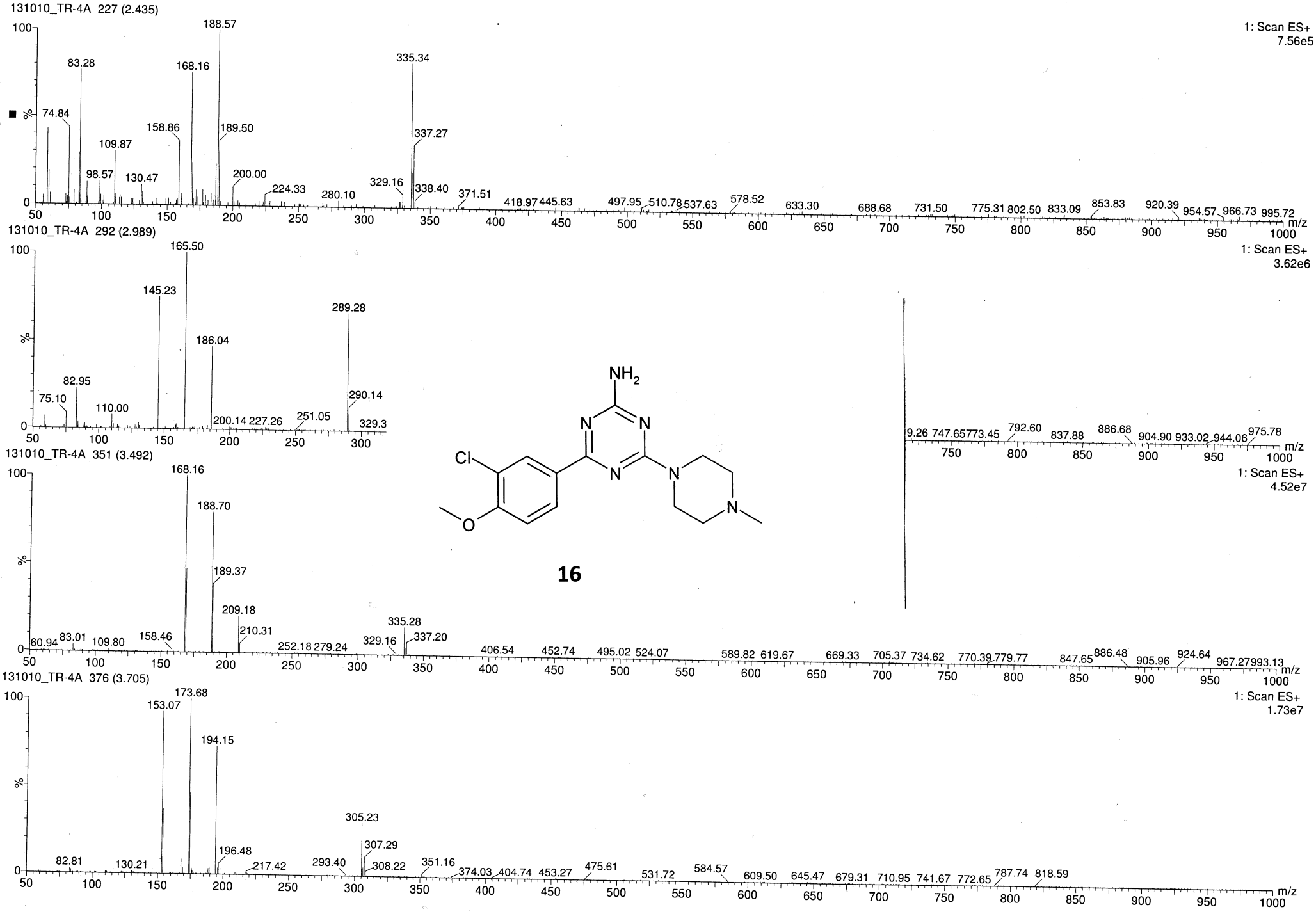
131010_TR-4A 227 (2.435)
1: Scan ES+
7.56e5
131010_TR-4A 292 (2.989)
1: Scan ES+
3.62e6
131010_TR-4A 351 (3.492)
1: Scan ES+
4.52e7
131010_TR-4A 376 (3.705)
1: Scan ES+
1.73e7
m/z
%
16

42.89
46.22
54.77
56.57
114.64
124.15
129.81
130.31
130.51
156.39
164.85
167.14
171.26
ppm (f1)
150
100
50
17

131010_TR-8A 230 (2.459)

1: Scan ES+
5.95e7

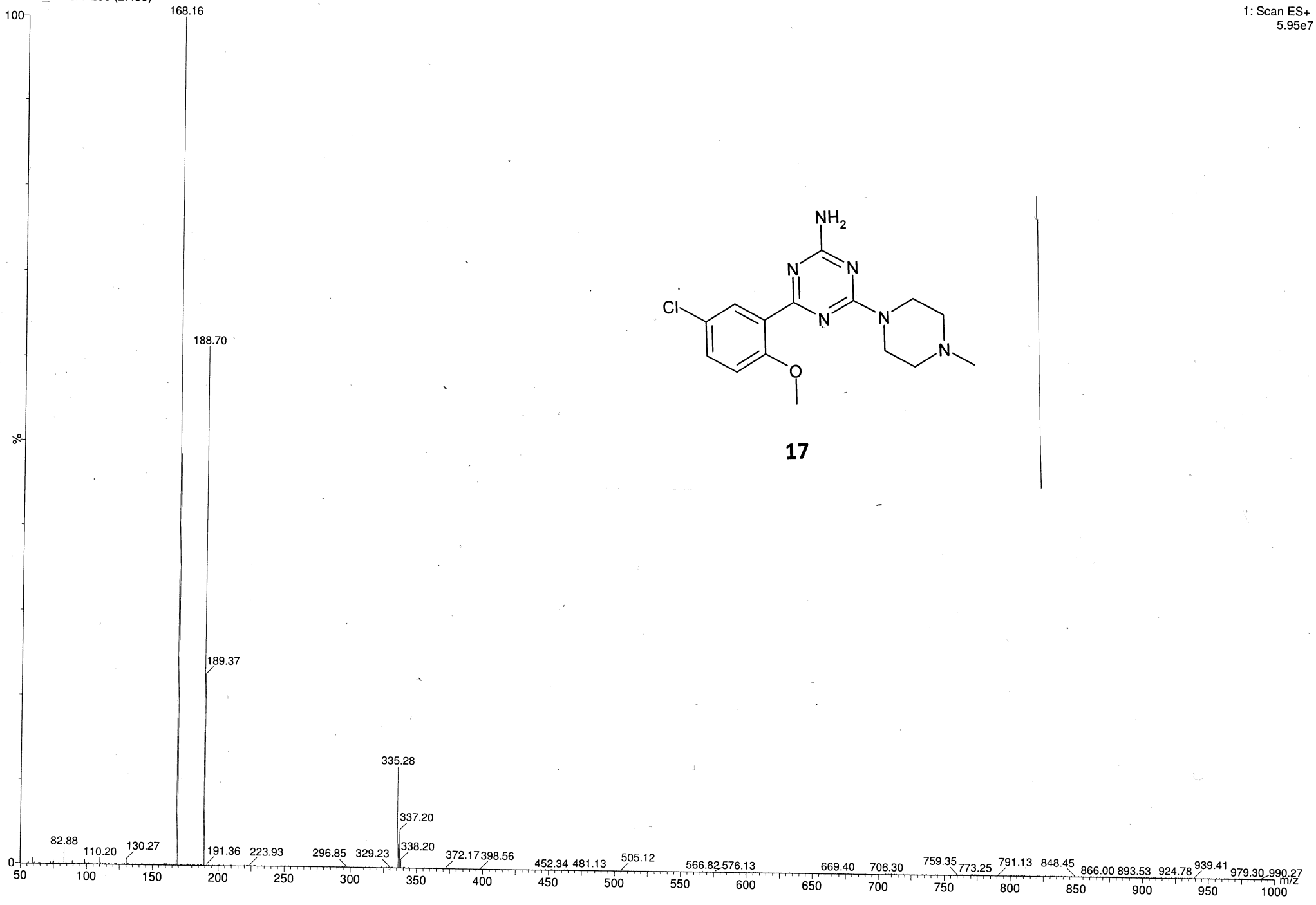

17

Uniwersytet Jagiellonski
Collegium Medicum
Pracownia Spektroskopii NMR
Jun 25 2013
Probka: JN-11
Rozpuszczalnik: dmso

Pulse Sequence: s2pul

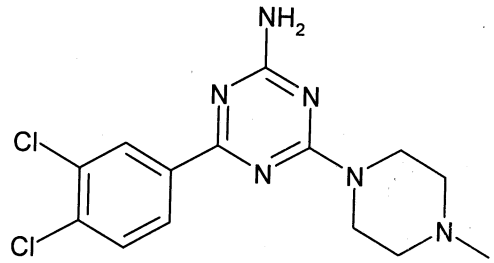

18

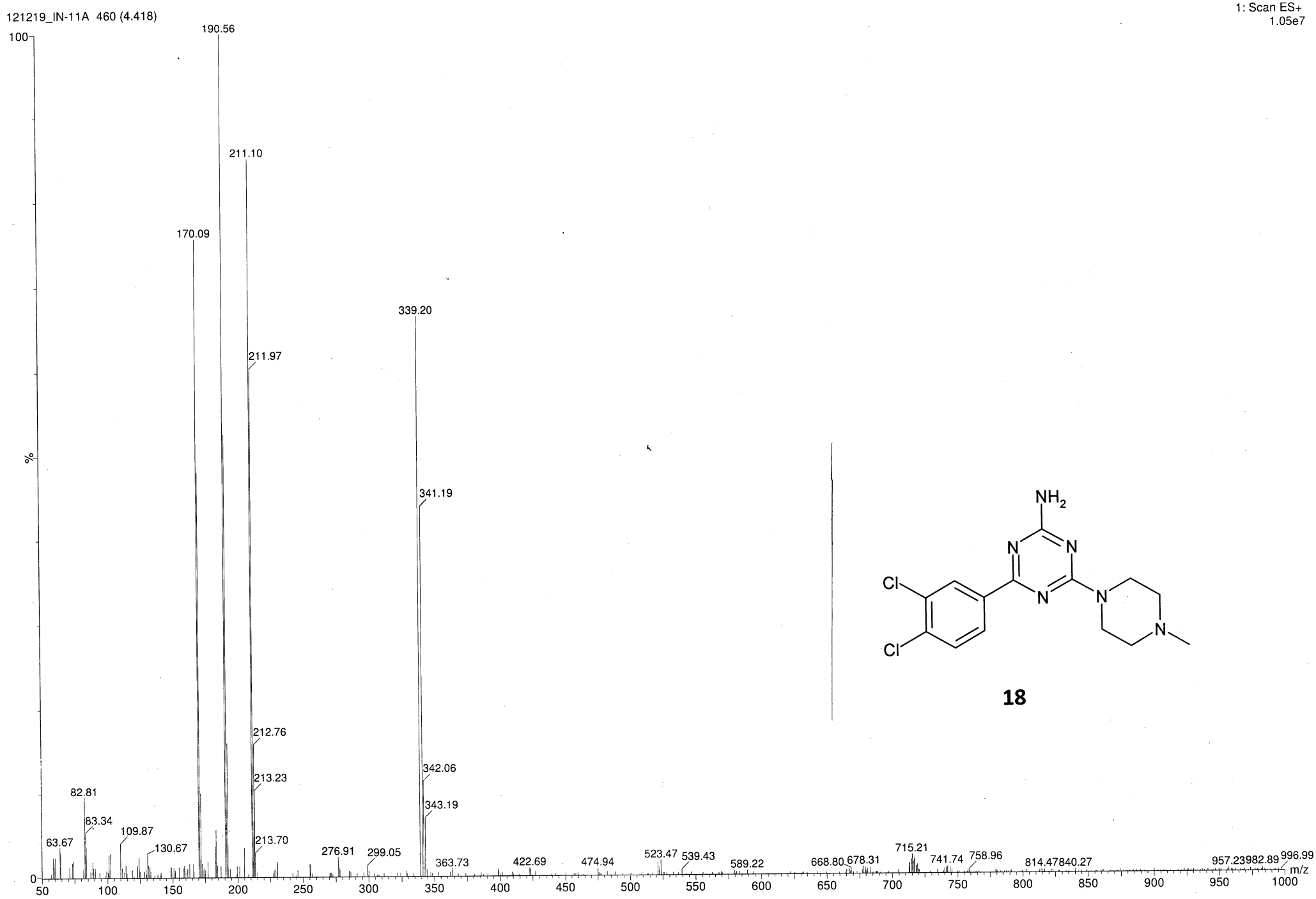
121219_IN-11A 460 (4.418)
1: Scan ES+
1.05e7
100
%
0
190.56
211.10
170.09
339.20
211.97
341.19
212.76
342.06
213.23
343.19
82.81
83.34
109.87
63.67
130.67
213.70
276.91
299.05
363.73
422.69
474.94
523.47
539.43
589.22
668.80
678.31
715.21
741.74
758.96
814.47
840.27
957.23
982.89
996.99
m/z
50
100
150
200
250
300
350
400
450
500
550
600
650
700
750
800
850
900
950
1000
NH2
N
N
N
N
N
Cl
Cl
18

Uniwersytet Jagiellonski
Collegium Medicum
Pracownia Spektroskopii NMR
Jun 24 2013
Probka: TR-13
Rozpuszczalnik: dmso

Pulse Sequence: s2pul

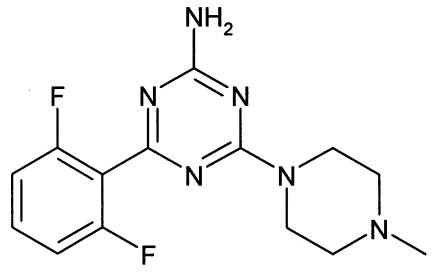

19

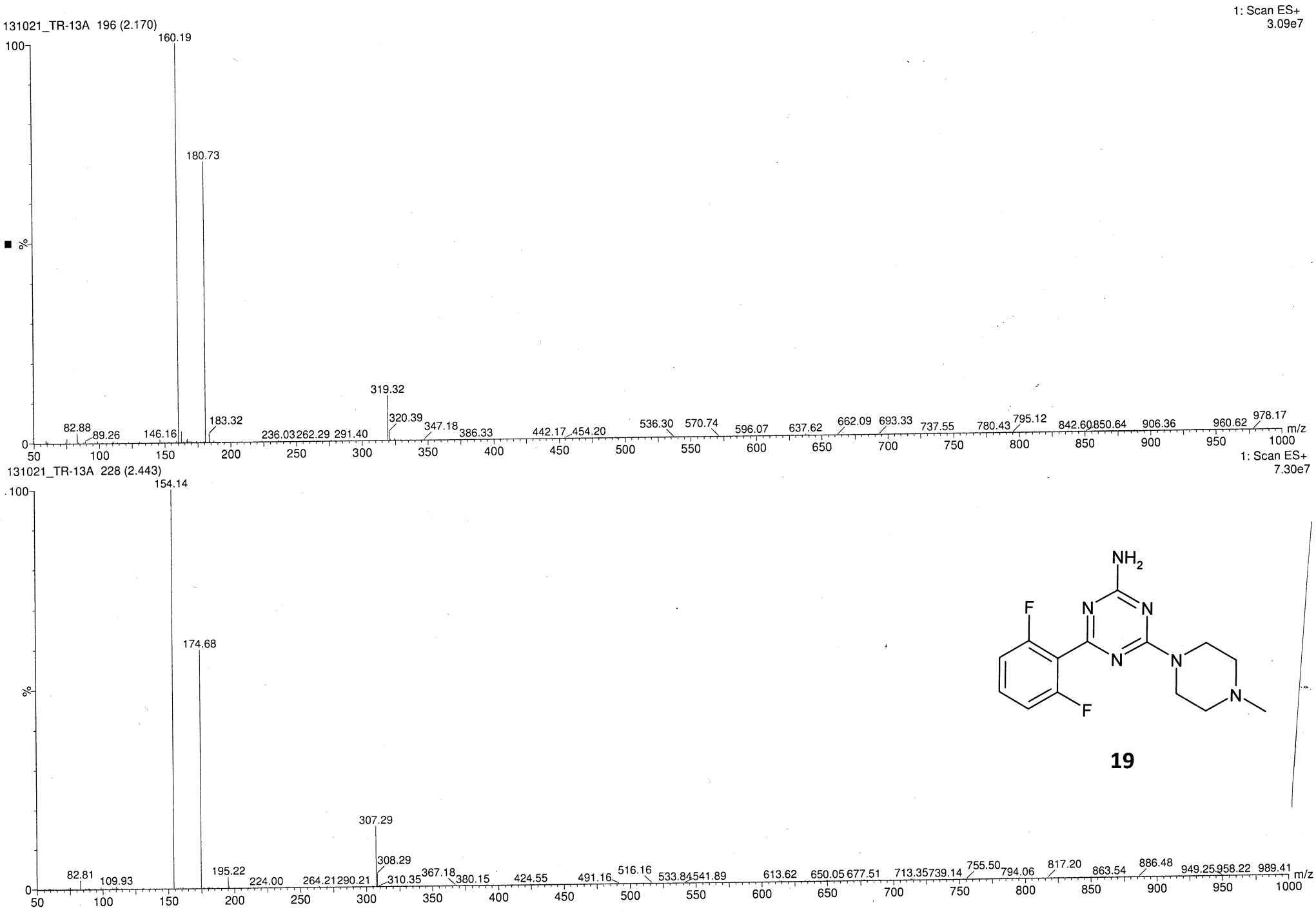
131021_TR-13A 196 (2.170)
1: Scan ES+
3.09e7
160.19
180.73
319.32
183.32
320.39
347.18
82.88
89.26
146.16
236.03
262.29
291.40
386.33
442.17
454.20
536.30
570.74
596.07
637.62
662.09
693.33
737.55
780.43
795.12
842.60
850.64
906.36
960.62
978.17
m/z
131021_TR-13A 228 (2.443)
1: Scan ES+
7.30e7
154.14
174.68
307.29
308.29
82.81
109.93
195.22
224.00
264.21
290.21
310.35
367.18
380.15
424.55
491.16
516.16
533.84
541.89
613.62
650.05
677.51
713.35
739.14
755.50
794.06
817.20
863.54
886.48
949.25
958.22
989.41
m/z
NH2
F
N
N
N
N
N
F
19

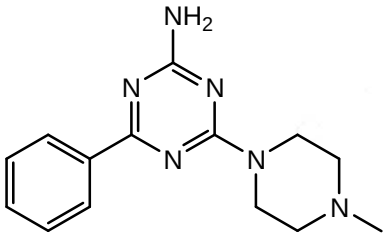
NH2
N
N
N
N
N

3

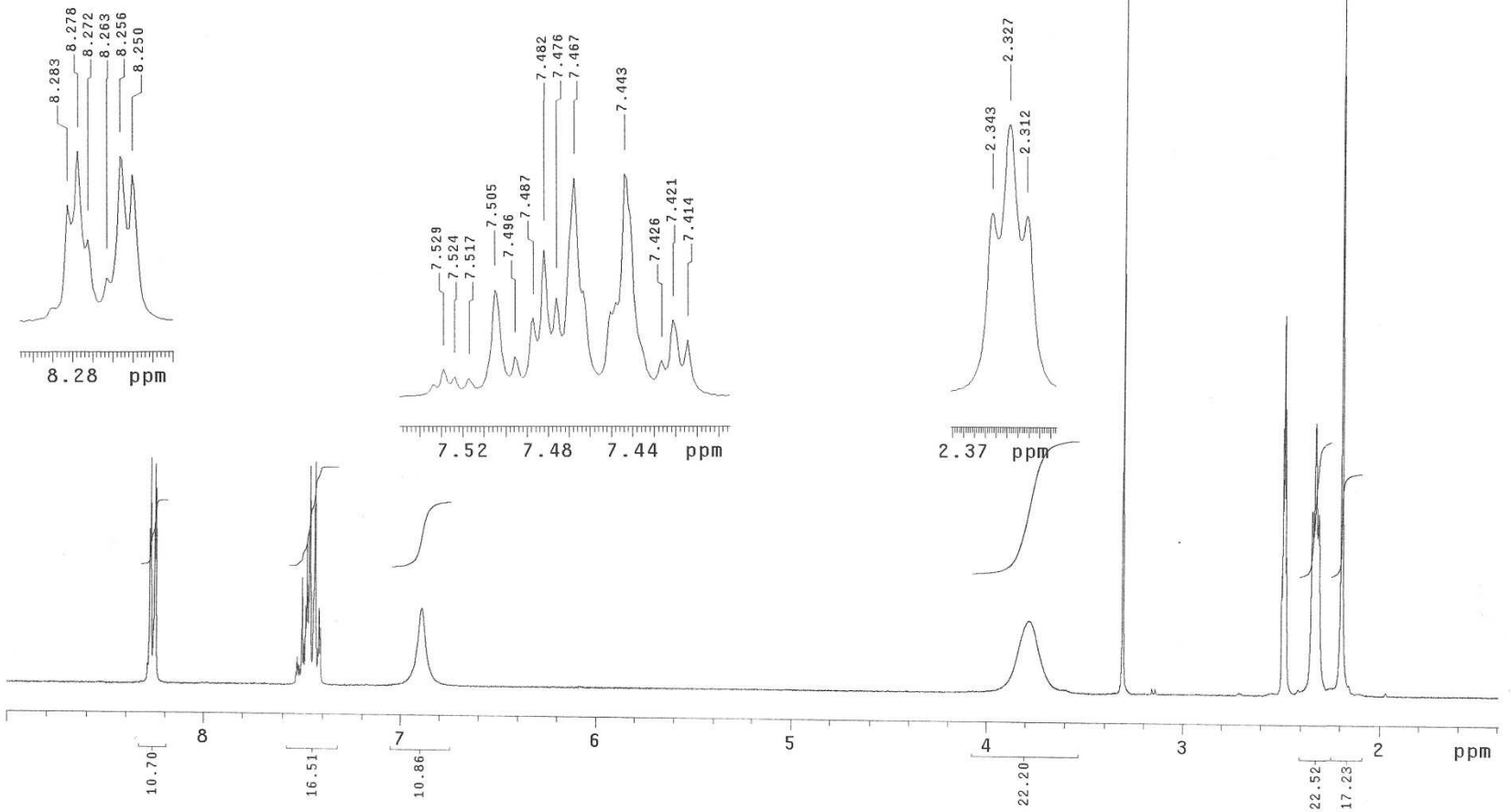
8.283
8.278
8.272
8.263
8.256
8.250
8.28 ppm
7.529
7.524
7.517
7.505
7.496
7.487
7.482
7.476
7.467
7.443
7.426
7.421
7.414
7.52 7.48 7.44 ppm
2.343
2.327
2.312
2.37 ppm
8
7
6
5
4
3
2
ppm
10.70
16.51
10.86
22.20
22.52
17.23

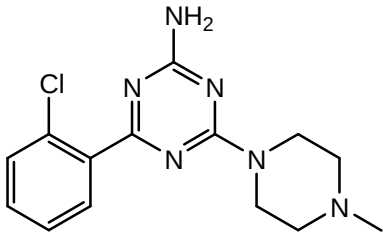
NH2
Cl
N
N
N
N
N

4

7.612
7.607
7.603
7.589
7.581
7.498
7.492
7.475
7.472
7.467
7.449
7.442
7.425
7.418
7.402
7.395
7.392
7.378
7.372
7.354
7.349
7.64 7.58 7.52 7.46 7.40 ppm
8
7
6
5
4
3
2
ppm
5.53
16.78
11.76
23.69
24.28
17.96

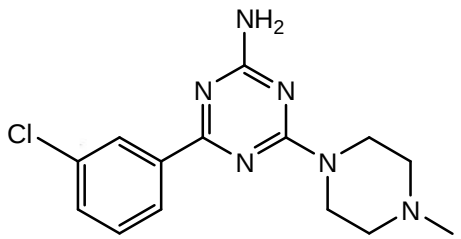
NH2
N
N
N
N
N
Cl

5

8.238
8.231
8.225
8.199
8.24 8.21 ppm
7.591
7.564
7.518
7.492
7.466
7.56 7.50 ppm
9
8
7
6
5
4
3
2
ppm
10.58
11.25
11.55
24.21
23.85
18.56

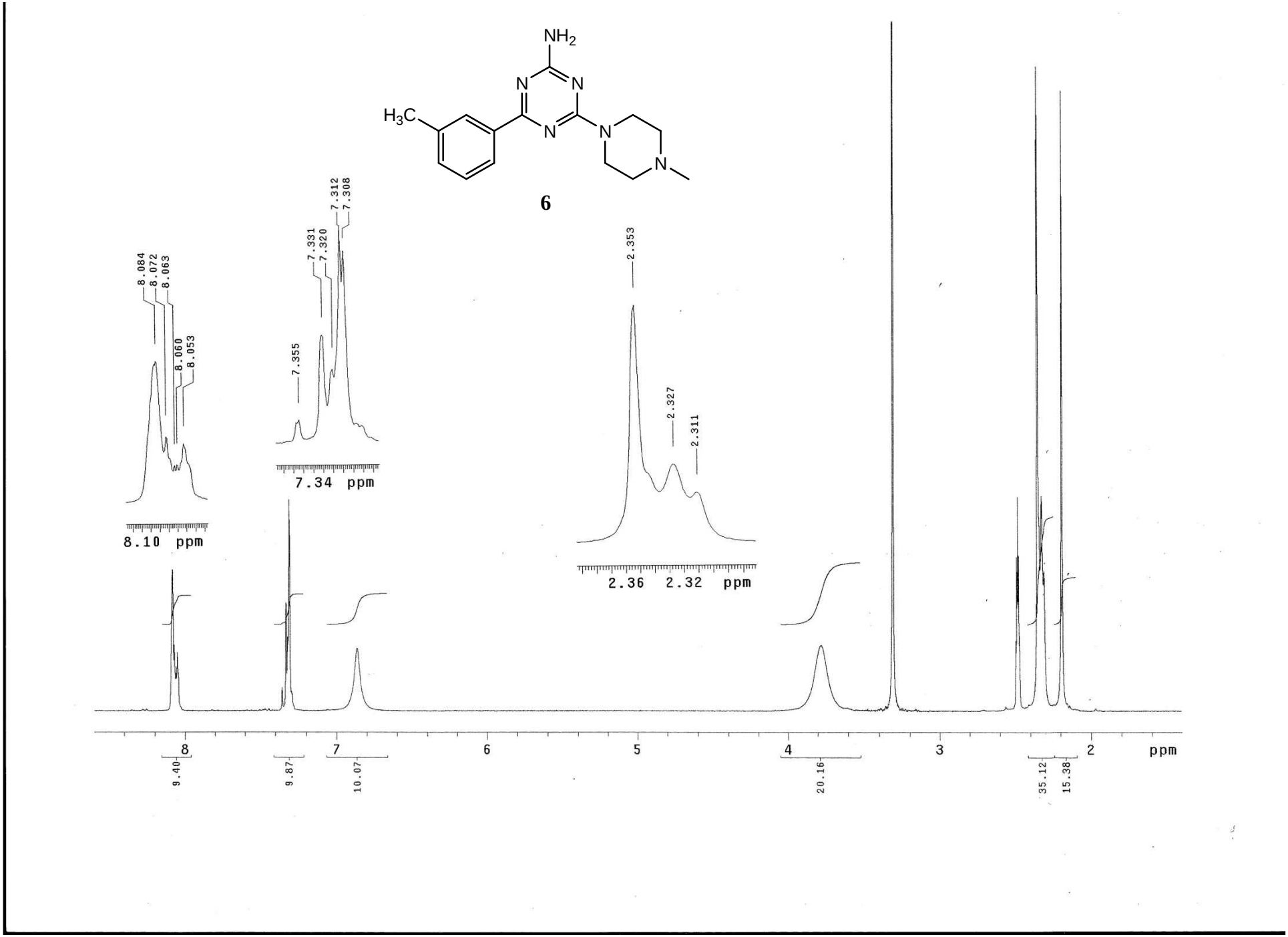
NH2
N
N
N
N
N
N
H3C
6
8.084
8.072
8.063
8.060
8.053
8.10 ppm
7.355
7.331
7.320
7.312
7.308
7.34 ppm
2.353
2.327
2.311
2.36 2.32 ppm
8
7
6
5
4
3
2
ppm
9.40
9.87
10.07
20.16
35.12
15.38

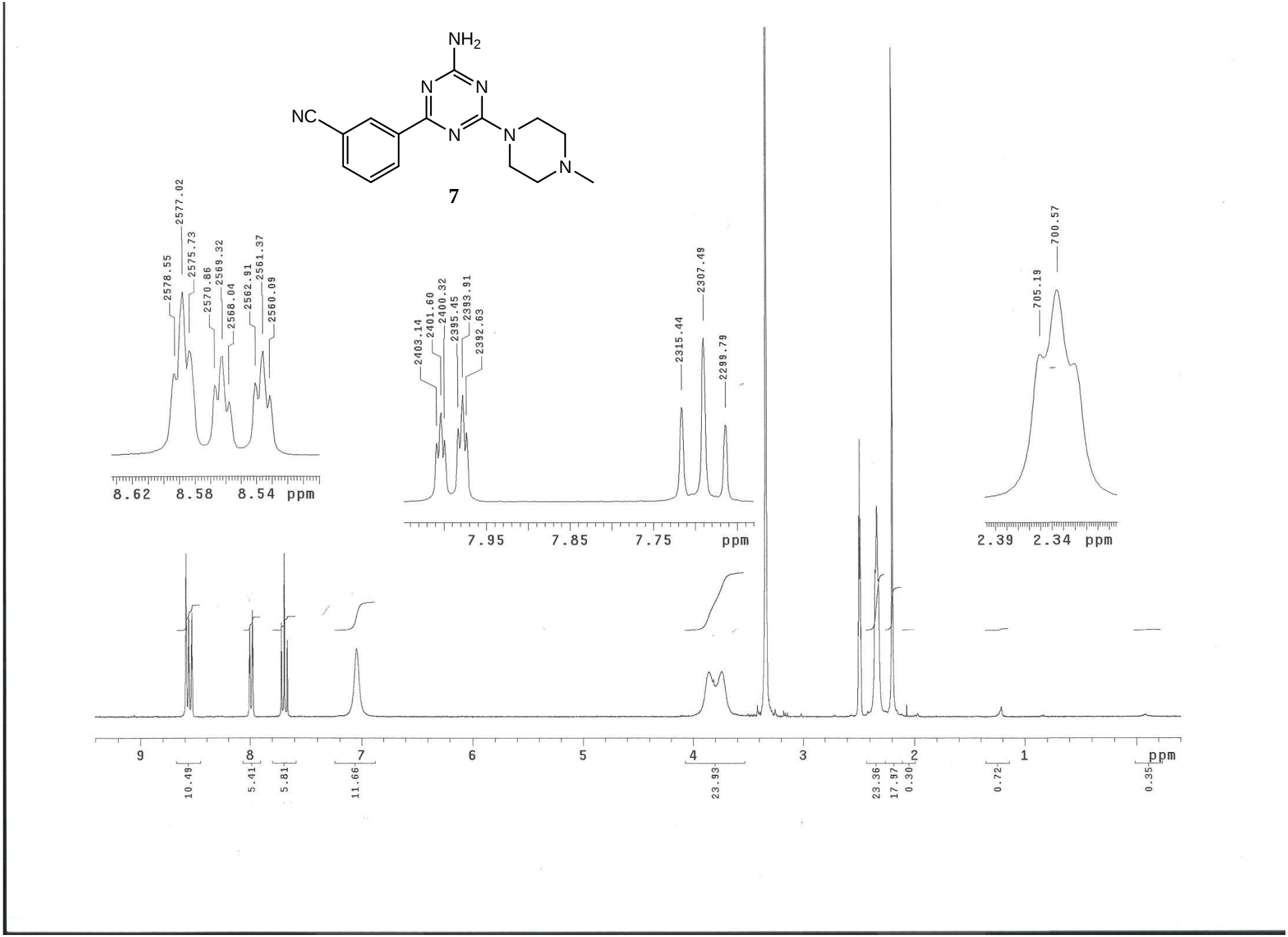
NH2
N
N
N
N
N
NC
7
2578.55
2577.02
2575.73
2570.86
2569.32
2568.04
2562.91
2561.37
2560.09
8.62 8.58 8.54 ppm
2403.14
2401.60
2400.32
2395.45
2393.91
2392.63
2315.44
2307.49
2299.79
7.95 7.85 7.75 ppm
705.19
700.57
2.39 2.34 ppm
9 8 7 6 5 4 3 2 1 ppm
10.49
5.41
5.81
11.66
23.93
23.36
17.97
0.30
0.72
0.35

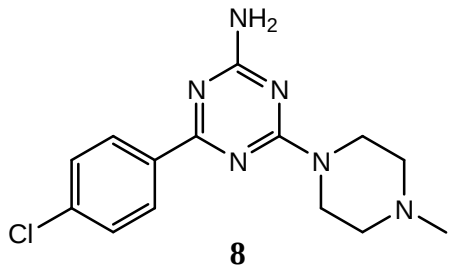

8

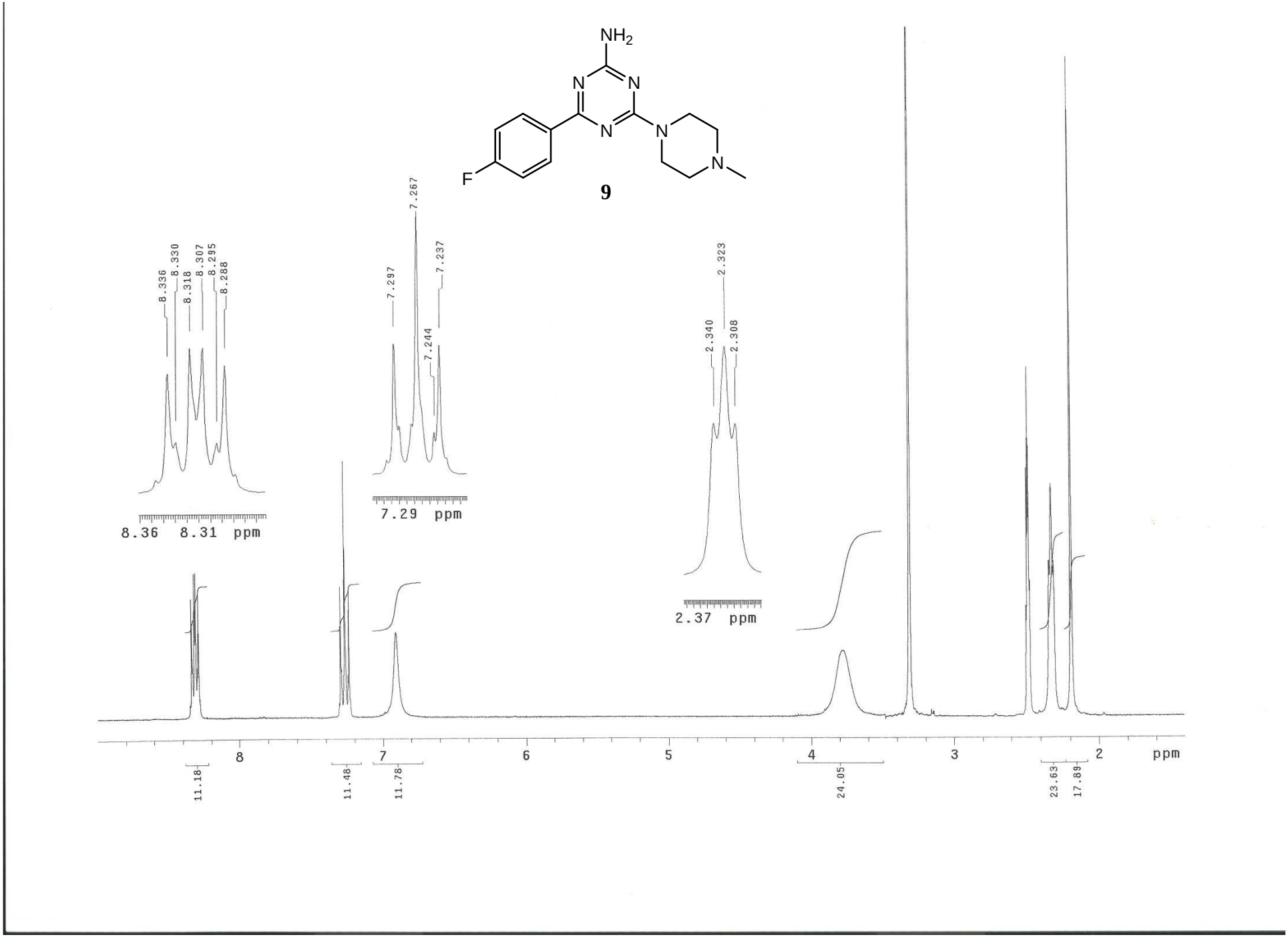
NH2
N
N
N
N
N
F
9
8.336
8.330
8.318
8.307
8.295
8.288
8.36 8.31 ppm
7.297
7.267
7.244
7.237
7.29 ppm
2.340
2.323
2.308
2.37 ppm
8
7
6
5
4
3
2
ppm
11.18
11.48
11.78
24.05
23.63
17.89

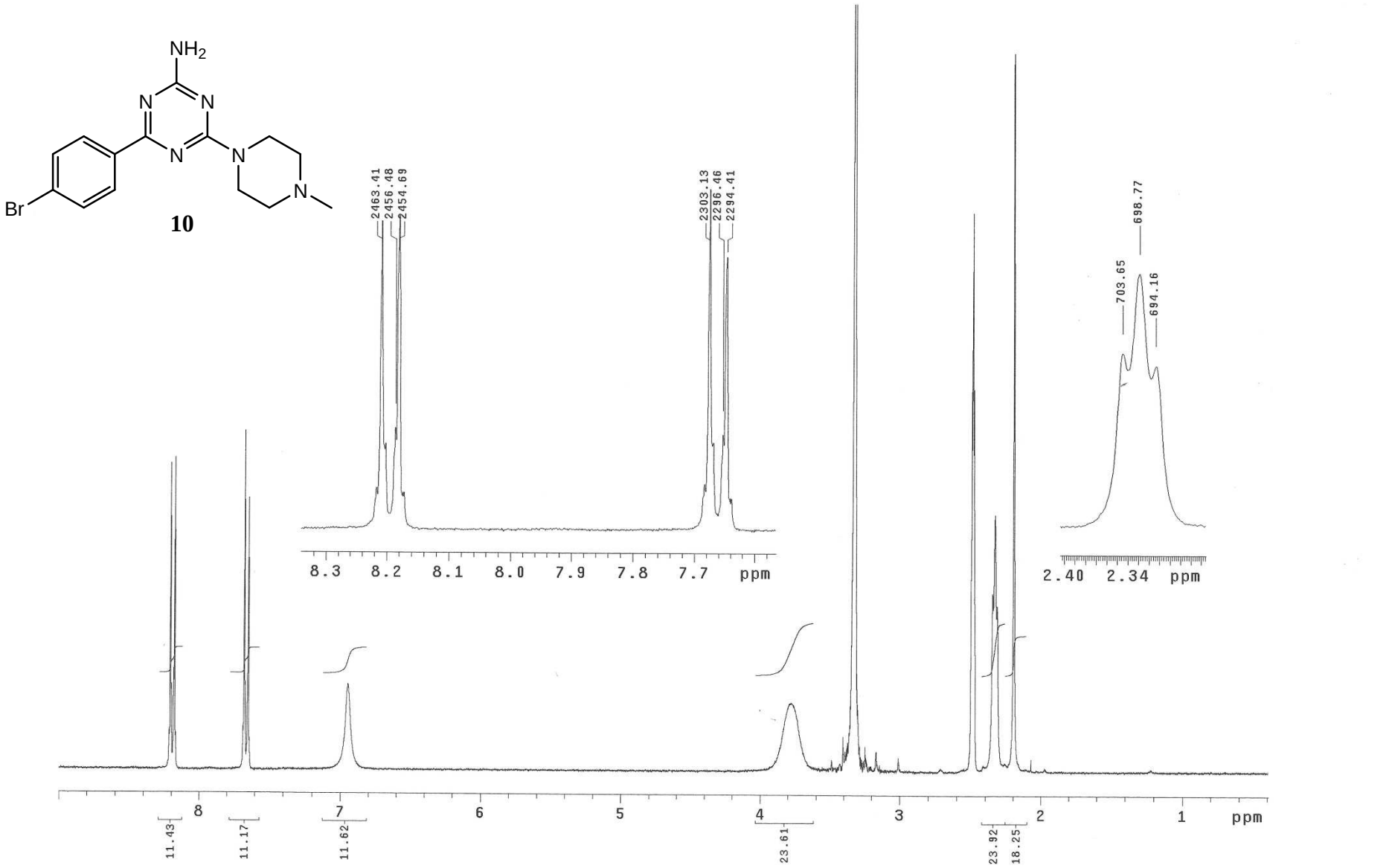
NH2
N
N
N
N
N
Br
10
2463.41
2456.48
2454.69
2303.13
2296.46
2294.41
703.65
698.77
694.16
8.3
8.2
8.1
8.0
7.9
7.8
7.7
ppm
2.40
2.34
ppm
8
7
6
5
4
3
2
1
ppm
11.43
11.17
11.62
23.61
23.92
18.25

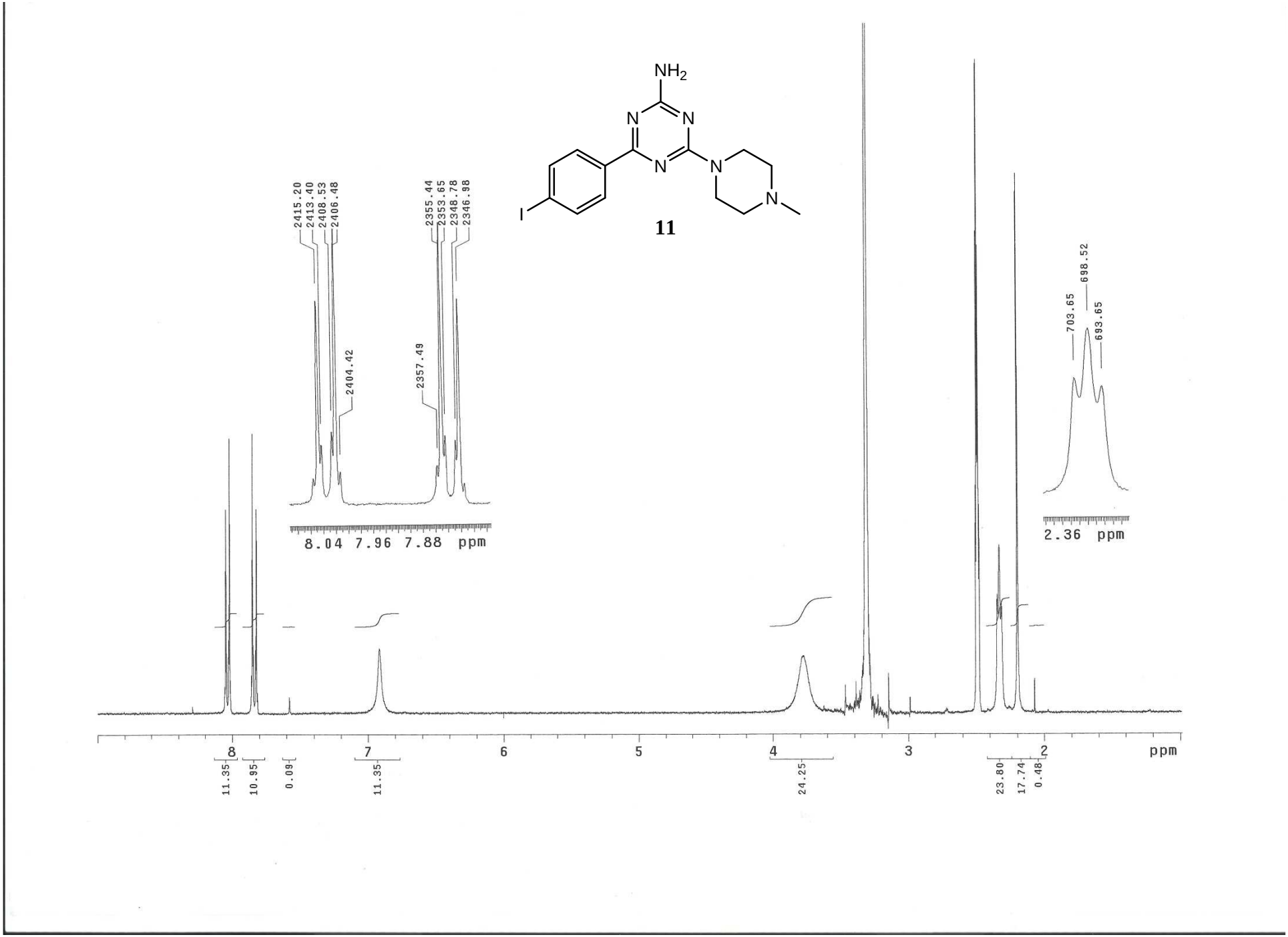
NH2
N
N
N
N
N
I
11
2415.20
2413.40
2408.53
2406.48
2404.42
2357.49
2355.44
2353.65
2348.78
2346.98
8.04 7.96 7.88 ppm
703.65
698.52
693.65
2.36 ppm
8
7
6
5
4
3
2
ppm
11.35
10.95
0.09
11.35
24.25
23.80
17.74
0.48

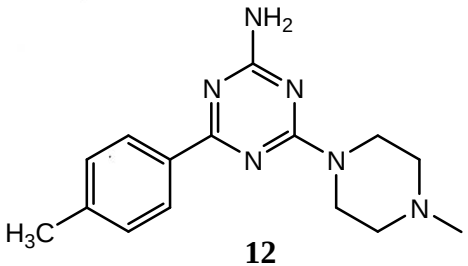
NH2
N
N
N
N
N
H3C

12

8.5
8.0
7.5
7.0
6.5
6.0
5.5
5.0
4.5
4.0
3.5
3.0
2.5
ppm
10.03
10.02
10.07
20.34
34.58
14.96

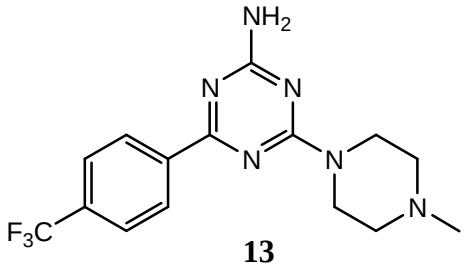
NH2
N
N
N
N
N
F3C

13

8.5
8.0
7.5
7.0
6.5
6.0
5.5
5.0
4.5
4.0
3.5
3.0
2.5
2.0
1.5
1.0
ppm
1.00
1.00
0.98
1.98
1.92
1.49
0.20

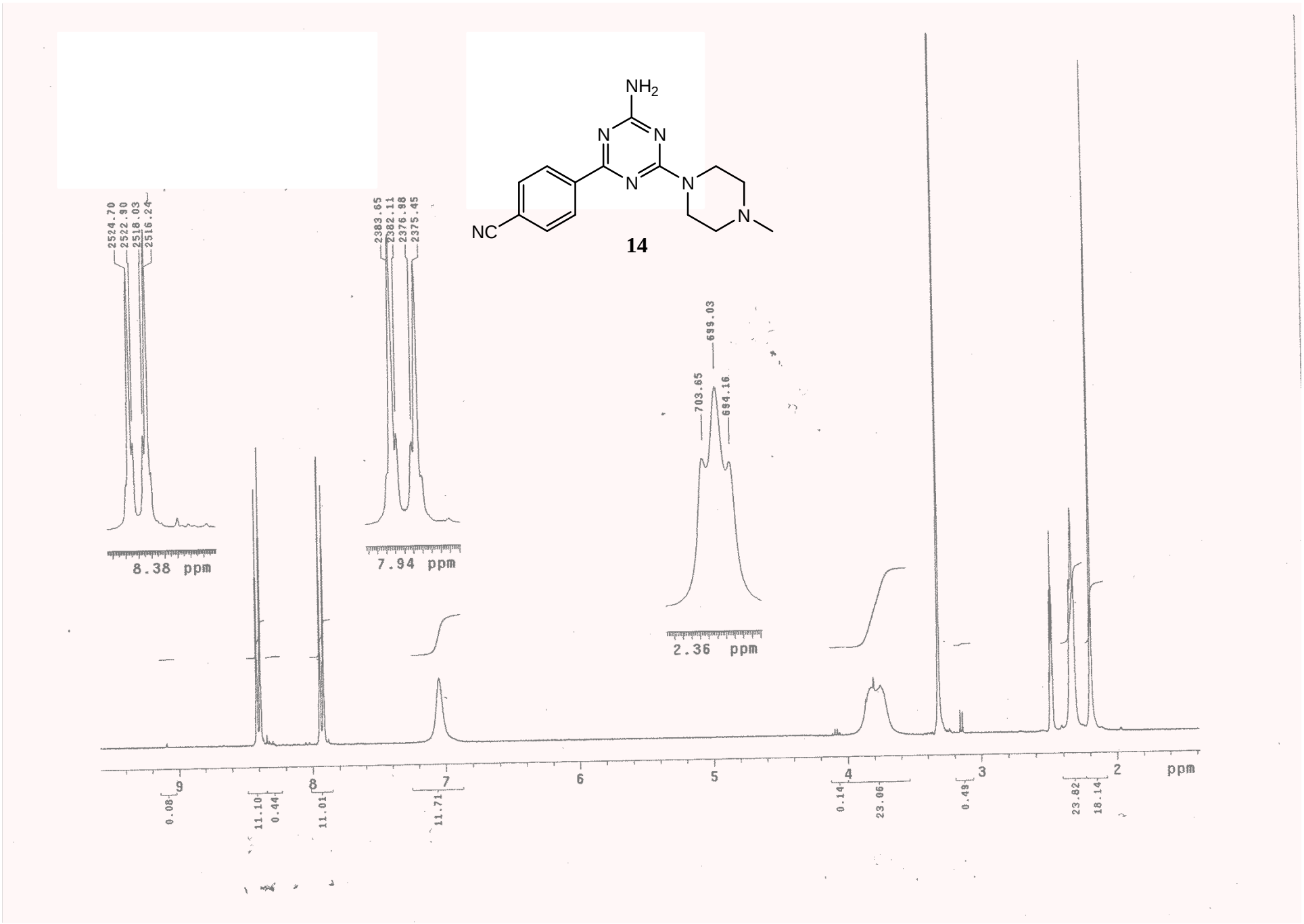
NH2
N
N
N
N
N
NC
14
2524.70
2522.90
2518.03
2516.24
8.38 ppm
2383.65
2382.11
2376.98
2375.45
7.94 ppm
699.03
703.65
694.16
2.36 ppm
9
8
7
6
5
4
3
2
ppm
0.08
11.10
0.44
11.01
11.71
0.14
23.06
0.49
23.82
18.14


NH2
N
N
N
N
N
(H3C)2N
15
2438.79
2429.81
8.12 ppm
2015.90
2006.93
1997.69
6.73 6.67 ppm
698.52
693.65
689.03
2.35 ppm
8
7
6
5
4
3
2
ppm
8.47
17.26
16.94
26.52
17.17
13.63

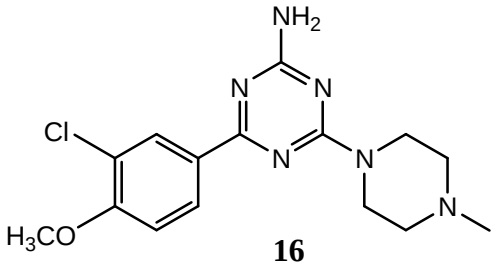
NH2
N
N
N
N
N
Cl
H3CO

16

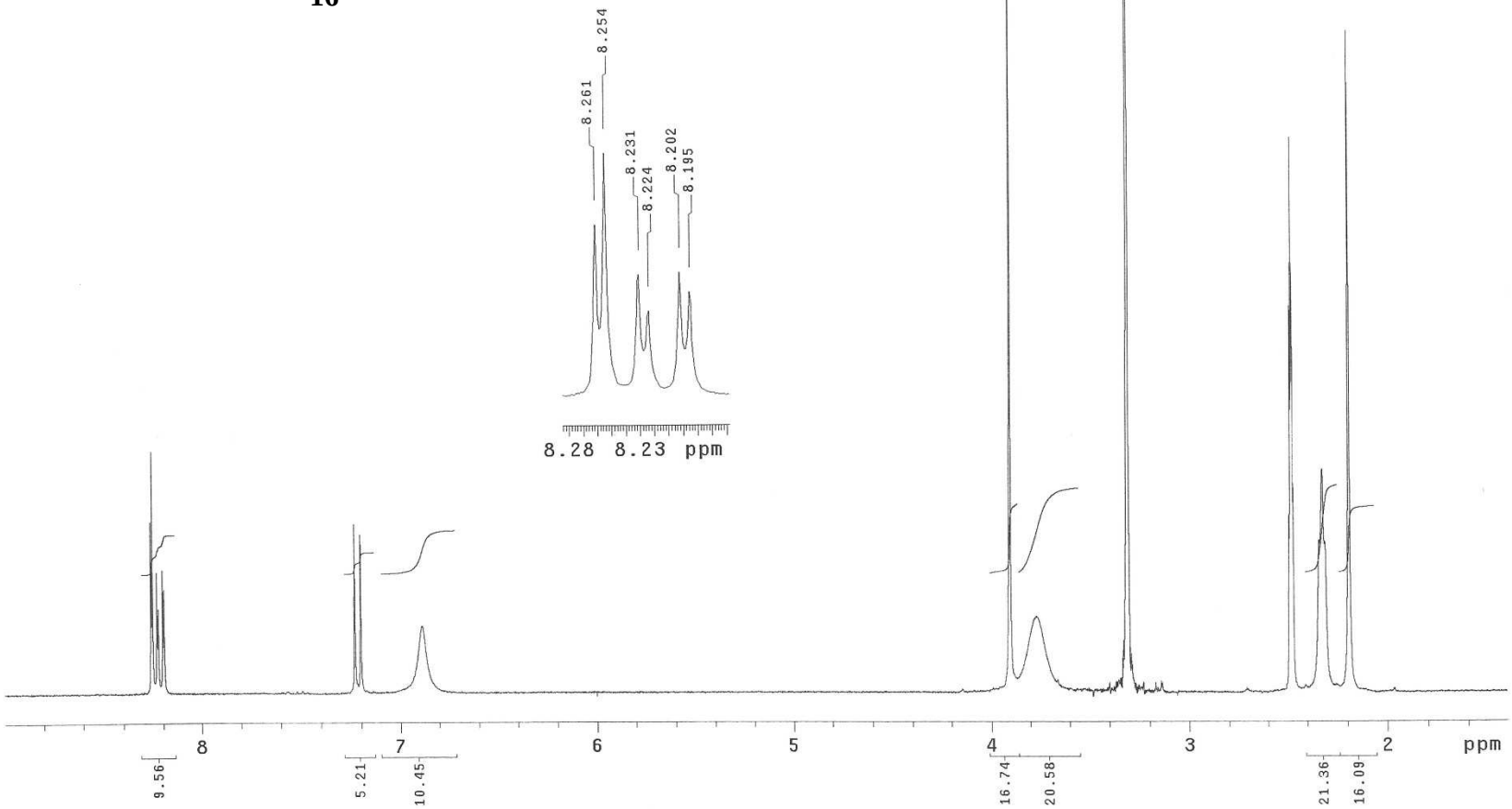
8.261
8.254
8.231
8.224
8.202
8.195
8.28 8.23 ppm
8
7
6
5
4
3
2
ppm
9.56
5.21
10.45
16.74
20.58
21.36
16.09

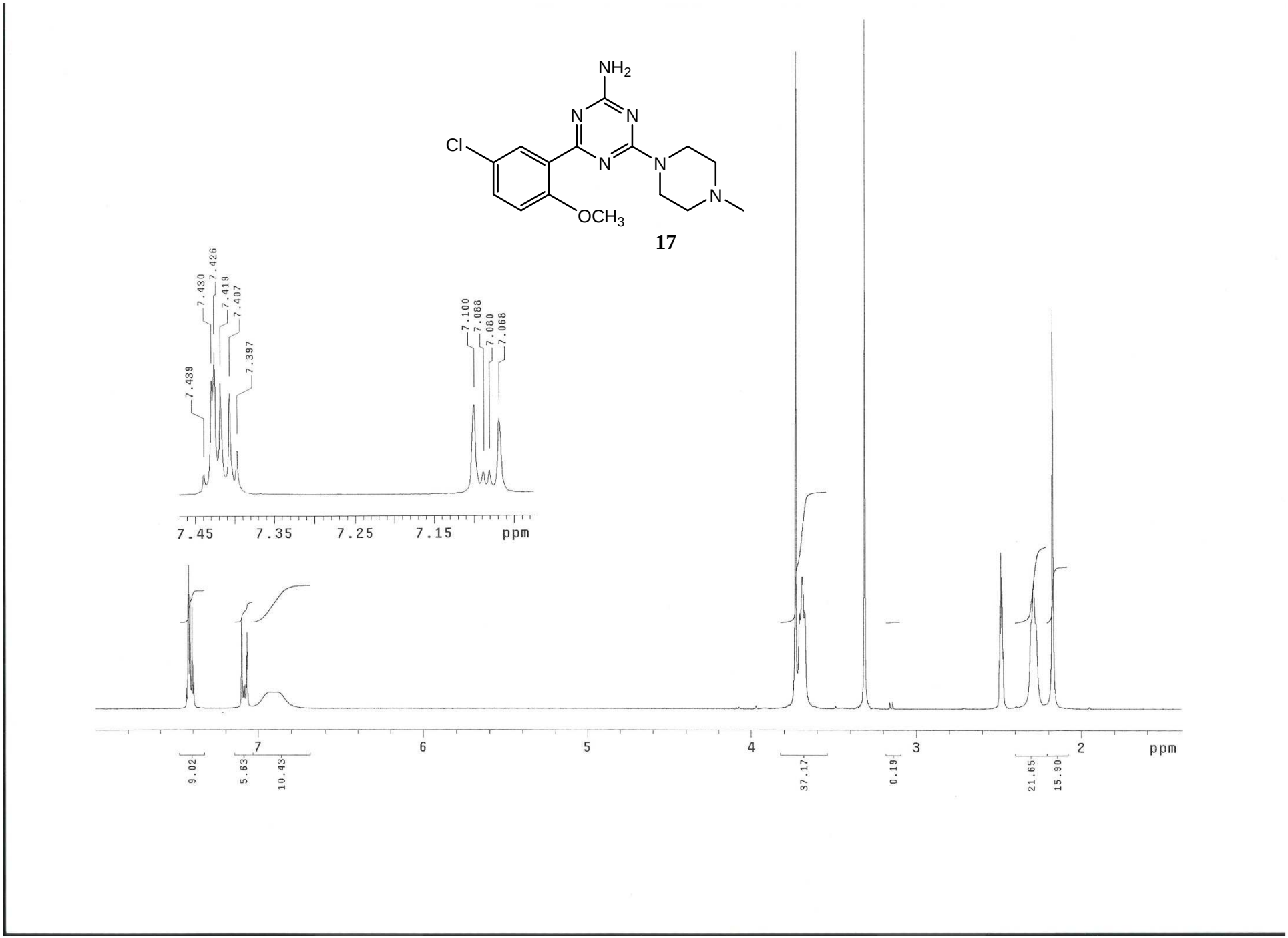
NH2
N
N
N
N
N
Cl
OCH3
7.439
7.430
7.426
7.419
7.407
7.397
7.100
7.088
7.080
7.068
7.45
7.35
7.25
7.15
ppm
7
6
5
4
3
2
ppm
9.02
5.63
10.43
37.17
0.19
21.65
15.90

17

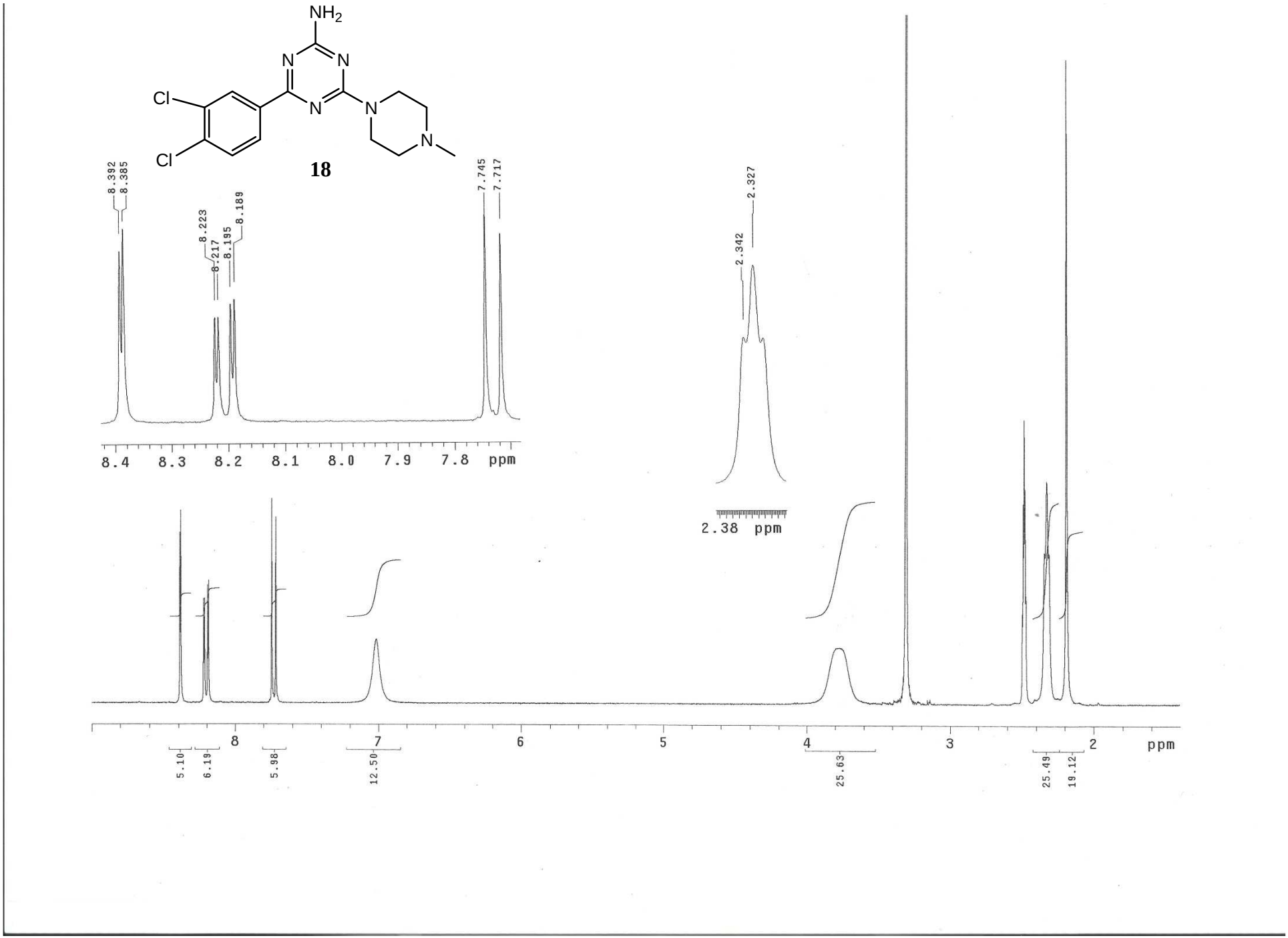
NH2
N
N
N
N
N
Cl
Cl
18
8.392
8.385
8.223
8.217
8.195
8.189
7.745
7.717
8.4
8.3
8.2
8.1
8.0
7.9
7.8
ppm
2.342
2.327
2.38 ppm
8
7
6
5
4
3
2
ppm
5.10
6.19
5.98
12.50
25.63
25.49
19.12

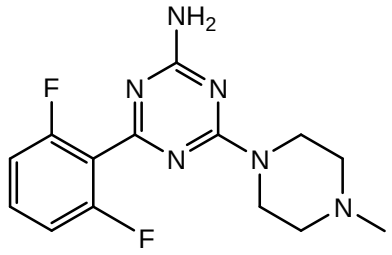
NH2
F
N
N
N
N
N
F

19

2262.61
2256.20
2254.14
2247.73
2240.81
2239.27
2232.60
2152.59
2144.64
2136.43
2132.59
7.50
7.40
7.30
7.20
ppm
8
7
6
5
4
3
2
1
ppm
6.10
24.11
25.17
25.28
18.99
0.35

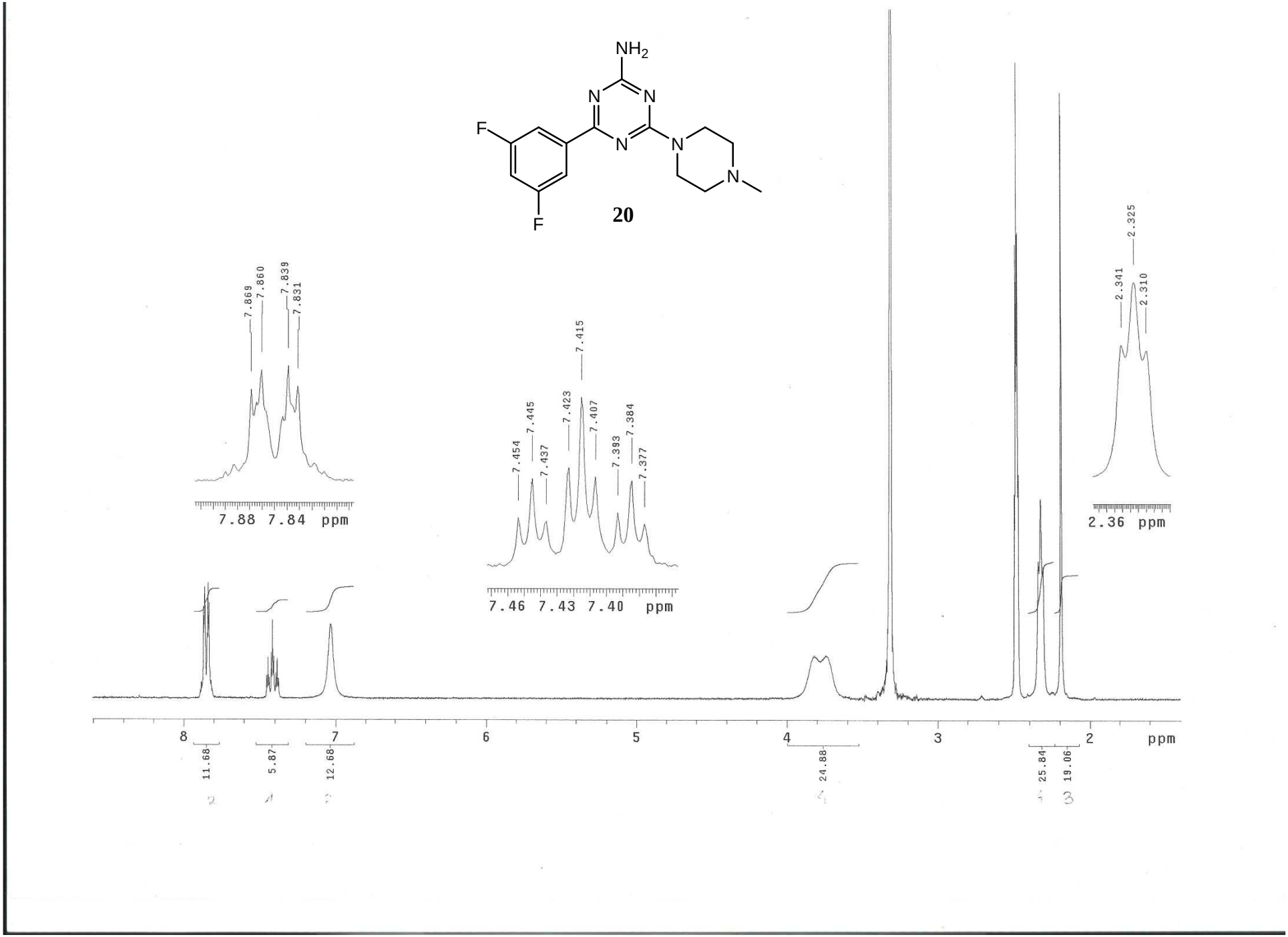
NH2
N
N
N
N
N
F
F
20
7.869
7.860
7.839
7.831
7.88 7.84 ppm
7.454
7.445
7.437
7.423
7.415
7.407
7.393
7.384
7.377
7.46 7.43 7.40 ppm
2.341
2.325
2.310
2.36 ppm
8
7
6
5
4
3
2
ppm
11.68
5.87
12.68
24.88
25.84
19.06

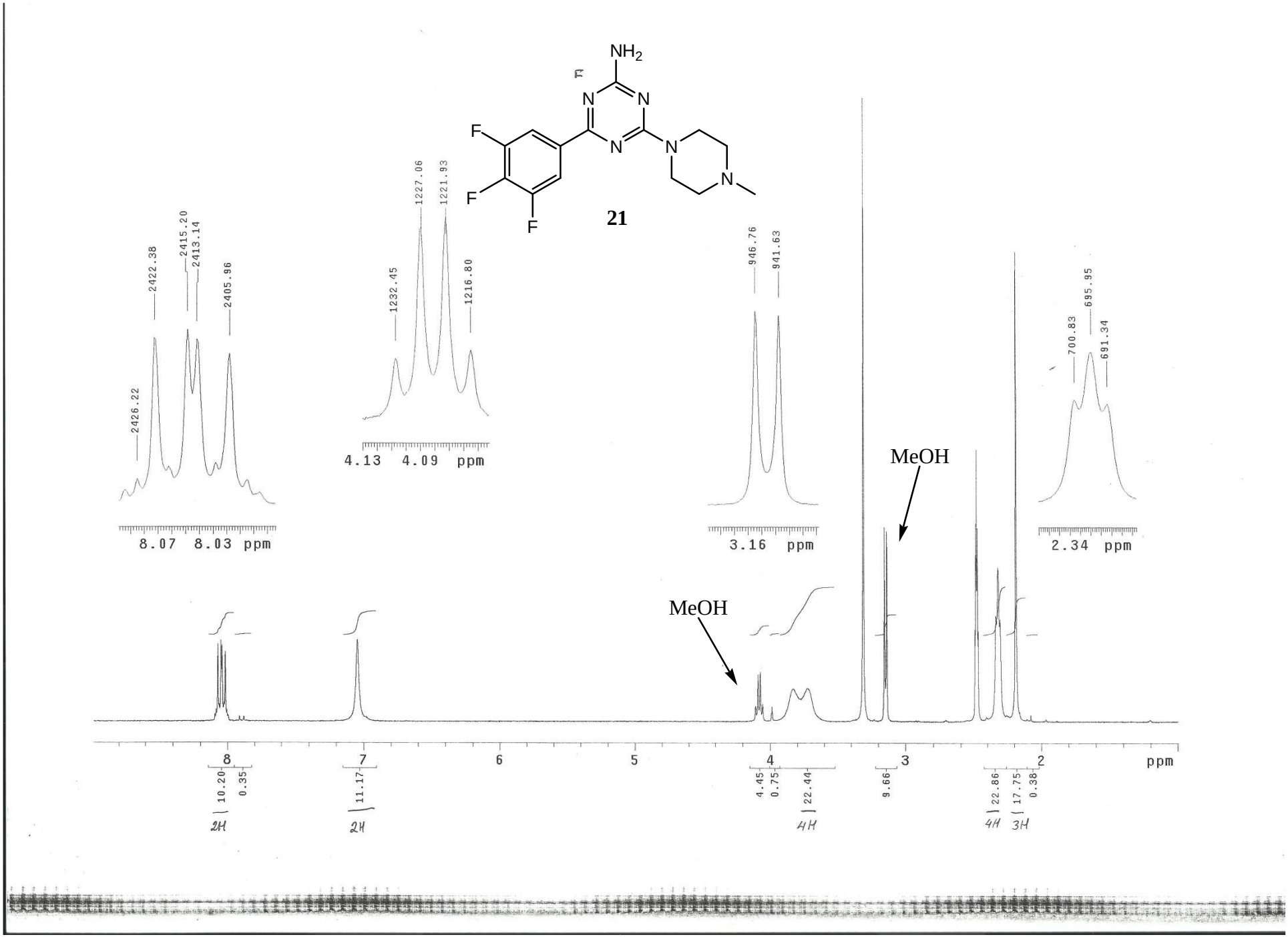
NH2
F
F
F
N
N
N
N
N
21
2426.22
2422.38
2415.20
2413.14
2405.96
8.07 8.03 ppm
1232.45
1227.06
1221.93
1216.80
4.13 4.09 ppm
946.76
941.63
3.16 ppm
MeOH
MeOH
700.83
695.95
691.34
2.34 ppm
8
7
6
5
4
3
2
ppm
10.20
0.35
11.17
4.45
0.75
22.44
9.66
22.86
17.75
0.38
2H
2H
4H
4H
3H

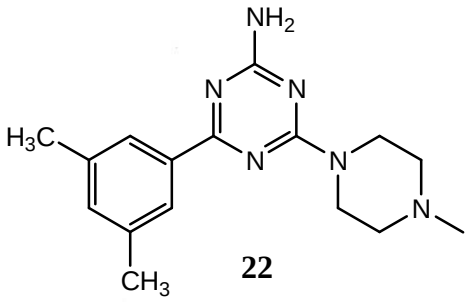

22

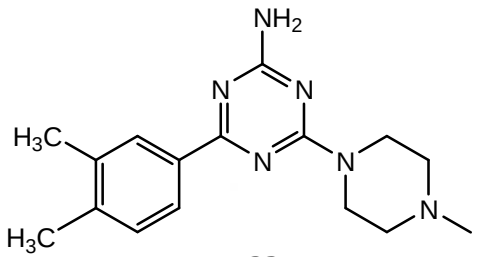
NH2
N
N
N
N
N
N
H3C
H3C

23

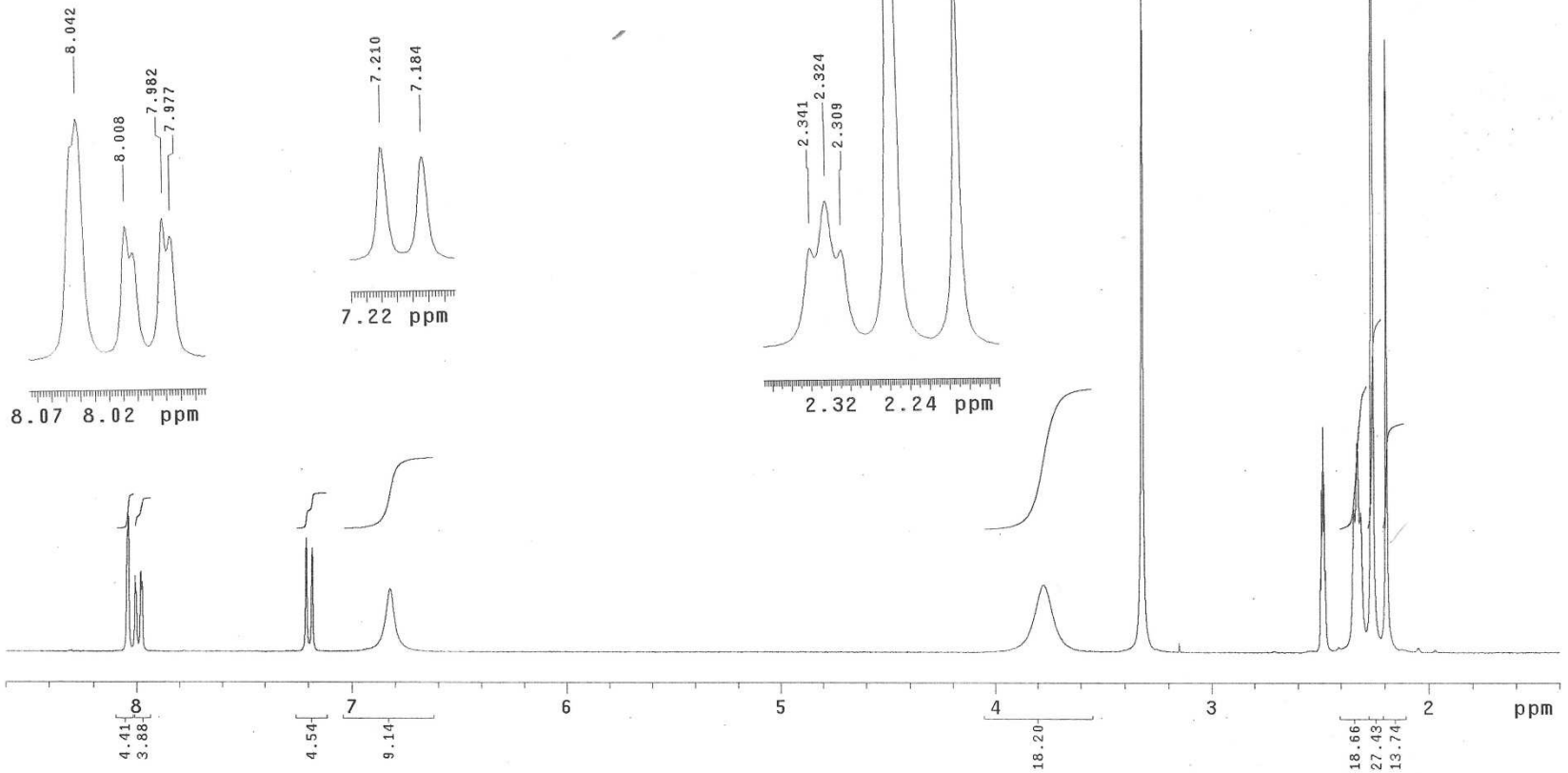
8.042
8.008
7.982
7.977
8.07 8.02 ppm
7.210
7.184
7.22 ppm
2.341
2.324
2.309
2.257
2.192
2.32 2.24 ppm
8
7
6
5
4
3
2
ppm
4.41
3.88
4.54
9.14
18.20
18.66
27.43
13.74

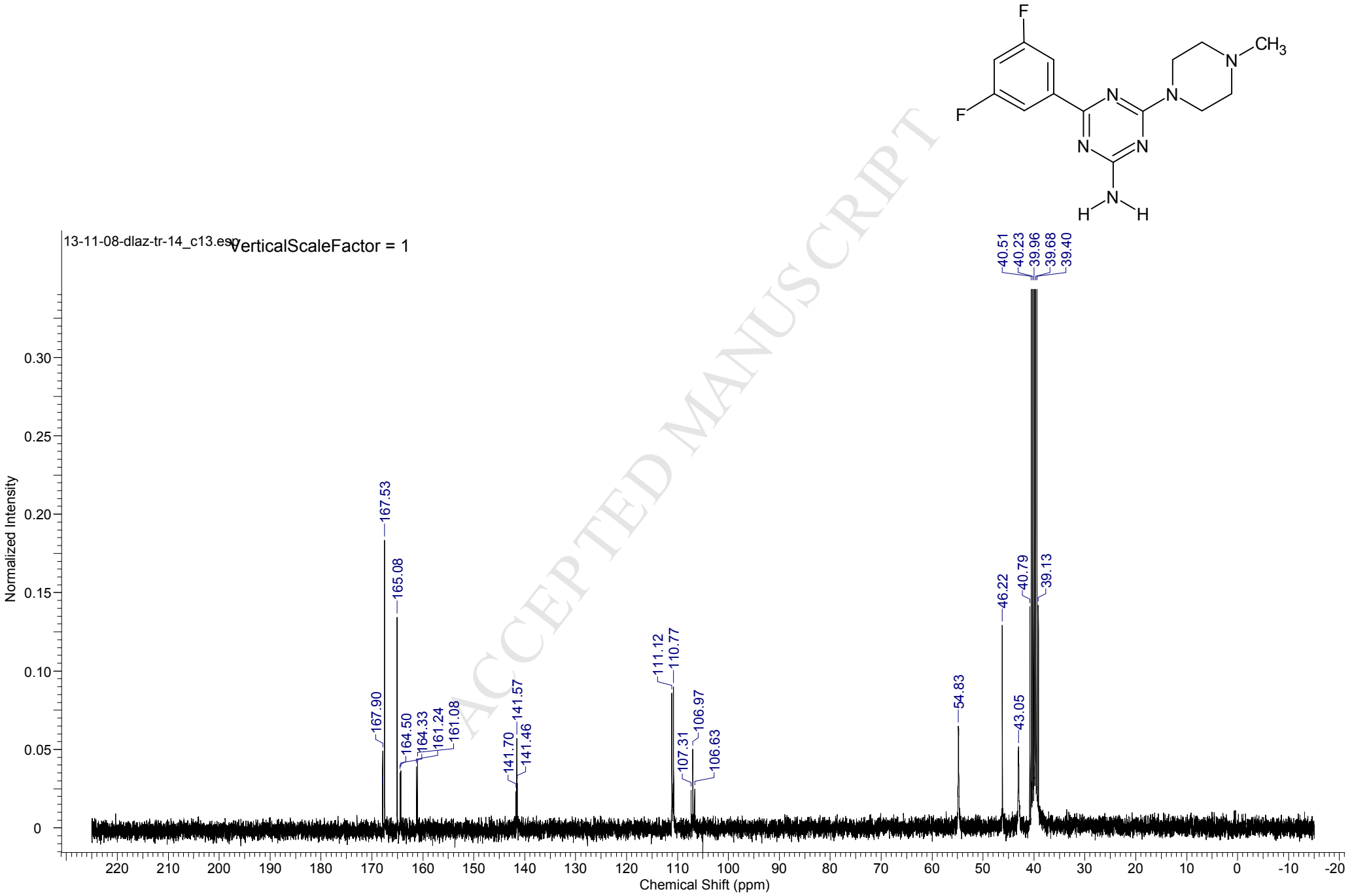

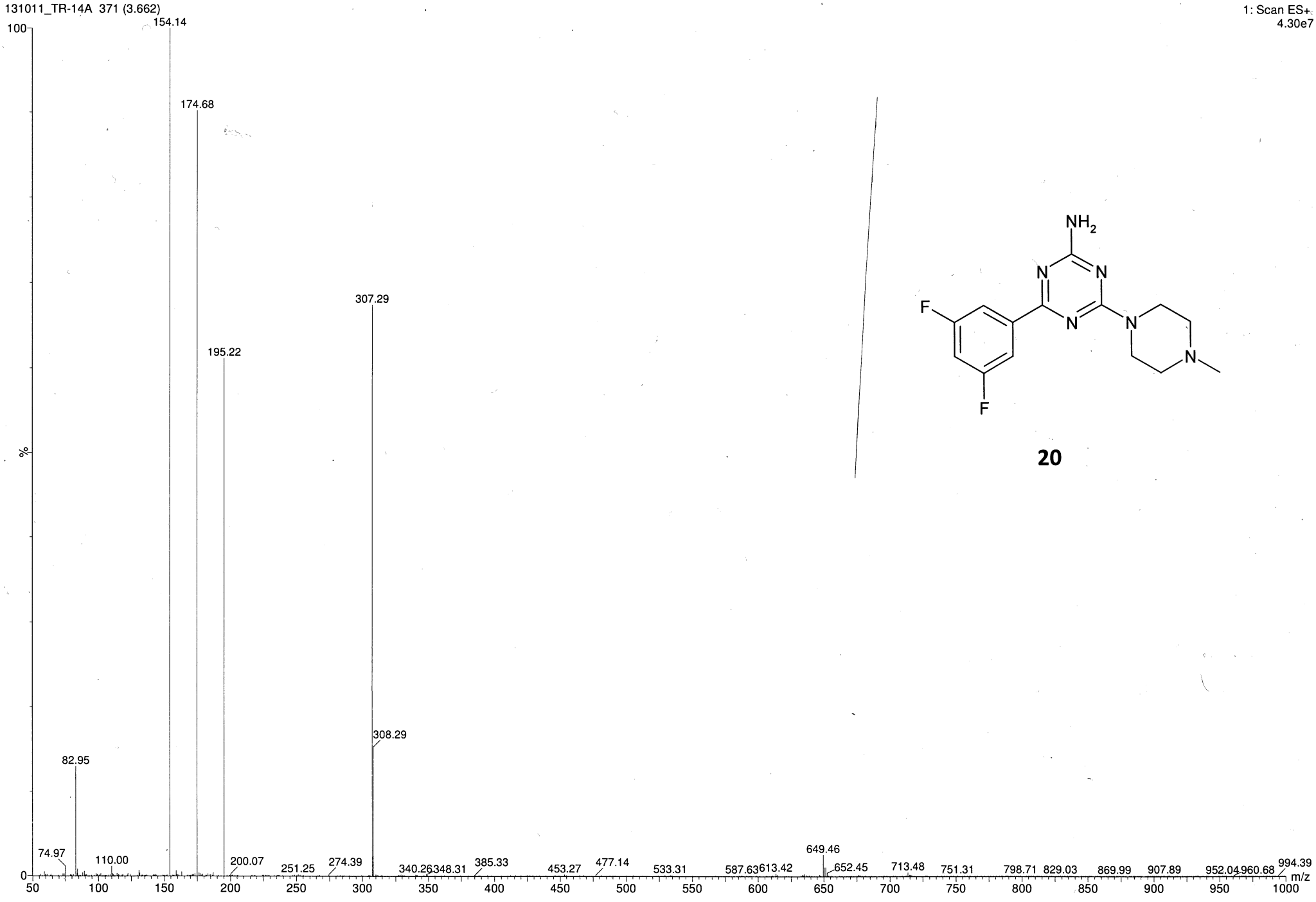
131011_TR-14A 371 (3.662)
1: Scan ES+
4.30e7
100
%
0
154.14
174.68
195.22
307.29
308.29
82.95
74.97
110.00
200.07
251.25
274.39
340.26
348.31
385.33
453.27
477.14
533.31
587.63
613.42
649.46
652.45
713.48
751.31
798.71
829.03
869.99
907.89
952.04
960.68
994.39
m/z
50
100
150
200
250
300
350
400
450
500
550
600
650
700
750
800
850
900
950
1000

NH2
N
N
N
N
N
F
F

20

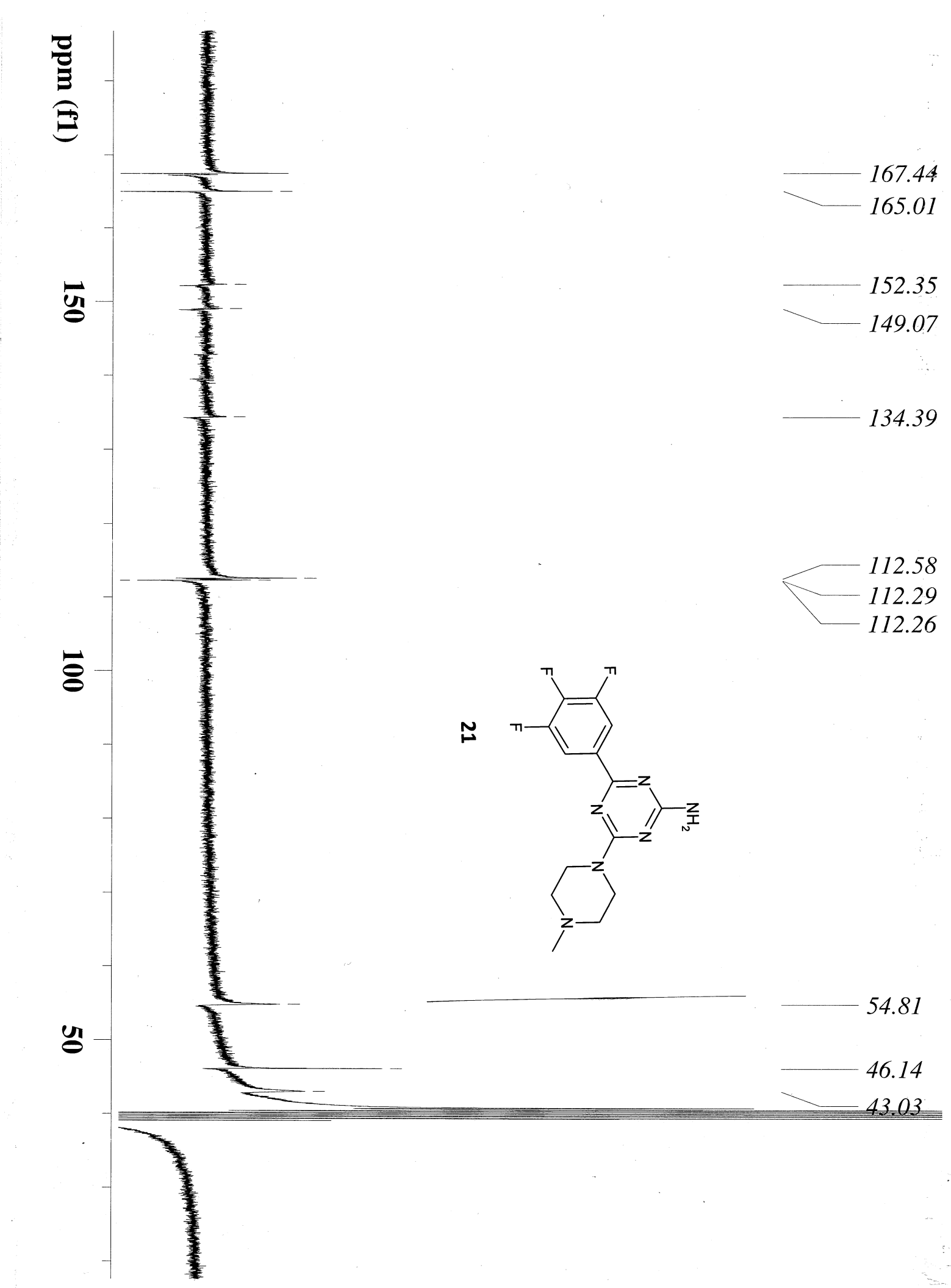
ppm (f1)
150
100
50
167.44
165.01
152.35
149.07
134.39
112.58
112.29
112.26
54.81
46.14
43.03
21
F
F
F
N
N
N
NH2
N
N

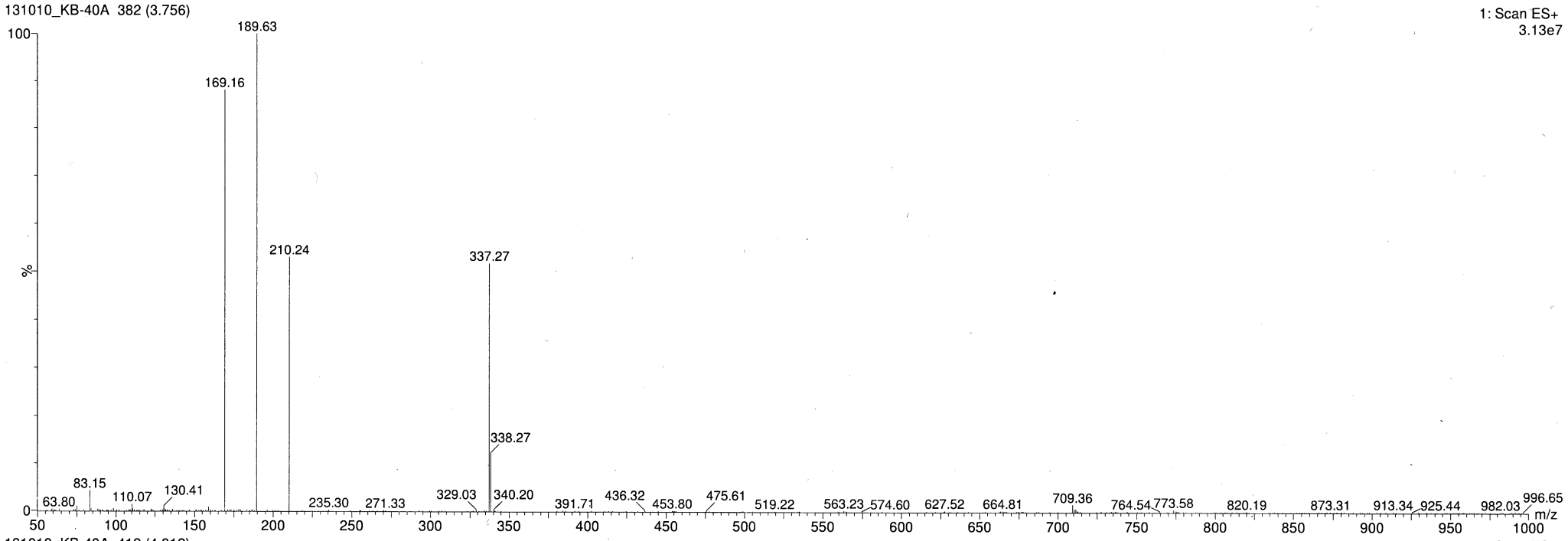
131010_KB-40A 382 (3.756)
1: Scan ES+
3.13e7
100
%
0
189.63
169.16
210.24
337.27
338.27
83.15
63.80
110.07
130.41
235.30
271.33
329.03
340.20
391.71
436.32
453.80
475.61
519.22
563.23
574.60
627.52
664.81
709.36
764.54
773.58
820.19
873.31
913.34
925.44
982.03
996.65
m/z
50
100
150
200
250
300
350
400
450
500
550
600
650
700
750
800
850
900
950
1000

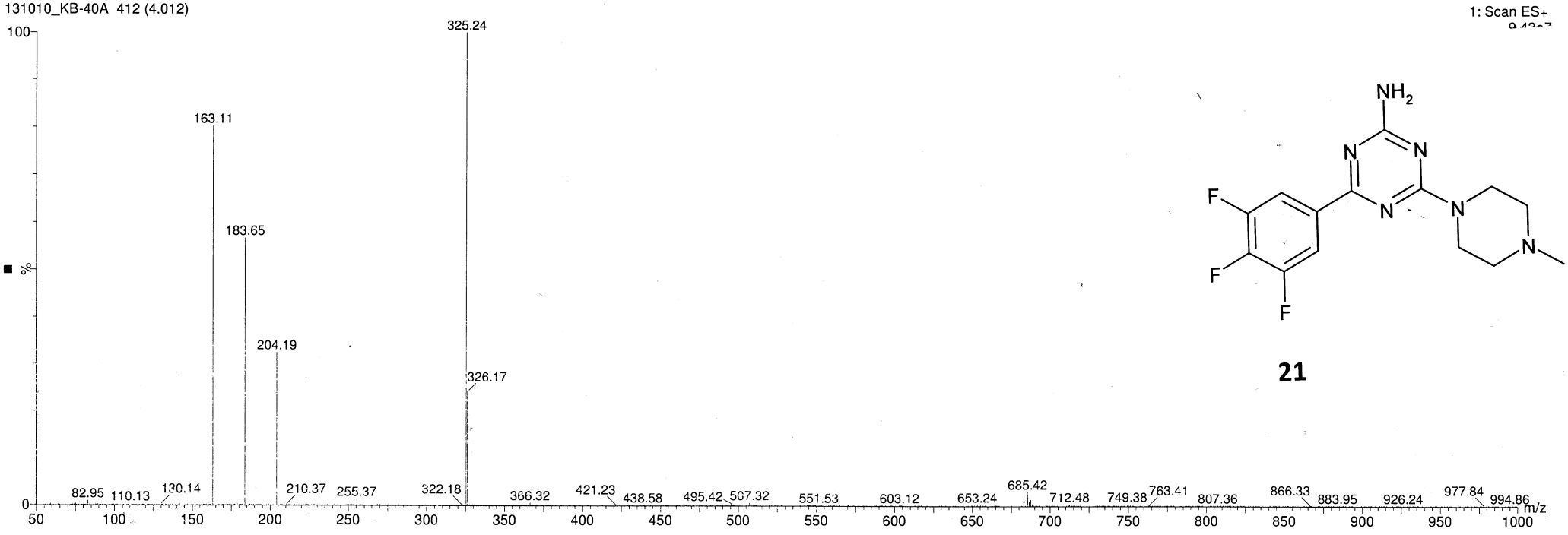
131010_KB-40A 412 (4.012)
1: Scan ES+
100
%
0
325.24
163.11
183.65
204.19
326.17
82.95
110.13
130.14
210.37
255.37
322.18
366.32
421.23
438.58
495.42
507.32
551.53
603.12
653.24
685.42
712.48
749.38
763.41
807.36
866.33
883.95
926.24
977.84
994.86
m/z
50
100
150
200
250
300
350
400
450
500
550
600
650
700
750
800
850
900
950
1000

NH2
N
N
N
N
N
F
F
F

21

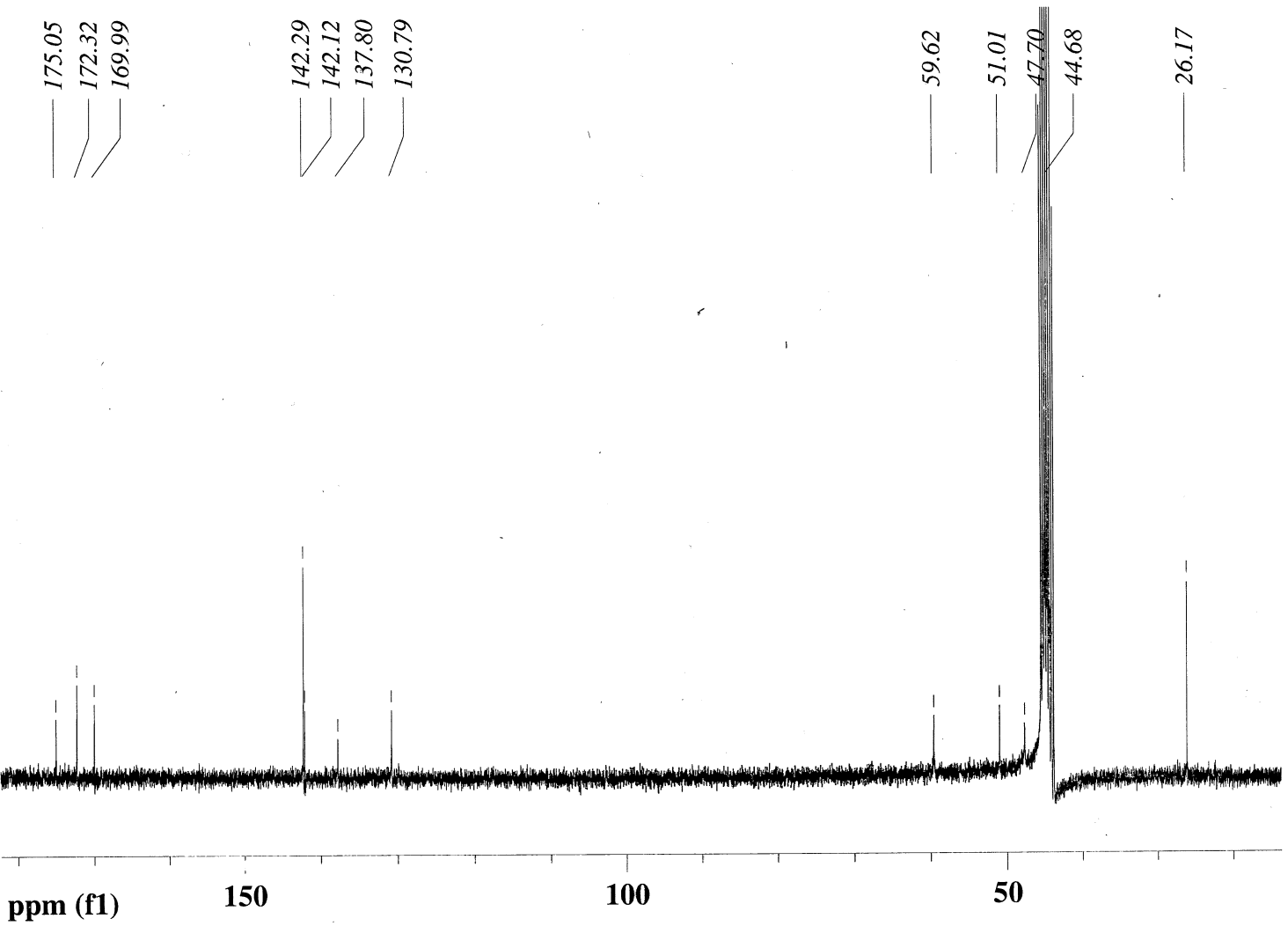
175.05
172.32
169.99
142.29
142.12
137.80
130.79
59.62
51.01
47.70
44.68
26.17
ppm (f1)
150
100
50

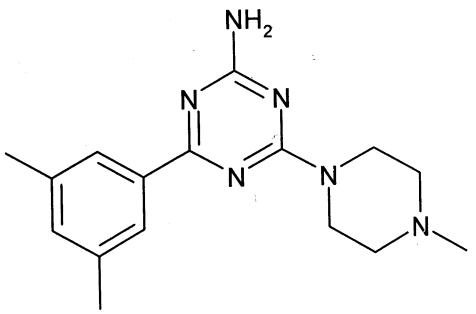
NH2
N
N
N
N
N

22

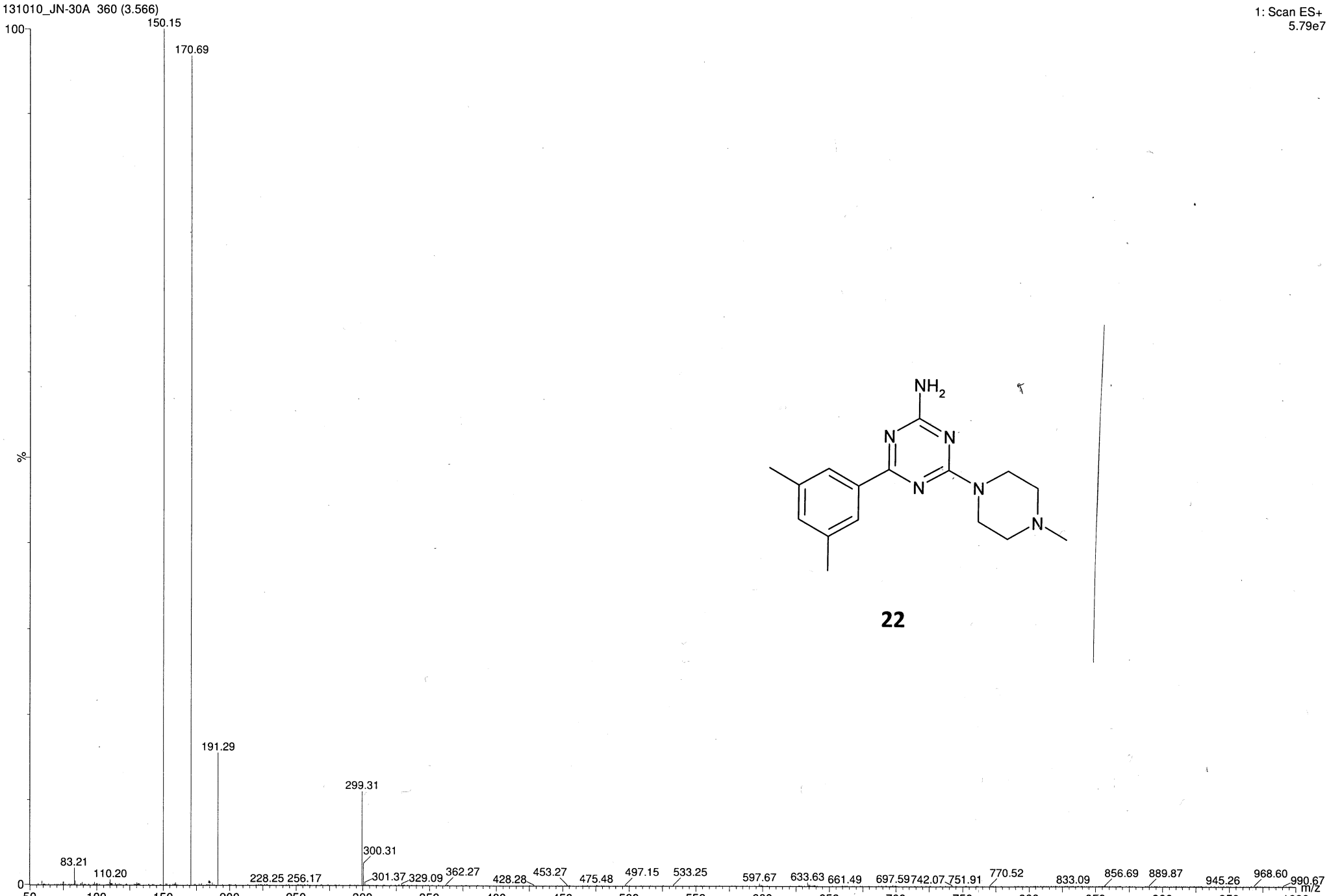
131010_JN-30A 360 (3.566)
1: Scan ES+
5.79e7
100
%
0
150.15
170.69
191.29
299.31
300.31
83.21
110.20
228.25
256.17
301.37
329.09
362.27
428.28
453.27
475.48
497.15
533.25
597.67
633.63
661.49
697.59
742.07
751.91
770.52
833.09
856.69
889.87
945.26
968.60
990.67
50
100
150
200
250
300
350
400
450
500
550
600
650
700
750
800
850
900
950
1000
m/z
NH2
N
N
N
N
N

22

Uniwersytet Jagiellonski
Collegium Medicum
Pracownia Spektroskopii NMR
Jun 24 2013
Probka: JN-31
Rozpuszczalnik: dmso

Pulse Sequence: s2pul

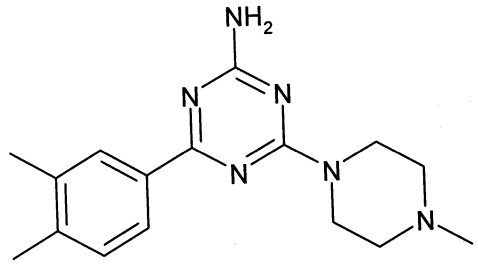

23

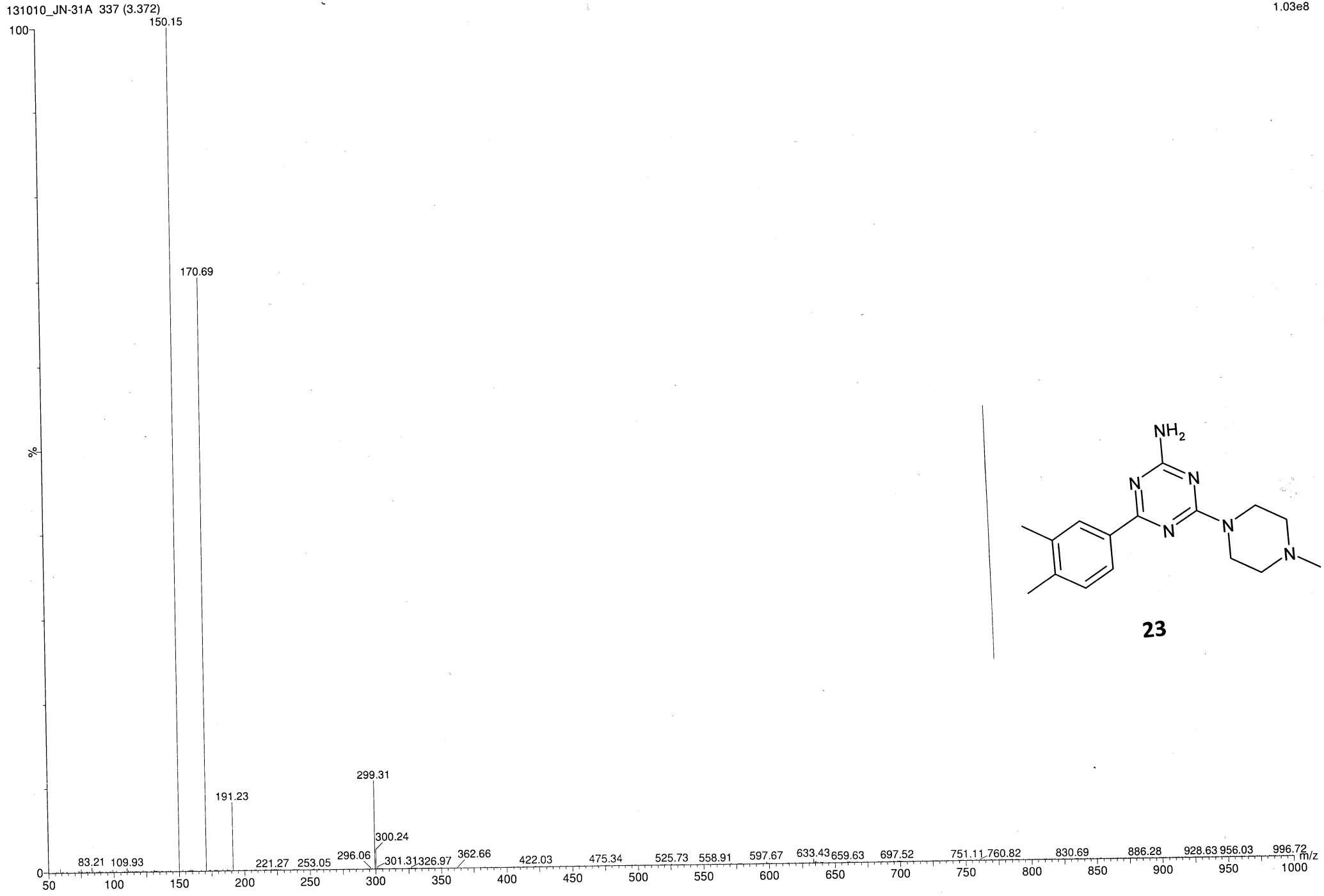
131010_JN-31A 337 (3.372)
1: Scan ES+
1.03e8
100
%
0
150.15
170.69
191.23
299.31
300.24
83.21
109.93
221.27
253.05
296.06
301.31
326.97
362.66
422.03
475.34
525.73
558.91
597.67
633.43
659.63
697.52
751.11
760.82
830.69
886.28
928.63
956.03
996.72
m/z
50
100
150
200
250
300
350
400
450
500
550
600
650
700
750
800
850
900
950
1000
NH2
N
N
N
N
N

23

Uniwersytet Jagiellonski
Collegium Medicum
Pracownia Spektroskopii NMR
Jul 2 2013
Probka: JN-20
Rozpuszczalnik: dmso

Pulse Sequence: s2pul

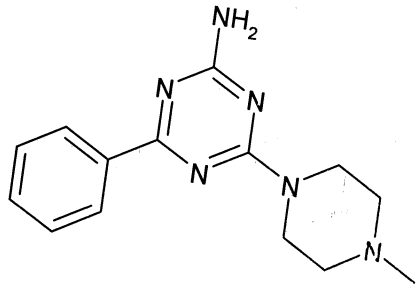

3

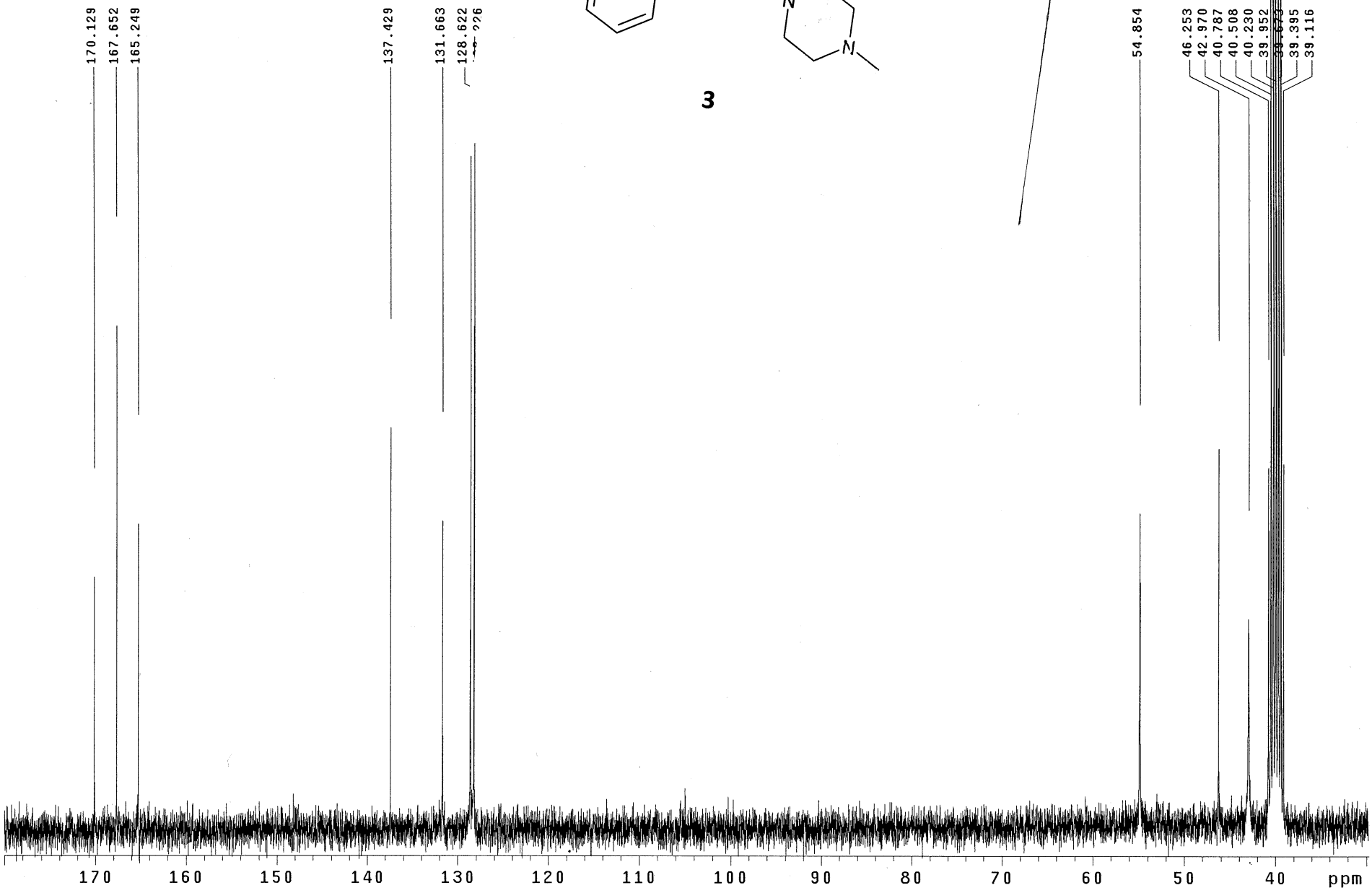

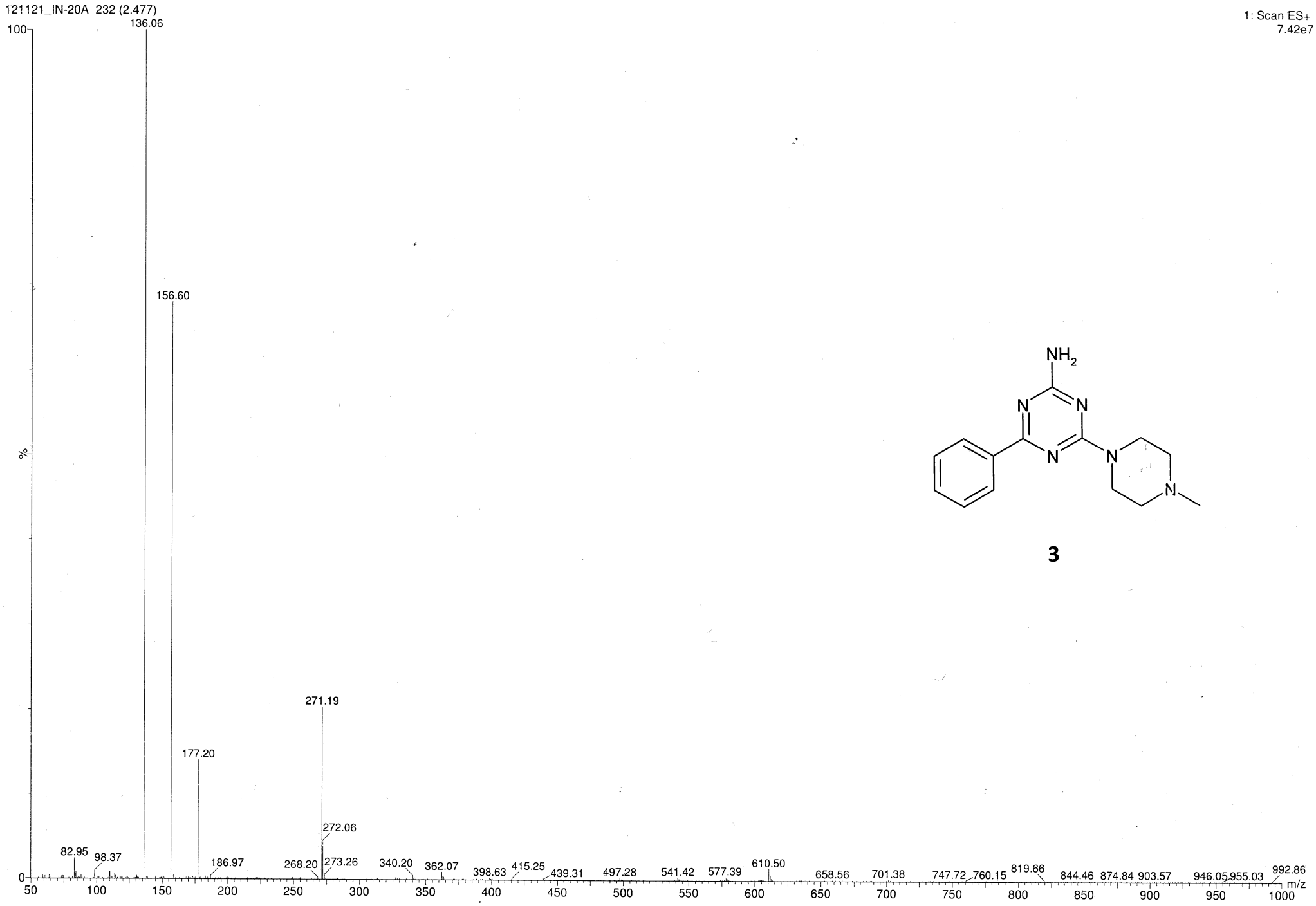
121121_IN-20A 232 (2.477)
1: Scan ES+
7.42e7
100
%
0
136.06
156.60
271.19
177.20
272.06
82.95
98.37
186.97
268.20
273.26
340.20
362.07
398.63
415.25
439.31
497.28
541.42
577.39
610.50
658.56
701.38
747.72
760.15
819.66
844.46
874.84
903.57
946.05
955.03
992.86
50
100
150
200
250
300
350
400
450
500
550
600
650
700
750
800
850
900
950
1000
m/z

NH2
N
N
N
N
N

3

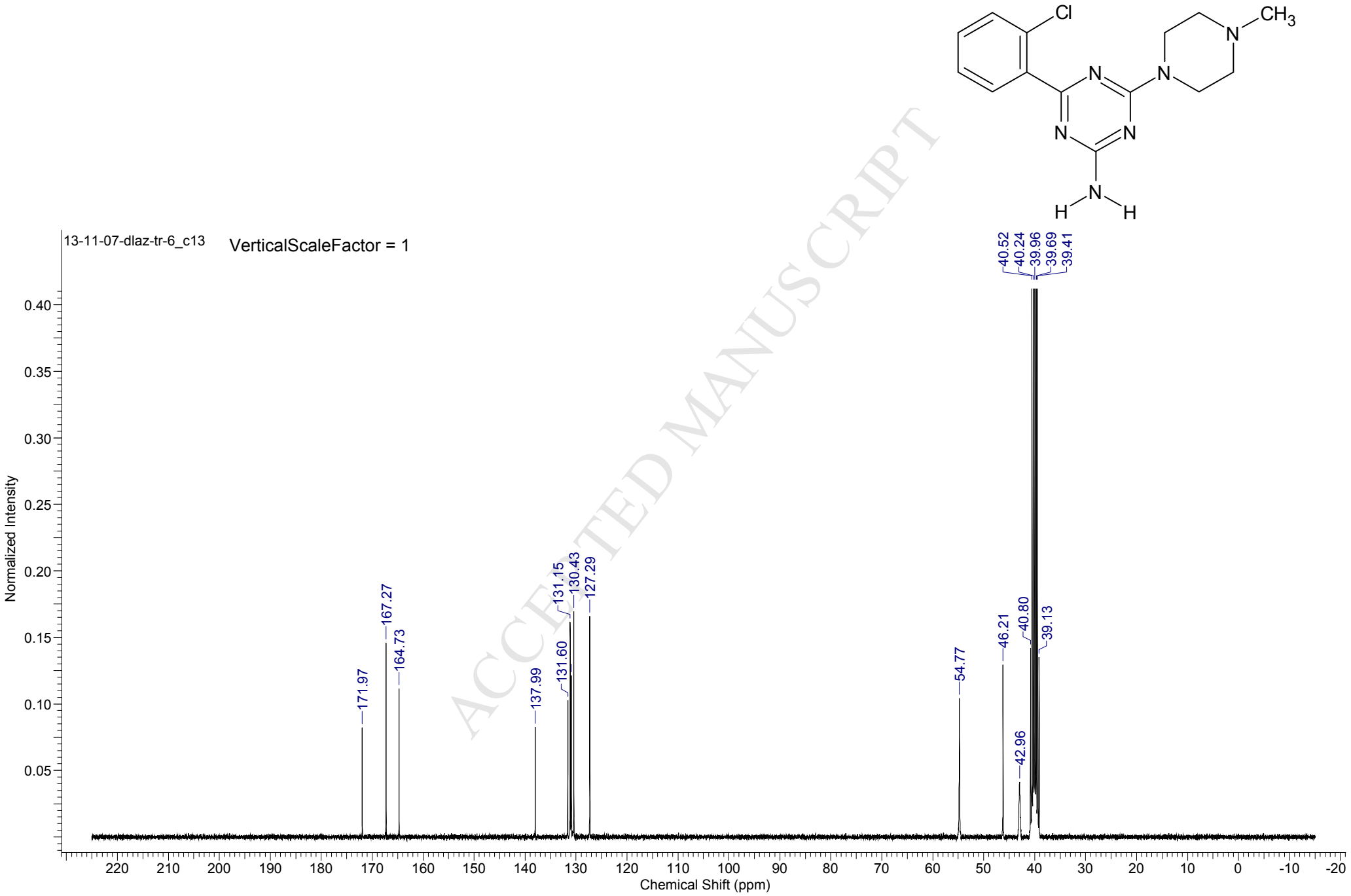


121219_TR-6A 250 (2.631)
1: Scan ES+
7.06e7
100
%
0
153.14
173.68
174.54
305.16
307.22
308.02
82.81
58.95
110.27
194.09
195.15
223.33
250.26
327.03
362.07
370.57
423.02
447.09
491.23
531.12
569.28
609.77
644.54
675.52
710.22
730.70
763.88
806.36
868.06
891.60
949.31
965.27
992.00
50
100
150
200
250
300
350
400
450
500
550
600
650
700
750
800
850
900
950
1000
m/z
NH2
Cl
N
N
N
N
N
4

Uniwersytet Jagiellonski
Collegium Medicum
Pracownia Spektroskopii NMR
Jul 2 2013
Probka: TR-3
Rozpuszczalnik: dmso

Pulse Sequence: s2pul

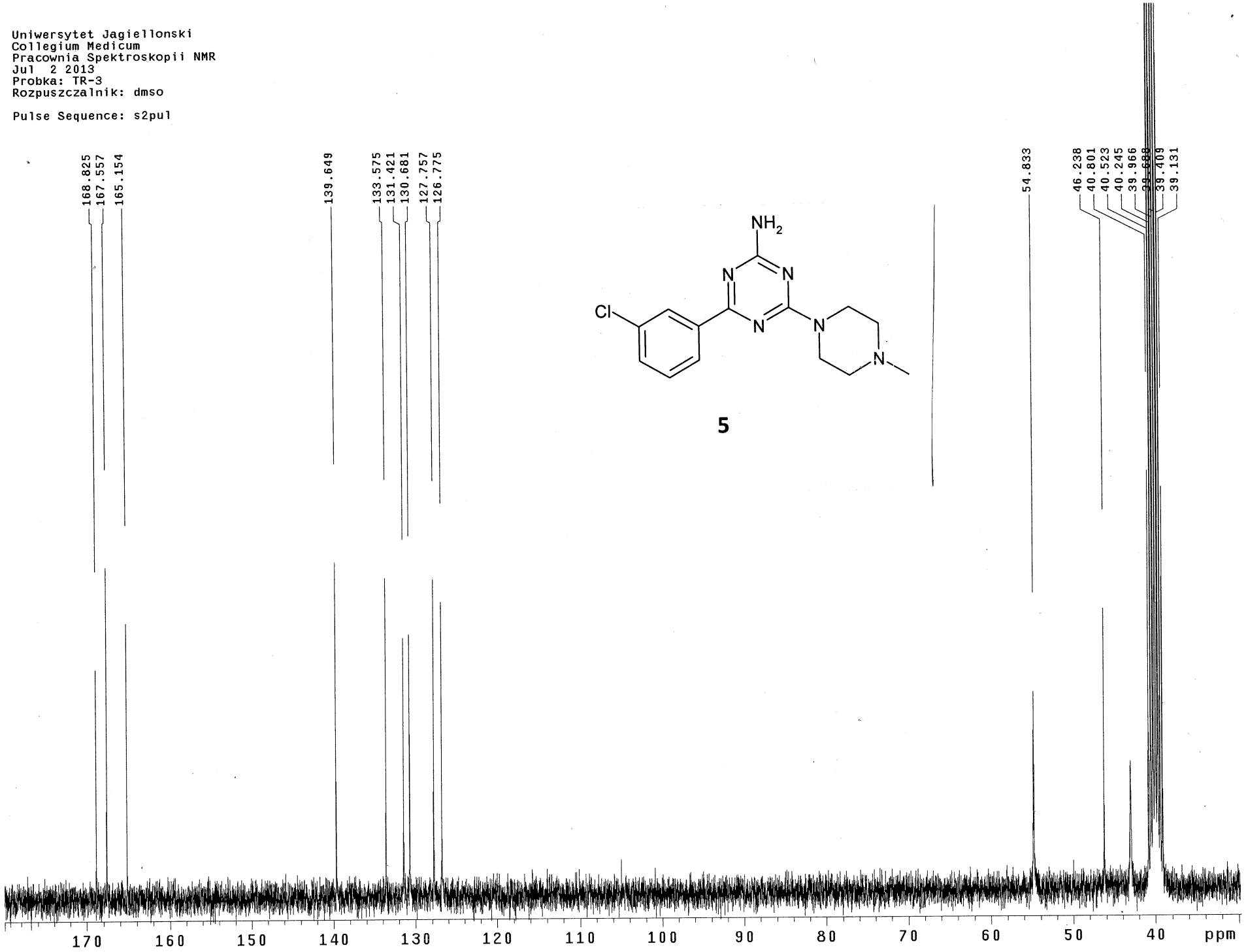

5

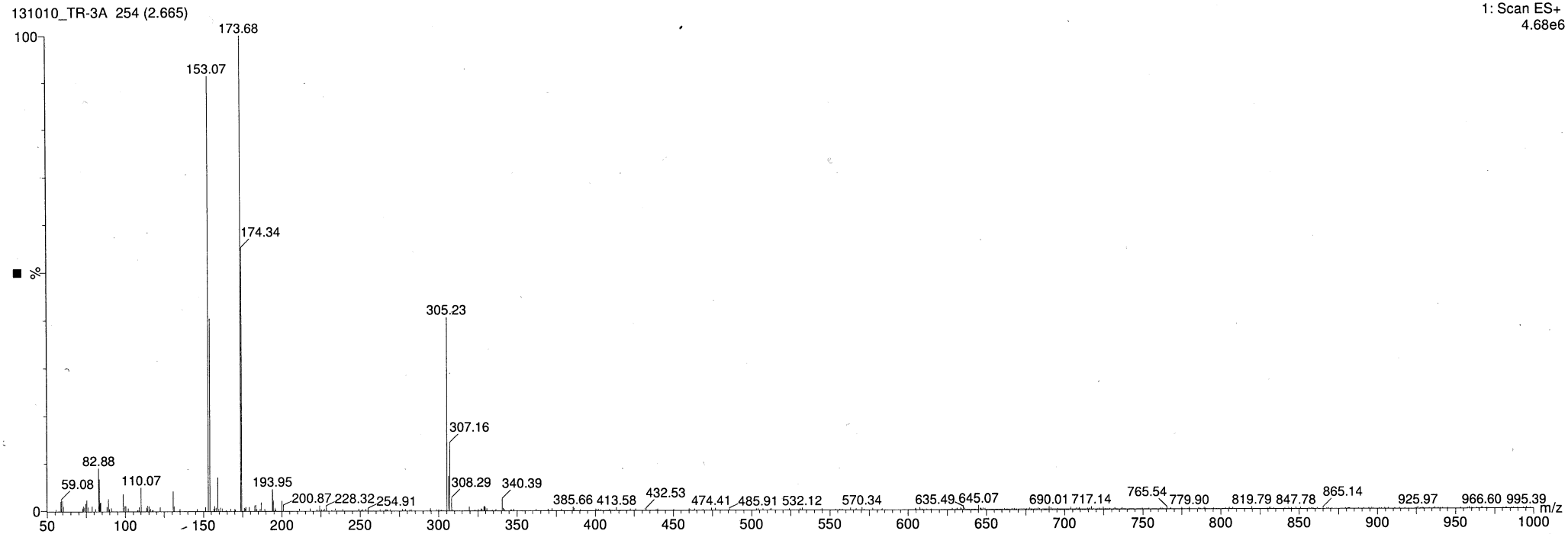
131010_TR-3A 254 (2.665)
1: Scan ES+
4.68e6
100
%
0
173.68
153.07
174.34
305.23
307.16
82.88
59.08
110.07
193.95
200.87
228.32
254.91
308.29
340.39
385.66
413.58
432.53
474.41
485.91
532.12
570.34
635.49
645.07
690.01
717.14
765.54
779.90
819.79
847.78
865.14
925.97
966.60
995.39
m/z
50
100
150
200
250
300
350
400
450
500
550
600
650
700
750
800
850
900
950
1000

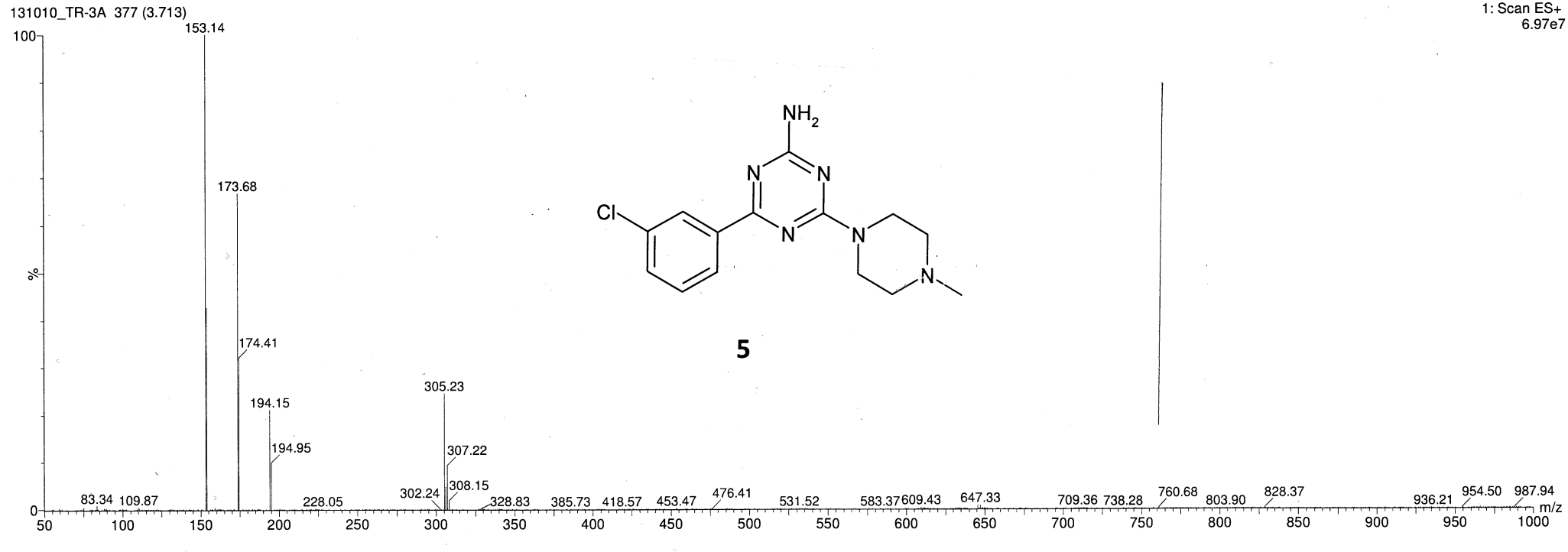
131010_TR-3A 377 (3.713)
1: Scan ES+
6.97e7
100
%
0
153.14
173.68
174.41
194.15
194.95
305.23
307.22
308.15
83.34
109.87
228.05
302.24
328.83
385.73
418.57
453.47
476.41
531.52
583.37
609.43
647.33
709.36
738.28
760.68
803.90
828.37
936.21
954.50
987.94
m/z
50
100
150
200
250
300
350
400
450
500
550
600
650
700
750
800
850
900
950
1000

NH2
N
N
N
Cl
N
N

5

Uniwersytet Jagiellonski
Collegium Medicum
Pracownia Spektroskopii NMR
Jun 27 2013
Probka: JN-9
Rozpuszczalnik: dmso

Pulse Sequence: s2pul

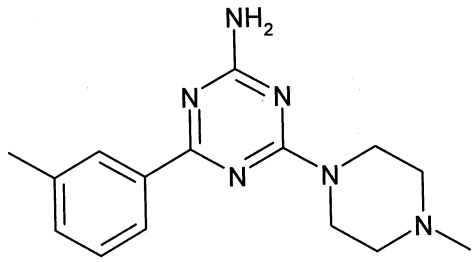

6

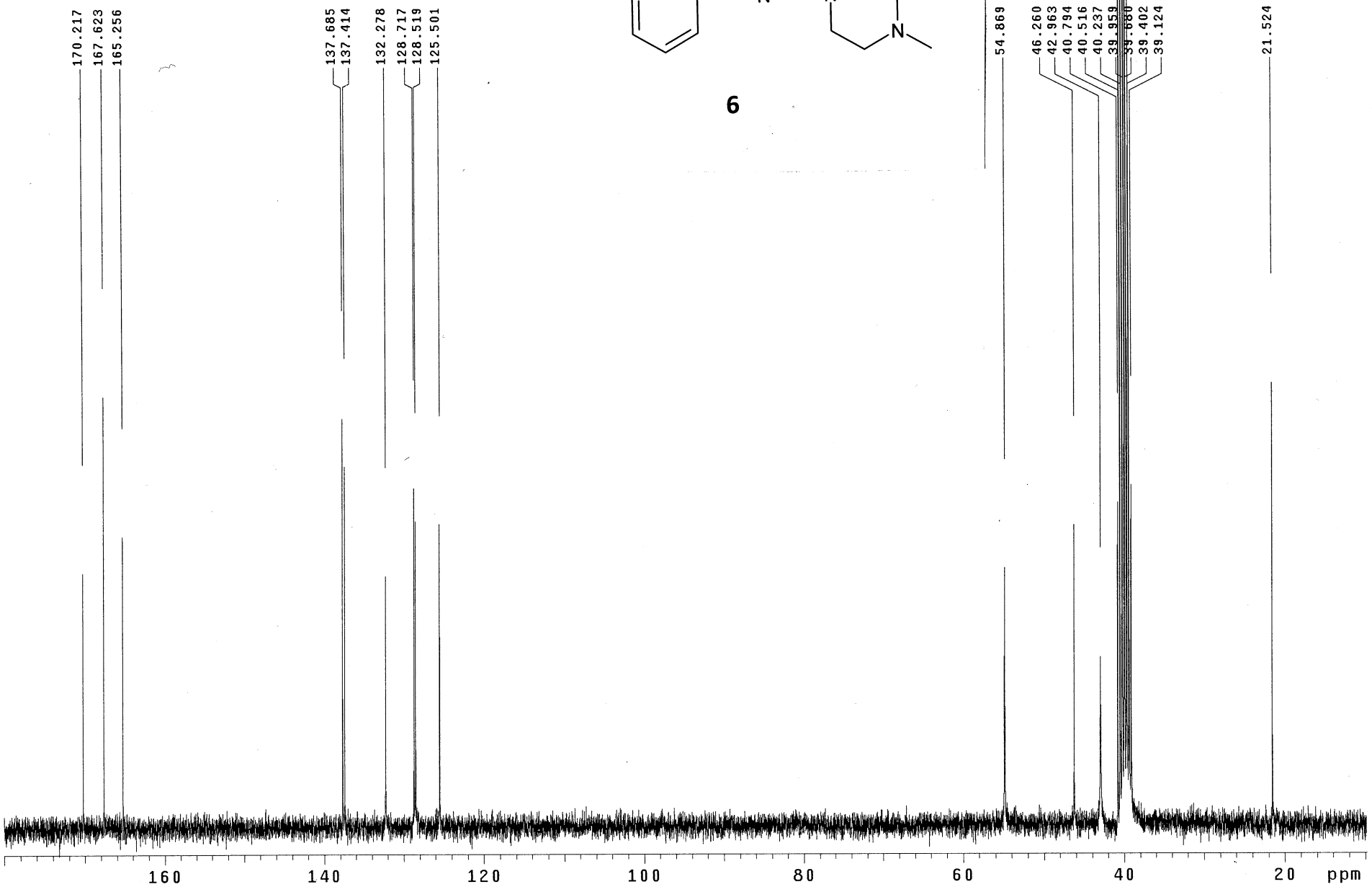

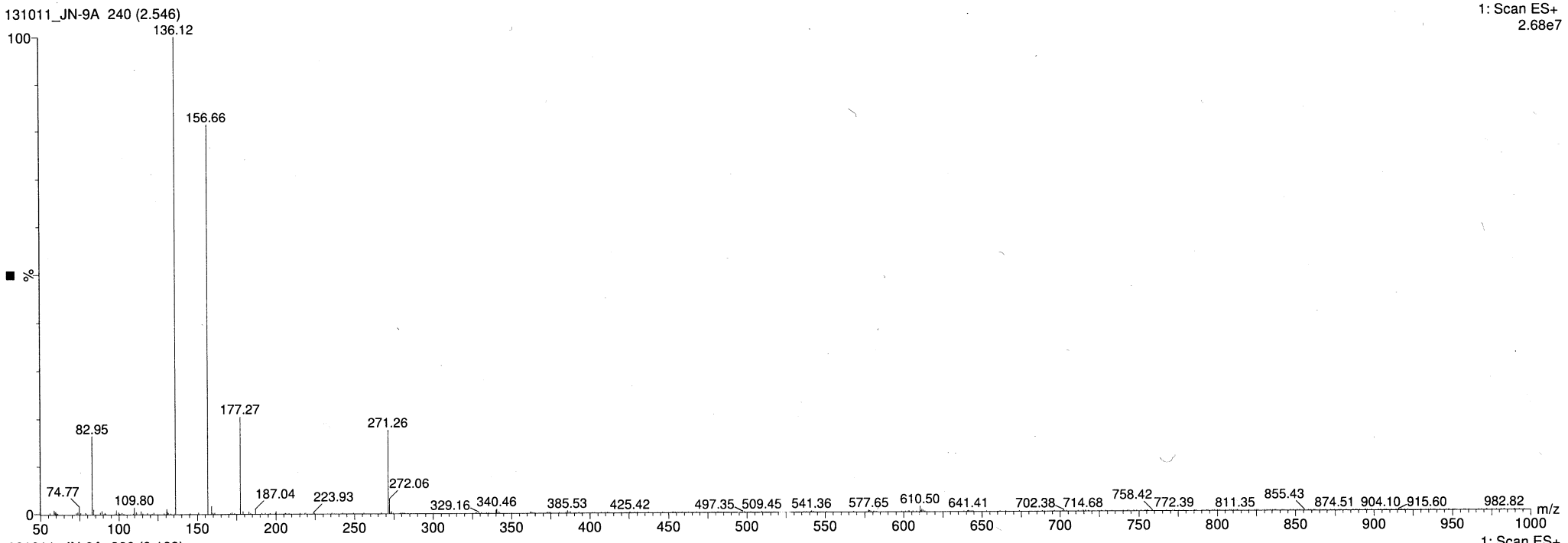
131011_JN-9A 240 (2.546)
1: Scan ES+
2.68e7
100
%
0
136.12
156.66
177.27
271.26
82.95
74.77
109.80
187.04
223.93
272.06
329.16
340.46
385.53
425.42
497.35
509.45
541.36
577.65
610.50
641.41
702.38
714.68
758.42
772.39
811.35
855.43
874.51
904.10
915.60
982.82
m/z
50
100
150
200
250
300
350
400
450
500
550
600
650
700
750
800
850
900
950
1000

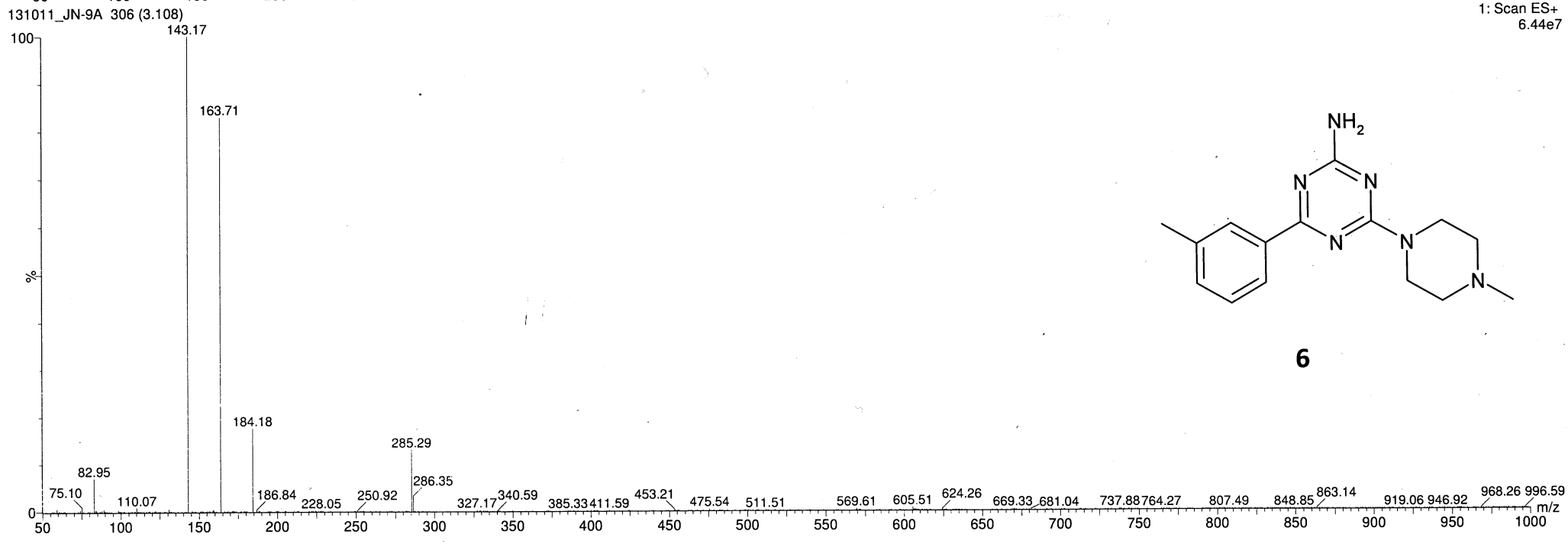
131011_JN-9A 306 (3.108)
1: Scan ES+
6.44e7
100
%
0
143.17
163.71
184.18
285.29
286.35
82.95
75.10
110.07
186.84
228.05
250.92
327.17
340.59
385.33
411.59
453.21
475.54
511.51
569.61
605.51
624.26
669.33
681.04
737.88
764.27
807.49
848.85
863.14
919.06
946.92
968.26
996.59
m/z
50
100
150
200
250
300
350
400
450
500
550
600
650
700
750
800
850
900
950
1000

NH2
N
N
N
N
N

6

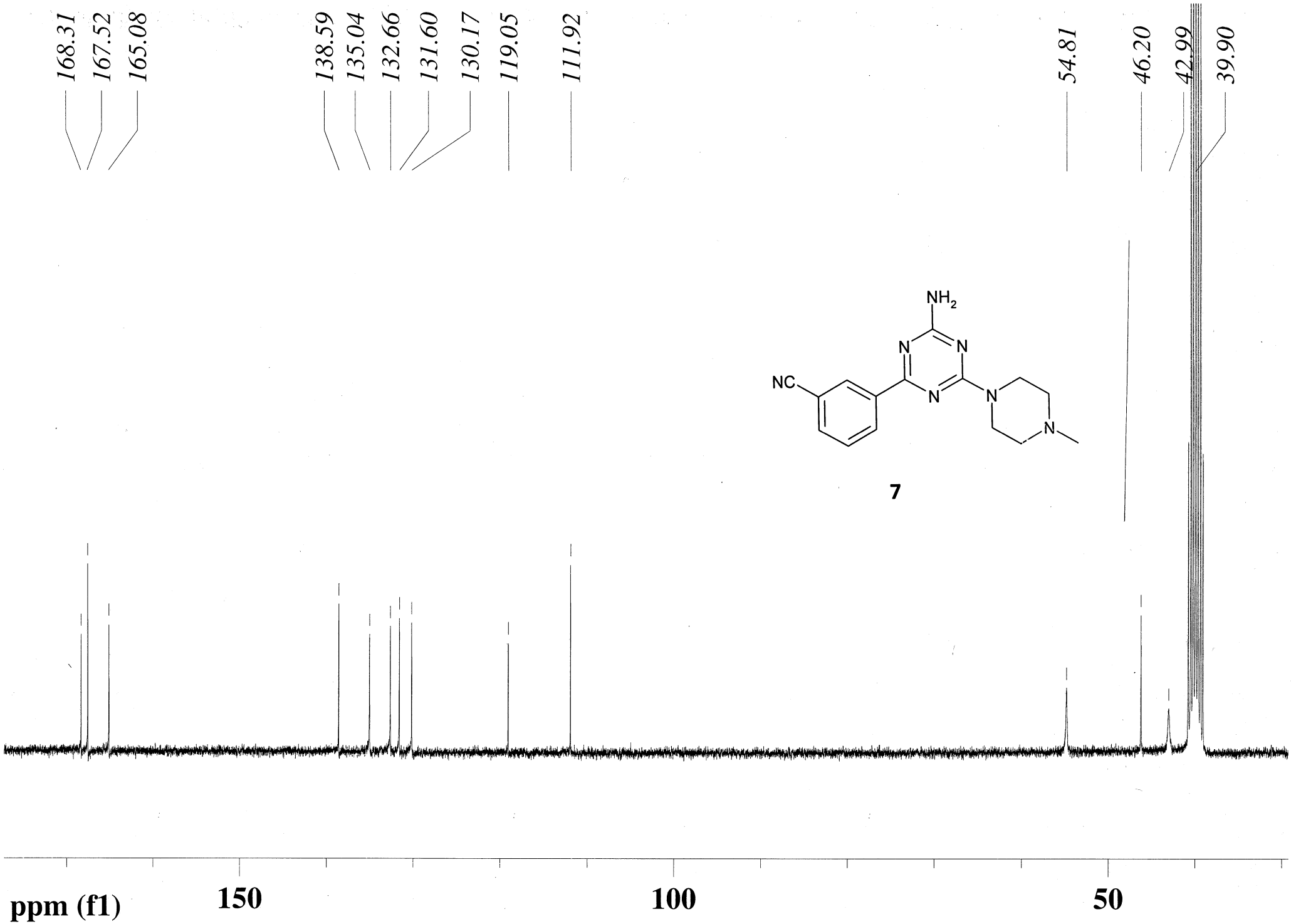
168.31
167.52
165.08
138.59
135.04
132.66
131.60
130.17
119.05
111.92
54.81
46.20
42.99
39.90
NH2
N
N
N
NC
N
N
7
ppm (f1)
150
100
50

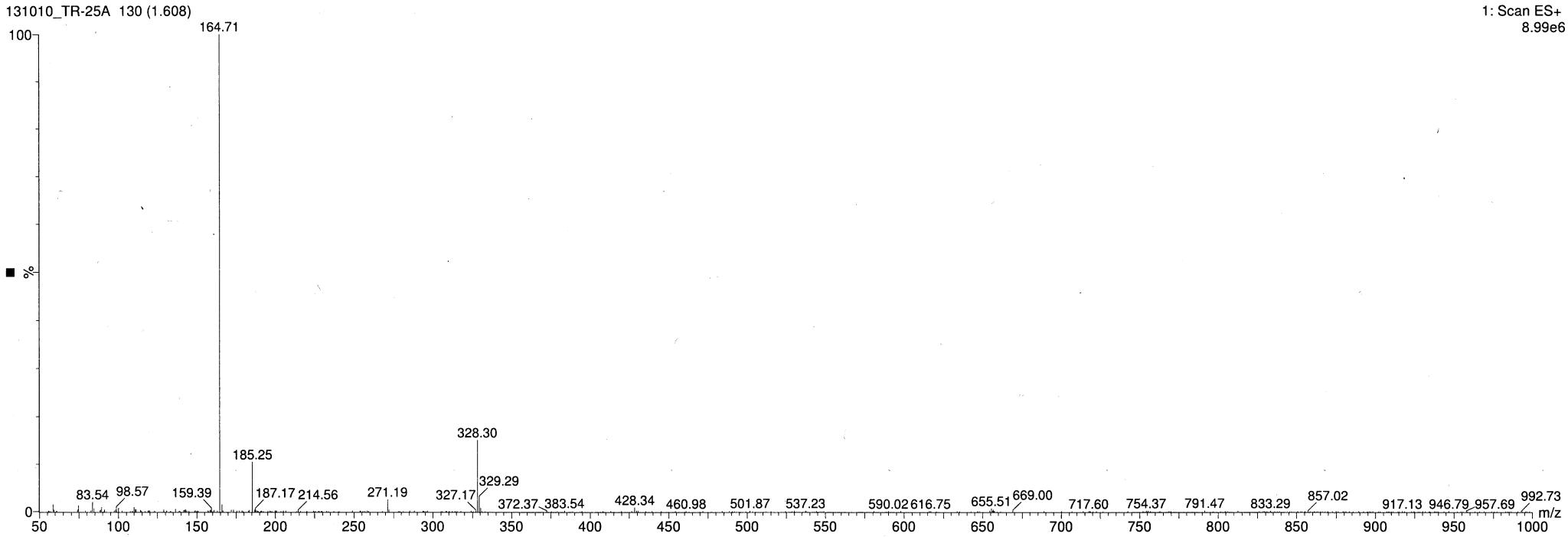
131010_TR-25A 130 (1.608)
1: Scan ES+
8.99e6
100
%
0
164.71
328.30
185.25
329.29
83.54
98.57
159.39
187.17
214.56
271.19
327.17
372.37
383.54
428.34
460.98
501.87
537.23
590.02
616.75
655.51
669.00
717.60
754.37
791.47
833.29
857.02
917.13
946.79
957.69
992.73
50
100
150
200
250
300
350
400
450
500
550
600
650
700
750
800
850
900
950
1000
m/z

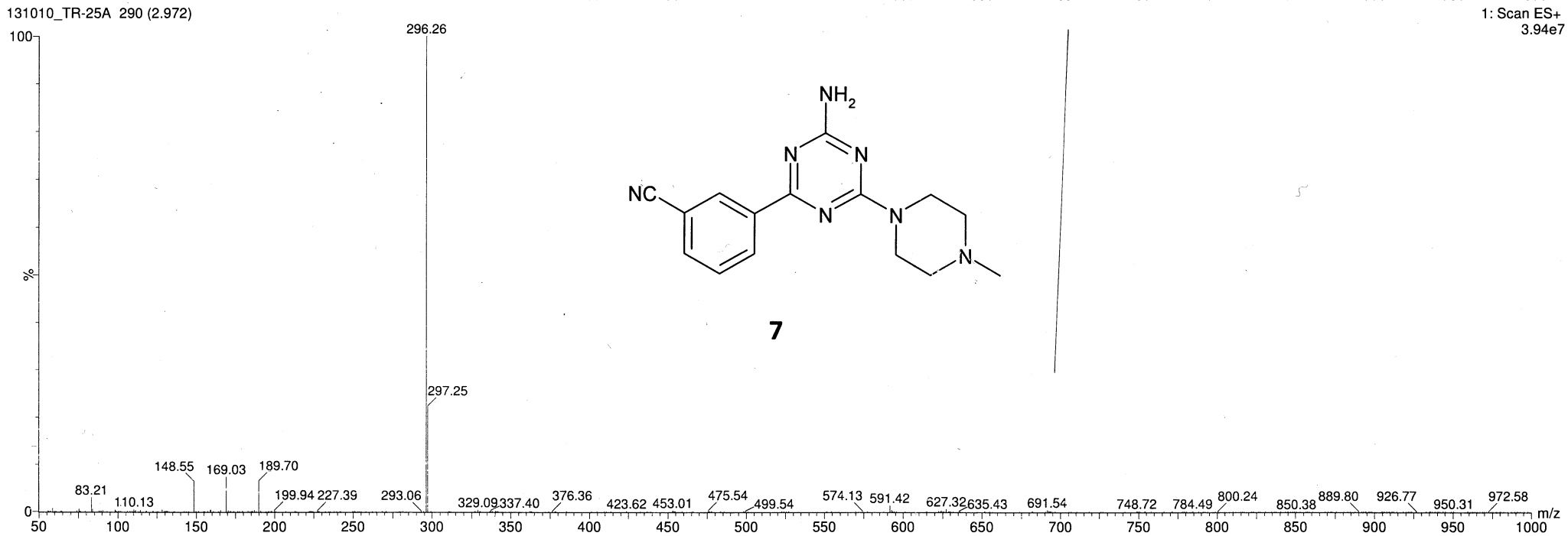
131010_TR-25A 290 (2.972)
1: Scan ES+
3.94e7
100
%
0
296.26
297.25
148.55
169.03
189.70
83.21
110.13
199.94
227.39
293.06
329.09
337.40
376.36
423.62
453.01
475.54
499.54
574.13
591.42
627.32
635.43
691.54
748.72
784.49
800.24
850.38
889.80
926.77
950.31
972.58
50
100
150
200
250
300
350
400
450
500
550
600
650
700
750
800
850
900
950
1000
m/z

NH2
N
N
N
NC
N
N

7

Uniwersytet Jagiellonski
Collegium Medicum
Pracownia Spektroskopii NMR
Jul 5 2013
Probka: TR-7
Rozpuszczalnik: dmso

Pulse Sequence: s2pul

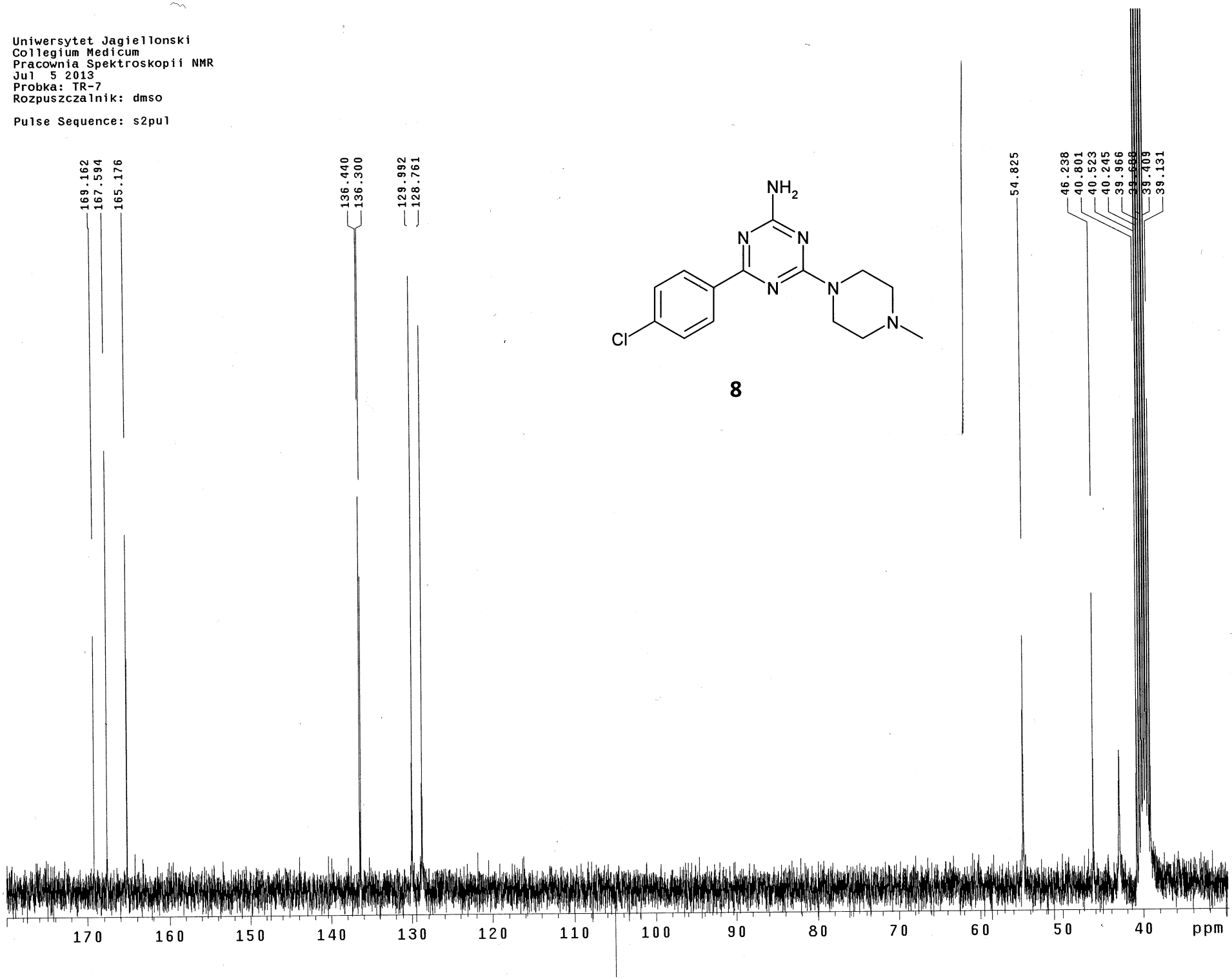

8

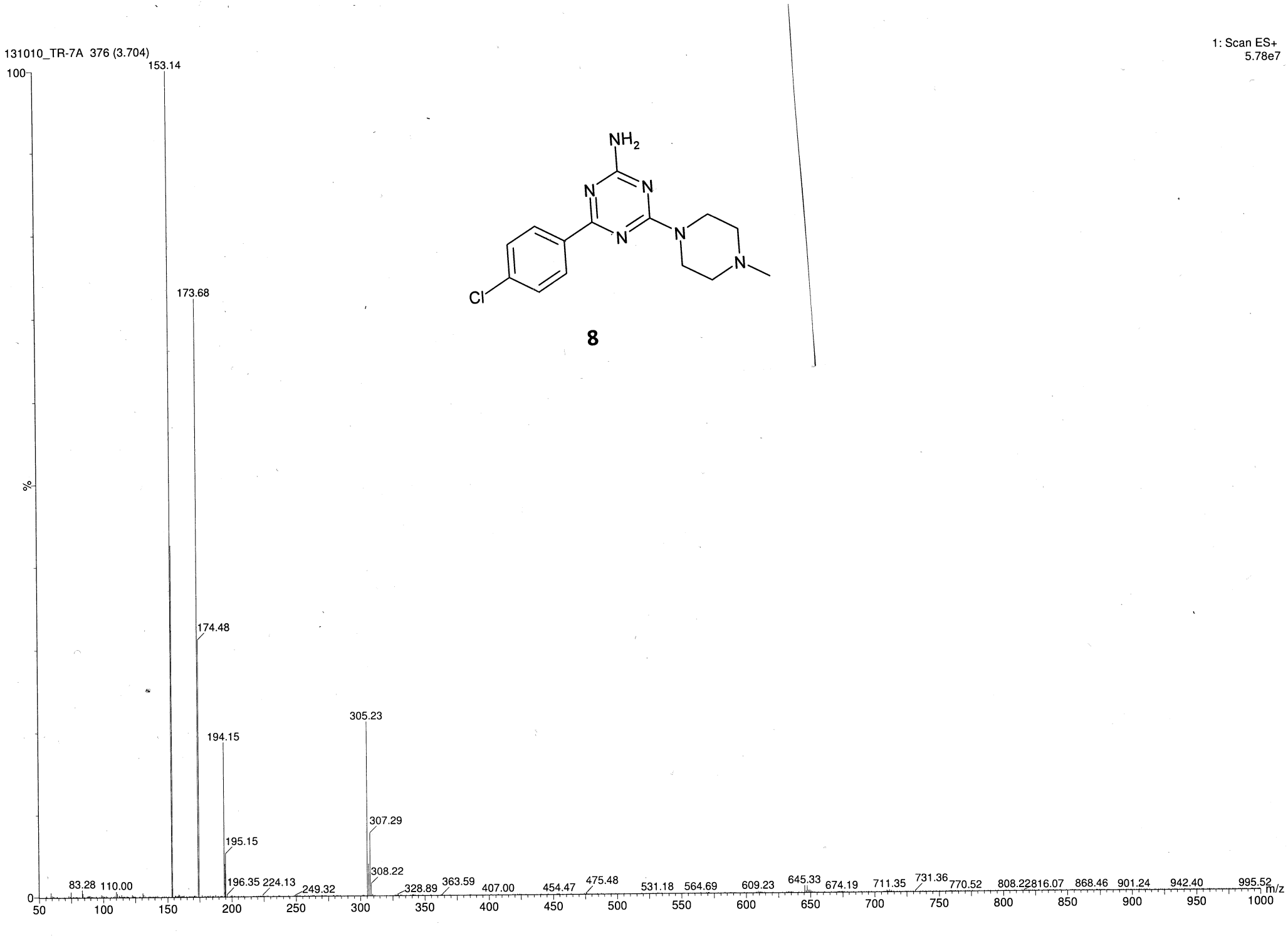
131010_TR-7A 376 (3.704)
1: Scan ES+
5.78e7
100
%
0
153.14
173.68
174.48
194.15
305.23
307.29
195.15
308.22
83.28
110.00
196.35
224.13
249.32
328.89
363.59
407.00
454.47
475.48
531.18
564.69
609.23
645.33
674.19
711.35
731.36
770.52
808.22
816.07
868.46
901.24
942.40
995.52
m/z
50
100
150
200
250
300
350
400
450
500
550
600
650
700
750
800
850
900
950
1000
NH2
N
N
N
N
Cl
8

Uniwersytet Jagiellonski
Collegium Medicum
Pracownia Spektroskopii NMR
Jul 4 2013
Probka: TR-5
Rozpuszczalnik: dmso

Pulse Sequence: s2pul

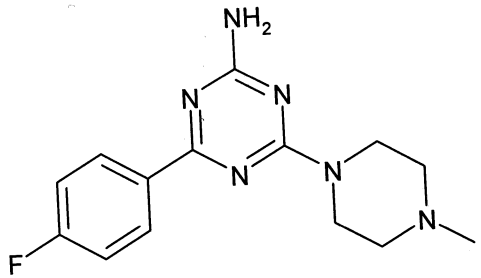

9

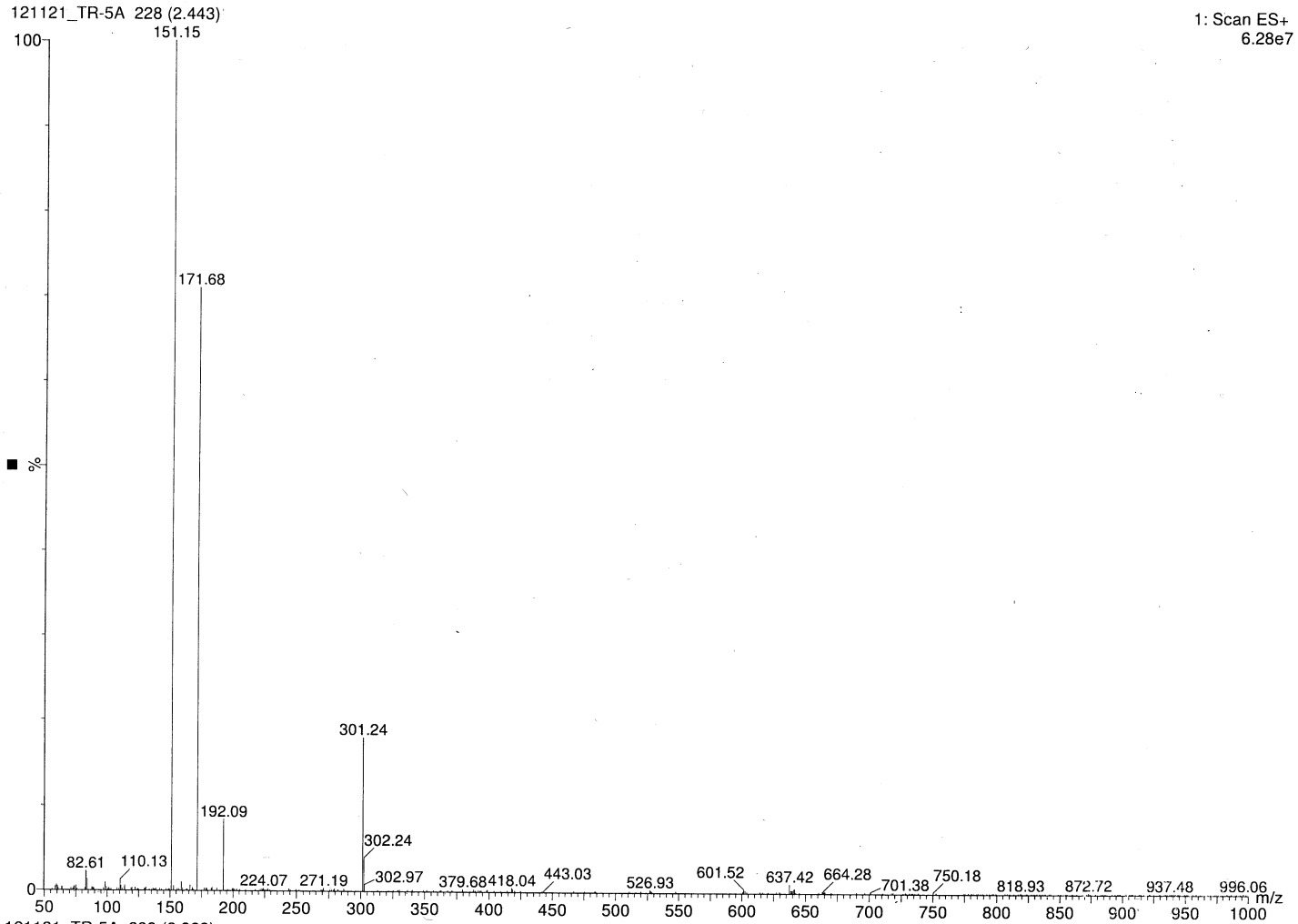
121121_TR-5A 228 (2.443)
1: Scan ES+
6.28e7
100
%
0
151.15
171.68
301.24
192.09
302.24
82.61
110.13
224.07
271.19
302.97
379.68
418.04
443.03
526.93
601.52
637.42
664.28
701.38
750.18
818.93
872.72
937.48
996.06
50
100
150
200
250
300
350
400
450
500
550
600
650
700
750
800
850
900
950
1000
m/z

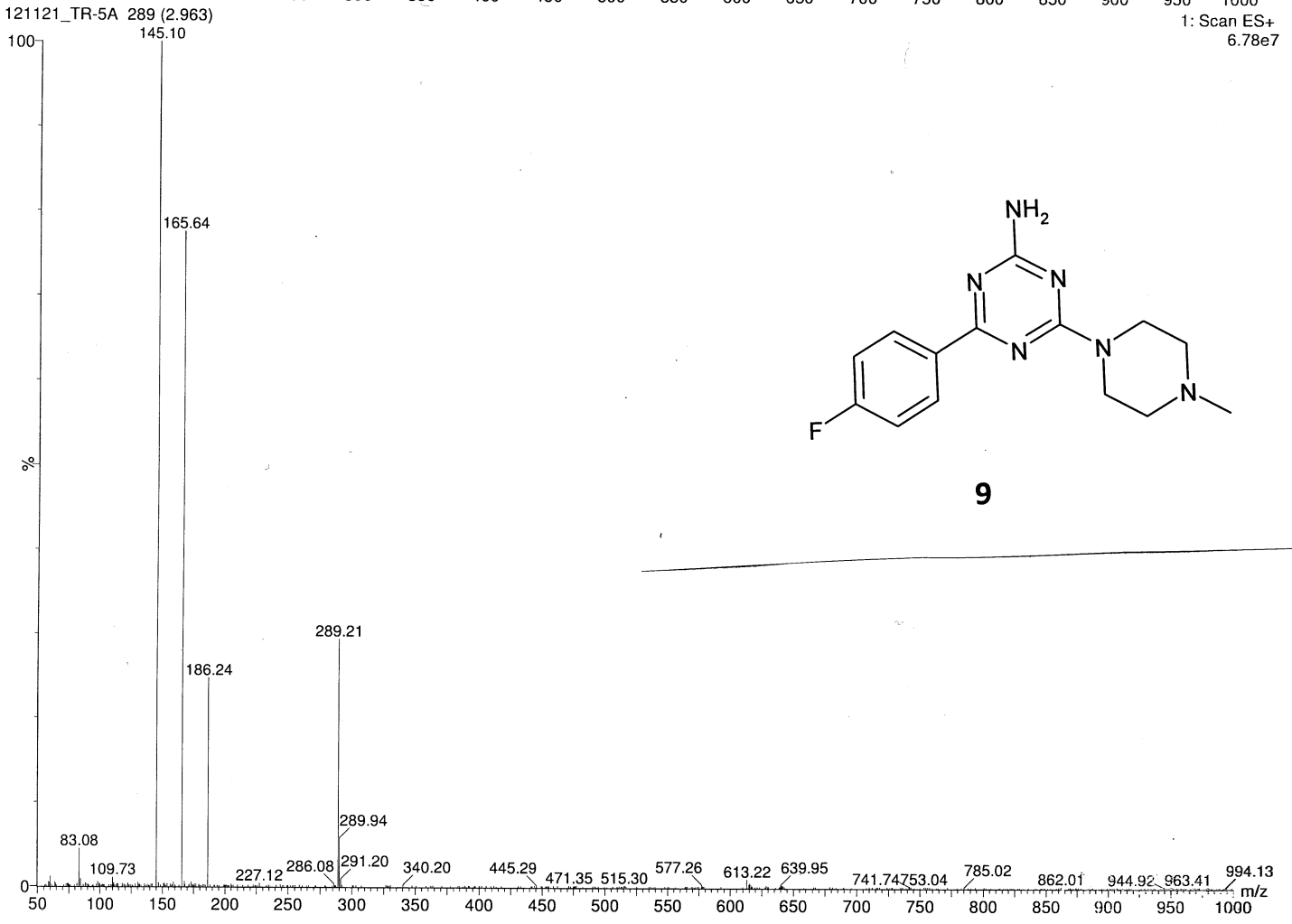
121121_TR-5A 289 (2.963)
1: Scan ES+
6.78e7
100
%
0
145.10
165.64
289.21
186.24
289.94
83.08
109.73
227.12
286.08
291.20
340.20
445.29
471.35
515.30
577.26
613.22
639.95
741.74
753.04
785.02
862.01
944.92
963.41
994.13
50
100
150
200
250
300
350
400
450
500
550
600
650
700
750
800
850
900
950
1000
m/z

NH2
N
N
N
N
N
F

9